5-7-2016

A Biogeochemistry Approach to Geographic Origin and Mortuary Arrangement at the Talgua Cave Ossuaries, Olancho, Honduras

Monica Michelle Warner

Follow this and additional works at: https://scholarsjunction.msstate.edu/td

A biogeochemistry approach to geographic origin and mortuary arrangement at the

Talgua cave ossuaries, Olancho, Honduras

By

Monica Michelle Warner

A Thesis
Submitted to the Faculty of
Mississippi State University
in Partial Fulfillment of the Requirements
for the Degree of Master of Arts
in Applied Anthropology
in the Department of Anthropology and Middle Eastern Cultures

Mississippi State, Mississippi

May 2016

A biogeochemistry approach to geographic origin and mortuary arrangement at the

Talgua cave ossuaries, Olancho, Honduras

By

Monica Michelle Warner

Approved:

_____
Nicholas P. Herrmann
(Major Professor)

_____
Molly K. Zuckerman
(Committee Member)

_____
David M. Hoffman
(Committee Member/Graduate Coordinator)

_____
R. Gregory Dunaway
Dean
College of Arts & Sciences

Name: Monica Michelle Warner

Date of Degree: May 7, 2016

Institution: Mississippi State University

Major Field: Applied Anthropology

Major Professor: Dr. Nicholas P. Herrmann

Title of Study: A biogeochemistry approach to geographic origin and mortuary
                    arrangement at the Talgua cave ossuaries, Olancho, Honduras

Pages in Study: 187

Candidate for Degree of Master of Arts

Isotopic assays, including stable carbon, stable oxygen, and radiogenic strontium were measured for 37 individuals from the Talgua cave ossuaries to understand human movement and mortuary practice during Formative Period Honduras. Likelihood assignment models demonstrated that the individuals had diverse childhood geographic origins within the surrounding valleys. This shows that different kin or ethnic groups from diverse geographic origins were utilizing the ossuaries. Five possible 'non-local' individuals were identified from the radiogenic strontium and stable oxygen isotope datasets, suggesting minimal human movement into northeast Honduras from outside Lower Central America. The low number of 'non-local' individuals at Talgua Caves also suggests that trade items were acquired by down-the-line exchange processes rather than through a long-distance trade connection. This type of trade network and bioarchaeological evidence of limited 'non-local' individuals at Talgua Caves suggests the surrounding region was culturally distinct from Mesoamerica during the Formative Period.

DEDICATION

To my sister and my mother

Last, but definitely not least, I would like to thank all of my family and friends for their support. Without you all, I would have never made it through this process.

TABLE OF CONTENTS

LIST OF TABLES

LIST OF FIGURES

CHAPTER I

THESIS OVERVIEW AND PURPOSES

1.1 Introduction

Pre-Columbian cultures in Central America and Mexico shared the ideology that

caves were associated with the origin of human creation (Prufer and Dunham, 2009).

Caves functioned as ossuaries, or repositories for the dead, and ritual spaces throughout

the Pre-Columbian region by many cultural traditions (Moyes and Brady, 2012). Ossuary

caves held elite and non-elite individuals, sacrificial offerings, and victims of conflict

(Prufer and Dunham, 2009). Ossuary caves contain a wealth of information, but are often

understudied resources, especially in Lower Central America. Biogeochemistry was used

in this study to improve scholarly understanding of the Talgua cave ossuaries through

studying the geographic origin and mortuary arrangement of the interred individuals.

Cueva del Río Talgua and Cueva de las Arañas (Talgua Caves) are two northeast

Honduran ossuary caves located in Lower Central America. Cueva del Río Talgua is a

protected eco-archaeological park located in the Sierra de Agalta National Park of the

Olancho Department. Based on six radiocarbon dates, the caves were used from

approximately 1605 BC to AD 852 (Brady et al., 2000). Little is known about the

geographic origins of the individuals interred in the Talgua Caves. In particular,

archaeological surveys failed to uncover any habitation sites associated with the

Formative Period (2000 BC to 300 BC) use of the ossuary caves (Dixon et al., 1998).

Many questions remain as to the origins and mortuary practices of these individuals. This research project aids in the understanding of northeast Honduran prehistory, especially the Olancho Valley, through the isotopic reconstruction of geographic origin and mortuary arrangement of the Talgua Cave individuals.

There were two primary research objectives: (1) assign geographic origin to a sample of individuals interred at the Talgua and Arañas ossuaries, and (2) to understand the mortuary arrangement in Cueva del Río Talgua using isotopic values. The first portion of the project used $^{87}Sr/^{86}Sr$ and $\delta^{18}O$ isotope analyses to assign geographic origin to 37 individuals from the Talgua Caves. Likelihood geographic assignment models using Bayesian probability were used to assign geographic origin on a small-scale quantitative level. These assignment models determined the probability of childhood origin using primarily the first and second molars, which form approximately at birth to three years of age and from two to eight years old, respectively. When individuals were assigned outside of the Olancho Valley, their probable geographic origins were explored in detail. The second portion of this research project used multivariate interpolation of $\delta^{13}C$, $\delta^{18}O$, and $^{87}Sr/^{86}Sr$ through inverse distance weighting (IDW) of each isotope dataset in Cueva del Río Talgua to understand the spatial arrangement of the interred individuals. Distinct spatial patterns within Cueva del Río Talgua were tested for differences in diet (i.e. $\delta^{13}C$), geographic origin (i.e. $\delta^{18}O$ and $^{87}Sr/^{86}Sr$), and presence of burial goods (i.e. $\delta^{13}C$ and $^{87}Sr/^{86}Sr$).

The secondary research objective in this project compared tooth dimensions to isotopic value ($\delta^{13}C$, $\delta^{18}O$, and $^{87}Sr/^{86}Sr$). Variation in tooth size may represent different ancestral groups or sexual dimorphism. For this study, tooth size was used as a proxy for

biological sex to look at gendered activities, such as differential diet (δ^{13}C) and change in residence (δ^{18}O and ^{87}Sr/^{86}Sr). Univariate normal finite mixture models were used to classify mesial-distal (MD) and buccal-lingual (BL) dental measurements into subgroups. A normal finite mixture model provides the framework to estimate the probability of sub-populations within the Talgua Caves sample population. Individuals from the sub-group with larger dentition were classified as possible male and individuals with smaller dentition were classified as possible female. Lastly, individuals with MD or BL values falling within the middle of the distribution were classified as indeterminate.

1.2   Research design

Dentition collected from the Talgua Caves was used in this research to determine childhood origin and explore the mortuary arrangement at Cueva del Río Talgua. Isotopic data generated from these two ossuary caves were used to answer three questions: (1) Did the individuals interred at Talgua Caves spend their childhoods in northeast Honduras? (2) Are there distinct isotopic patterns within or between the spatially structured subdivisions (lots) in the Cueva del Río Talgua ossuary? And finally, (3) Is there a relationship between isotopic value (δ^{13}C, δ^{18}O, and ^{87}Sr/^{86}Sr) and tooth size? All questions were addressed using hypothesis testing, and are stated in the following sections. Each research objective is divided by topic, (i.e. geographic origin, mortuary arrangement, and dental metric analysis), and discussed in detail in the remainder of this chapter.

1.2.1   Geographic origin

- Research objective 1: To determine the geographic origins of the individuals interred at Talgua Caves.

- Question 1: Do the individuals sampled from the Talgua Caves have a high probability of originating from northeast Honduras?

- H_0: The Talgua Cave $^{87}Sr/^{86}Sr$ and $\delta^{18}O$ bioavailable signatures are assigned with 90% probability to northeast Honduras.

The first research objective was designed to assign geographic origin to each individual sampled at Talgua Caves. It is possible that the interred individuals had diverse geographic origins based on the previous archaeological survey conducted along the Río Talgua drainage in the Olancho Valley. The archaeological survey resulted in the identification of 39 habitation sites, which all had Classic Period or Post-Classic Period components. Since five of the six radiocarbon dates from the Talgua Caves dated to the Formative Period, the absence of identified Formative Period habitation sites in the Olancho Valley is one possible reason the Talgua Cave individuals may have diverse geographic origins. The presence of exotic goods, such as jade, recovered in the Río Talgua Cave is additional evidence to support this possibility (Dixon et al., 1994). Another ossuary cave in the region, Cuyamel Caves, also contained exotic obsidian and pottery with Olmec motifs (Healy, 1974; Joyce and Henderson, 2010). This provides justification to infer that northeast Honduras had long distance exchange with areas in Mesoamerica, and that human movement may be associated with this interaction. The $^{87}Sr/^{86}Sr$ and $\delta^{18}O$ isotopes serve as geochemical signatures that source or trace individuals to geographic areas (Bentley, 2006), and were used to assign geographic

origin to the sampled individuals. Fourteen ^{87}Sr/^{86}Sr samples and four "binned" δ^{18}O

values were input into the corresponding assignment models. The output assignment data,

along with traditional archaeological 'non-local' identification techniques, were used to

assess the individuals' childhood origins.

The null was accepted and all the Talgua Cave ^{87}Sr/^{86}Sr and δ^{18}O bioavailable

signatures were assigned within the 90% probability range to northeast Honduras. The

acceptance of this hypothesis is informative. The Talgua Cave individuals sampled

appear to have all spent their childhoods in northeast Honduras, despite the evidence of

exotic goods found in northeast Honduran cave ossuaries. This provides the framework

for the inference that the non-local goods recovered in these Formative Period cave

ossuaries may have been acquired from down-the-line exchange networks, since

individuals living during the Formative Period in northeast Honduras were not changing

residence from far distances, such as Mesoamerica.

1.2.2   Mortuary arrangement

- Research objective 2: To understand the mortuary arrangement in Cueva
  del Río Talgua through isotope values.

- Question 2: Are there distinct isotopic patterns between the spatially
  structured subdivisions (lots) in the Río Talgua Cave ossuary?

- H$_0$: There are random patterns of δ^{13}C, δ^{18}O, and ^{87}Sr/^{86}Sr values between
  the lots in the Río Talgua Cave ossuary.

The second objective for the research project was designed to analyze the spatial

distributions of the ^{87}Sr/^{86}Sr, δ^{18}O, and δ^{13}C bioavailable signatures throughout Cueva del

Río Talgua. No evidence of trauma or human sacrifice was documented in the ossuary;

5

therefore the multiple-episode internments may suggest that the Talgua Caves represent family ossuaries on the basis of kinship or lineage (Somerville, 2010). Flowstone pools and niches, termed lots, act as discrete barriers within the Río Talgua Cave that may have been used to sub-divide individuals. Typically, intra-ossuary variation is studied using biodistance, DNA, body modifications, contextual artifacts, or historic records to fully understand the mortuary arrangement (Stojanowski and Schillaci, 2006). Since these types of data are unavailable, isotopes may assist in understanding the mortuary practices. Mortuary practices are shaped by biological, social, ideological, and taphonomic phenomena (Shimada et al., 2004), which help reconstruct social organization of populations.

The mean δ^{13}C and δ^{18}O lot values were input into the Inverse Distance Weighting (IDW) interpolation model. The IDW output was visually explored and any observed spatial patterns were tested for statistical significance using Kruskal-Wallis one-way analysis of variance tests. Lots with and without burial goods were also explored by ^{87}Sr/^{86}Sr, δ^{13}C, and δ^{18}O values, and tested for significance using student's t-tests.

The null was accepted and there were no statistical isotopic spatial variations between the lots in the Río Talgua cave ossuary. Although, there were observed differences between the lots with artifacts and the lots without artifacts by ^{87}Sr/^{86}Sr bioavailable signatures, the differences were not significant (p=0.11249). The lack of spatial patterning by isotopic signature is informative, and may suggest that Río Talgua Cave was used by one extended lineage over multiple generations, or population egalitarianism (Ashmore and Geller, 2005).

6

1.2.3 Dental metric analysis

- Secondary research objective: To determine if tooth size is related to geographic origin or diet.

- Question 3: Is there a relationship between isotopic value ($\delta^{13}C$, $\delta^{18}O_p$, $\delta^{18}O_c$, and $^{87}Sr/^{86}Sr$) and tooth size?

- H_0: There is no significant relationship between isotopic value and tooth size.

The secondary research objective was designed to compare tooth size to isotopic value ($\delta^{13}C$, $\delta^{18}O$, and $^{87}Sr/^{86}Sr$) for the Talgua Cave assemblage. Variation in tooth size includes relationships within and between populations, and between biological sex (i.e. sexual dimorphism) (Kieser, 1990; Joseph et al., 2013). For this study, tooth size was used as a proxy for biological sex to look at gendered activities, such as differential diet ($\delta^{13}C$) and change in residence ($\delta^{18}O$ and $^{87}Sr/^{86}Sr$). Change in residency occurs for many reasons, including marriage, resource acquisition, climate, trade, warfare, pilgrimage, and colonization (Schwarcz et al., 2010), and may be a 'woman', 'man', or 'other' gendered activity. Gendered access to food resources, or differential diet, may be elucidated with $\delta^{13}C$ values, since "the foods we eat become organically and socially embodied" (White, 2005: 357). Gender identity or gendered activities are unknown for the Formative Period in eastern Honduras (Hoopes, 2001). Therefore, there is not enough information to know whether gender identities were fluid or bimodal for Pre-Columbian northeast Honduras.

Dental metrics were used since no skeletal indicators were available for sex estimation. The metric distribution of tooth size for the Talgua Caves assemblage provides an overall distribution of sexual dimorphism. Univariate normal finite mixture

models were used to classify mesial-distal (MD) and buccal-lingual (BL) dental measurements into subgroups. Individuals from the sub-group with larger dentition were classified as possible male and individuals with smaller dentition were classified as possible female. Lastly, individuals with MD or BL values falling within the middle of the distribution were classified as indeterminate.

The null hypothesis was accepted and there were no differences between isotope values and tooth size. For the subsample of isotope measurements, two possible males, six possible females, and five indeterminate individuals were identified No significant relationships between $\delta^{13}C$ (p=0.16877), $\delta^{18}O_p$ (p=0.38225), or $\delta^{18}O_c$ (p=0.90604) and tooth size were present. However, this null relationship of $\delta^{13}C$ provides evidence for equal access to food resources in the Olancho Valley during the Formative Period.

1.3   Chapter organization

This thesis is divided into seven chapters. Chapter II is a discussion of the biocultural context for the northeast Honduras, specifically defining the temporal periods, and reviewing the archaeology of the region. Importantly, the theoretical view of Lower Central America and gender are addressed, and why the term *Intermediate Area* was traditionally used for this region. Chapter III is the literature review for biogeochemistry, which details the theories and principles of isotope analysis. A review of isoscapes is listed in this chapter, and is important for understanding the application of assignment models. The Talgua and Arañas ossuary caves are discussed in Chapter IV, along with the environmental setting of the region. The sample selection for the isotopic analysis is also addressed in this chapter, since the description of the lots relate to what individuals were selected. The methods and procedures are fully detailed in chapter V, including the

likelihood geographic assignment models, isoscape maps used, and all formulas and equations. The results chapter, Chapter VI, includes an in depth descriptions of all preliminary exploratory results and the outcomes of hypotheses testing. The final chapter provides a summary of all the research findings and some possible interpretations of the results.

CHAPTER II

BIOCULTURAL CONTEXT FOR NORTHEAST HONDURAS

2.1   Beyond the Frontier

Lower Central America includes the modern countries of Costa Rica, Nicaragua, Panama, and most of El Salvador and Honduras (Figure 2.1). In Honduras, the cultural boundary separating Mesoamerica from Lower Central America typically follows the Ulúa River in western Honduras (Henderson and Hudson, 2012). Traditionally, *Intermediate Area* was used to define Lower Central America, but this term limits the cultural diversity and independence of the region. This term depicts the region as a geographical entity that lies between the major cultural complexes of Mesoamerica and South America. These early ideas of the Intermediate Area as a product of the intrusion of core cultural areas devalue Honduran prehistory (Lang and Stone, 1984). Intermediate Area also implies the area is not as complex, invoking a hierarchal cultural evolutionary history (Lang and Stone, 1984). This way of thinking is a consequence of limited research conducted in northeast Honduras, and the lack of Mesoamerican-like architecture and monuments. A less controversial term, *Isthmo-Colombian Area*, has more recently been proposed for the region, and encompasses parts of Columbia with cultural and linguistic similarities (Hoopes and Fonseca, 2003). For ease, the term Lower Central America was used in this research.

Figure 2.1   Formative Period Sites with Mesoamerican Boundary

Linguistic research suggests a connection between Lower Central American and South American populations. Historical documentation shows that at Spanish contact northeast Honduras was home to Lenca, Pech, Tawaka, Tolupanes, and Nahua indigenous groups (Strong, 1948). The Pech is the only remaining indigenous group living in the Olancho Department of Honduras today, who speak a Chibchan language variant that is similar to the speakers of northern South America (Begley, 1999). In addition, linguistic evidence suggests that the Chibchan speaking people of Costa Rica and Panama have spoken this language since the late Archaic (Barrantes, 1993).

Therefore, it is suggested that the Pech are biologically affiliated with individuals who migrated from South America at least 3,000 years ago (Cuddy, 2007).

Alternatively, Melton (2008) demonstrated a shared paternal biological (Y-chromosome) relationship between K'iche Maya and northern Chibchan populations in Nicaragua. There was also a genetic relationship between southern Chibchan and South American groups. The stronger Y chromosome and lower mtDNA haplotypes implied male dominated movement or possible change in residence by male individuals (Melton, 2008). Based on the linguistic and genetic evidence an early migration event occurred into Lower Central America by at least the Archaic Period, followed by later male dominated changes in residential history into northern Chibchan speaking areas (Melton et al., 2013).

Although linguistic, biological, and cultural similarities are apparent, classifying the cultural affiliation for northeast Honduras is difficult. Some have even suggested that the indigenous groups that historically and currently reside in northeast Honduras are not ancestral to the individuals who built many of the archaeological sites in the area (Lara Pinto and Hasemann, 1988). In Lower Central America, there are trade goods from both Mesoamerica and South America, but also distinctions in material culture (see discussion in next section). Thus, the question of the ancestral affiliation of pre-Columbian northeast Honduras remains.

2.2   Archaeology of northeast Honduras

There are six different archaeological regions in Honduras: the Far West (includes the Department of Copán), Lake Yojoa region, Ulua-Chamelecon-Sula region, Central Honduras, Southern Pacific, and the Northeast region (Healy, 1984). The archeological

region of northeast Honduras extends from the Bay Islands to the Río Patuca, and includes the Departments of Olancho, Colón, and the western portion of Gracias a Dios. This region also contains the Aguan Valley of eastern Honduras, which is one of the most agriculturally productive valleys in Honduras, rich in alluvial mountain soil. The Department of Olancho, the location of the sites used in this research project, is larger in area than the country of El Salvador. Northeast Honduras "remains one of the least studied and least understood regions in Lower Central America" (Dennett and McCafferty, 2012: 52). The earliest archaeological investigations of northeast Honduras focused on the north coast and Bay Islands by Junius Bird, during his time at the American Museum of Natural History that was published by Strong (1935), and Stone (1941). Epstein (1957) developed the first chronological sequence for northeast Honduras based on the coastal and island pottery. The chronology was later simplified during the *Advanced Seminar on lower Central American Archaeology* in 1980, and further improved upon by Dennett (2007) (Figure 2.2).

	Talgua Caves	Northeast Honduras	Lower Central America	Mesoamerica
1500		Late Cocal Period	Late Period	Late Post Classic
1400				
1350		Early Cocal Period		
1250				
1000				Early Post Classic
1000				
900		Transitional Selin	Regional Development Period	Terminal Classic
800				
700	Classic Period	Basic Selin		Classic
650				
500		Early Selin		
400				
300			Formative Period	
250				
100				Late Pre-Classic
0				
100				
200				
300				
400	Middle Formative	Cuyamel Period		
500				Middle Pre-Classic
600				
700				
800				
900				
1000				
1100	Early Formative		Early Ceramic Period	Early Pre-Classic
1200				
1300				
1400				
1500				
1600				

Figure 2.2   Chronology at Talgua Caves (adopted from Dennett, 2007)

Paul Healy and Chris Begley worked extensively in northeast Honduras at the following sites: Cuyamel Caves (Healy, 1974); William's Ranch (Healy, 1975); Selin Farm (Healy, 1978a); Río Claro (Healy, 1978b); Calientes, Peroles, Piedra Blanca,

Talgua Village, and Tayaco (Begley, 1999). The majority of their research focused on documenting unidentified archaeological sites, studying settlement patterns, ceramic chronological sequencing, and identifying the cultural affiliation of the region. Paul Healy was the pioneering archaeologist in northeastern Honduras and was the first to conduct systematic research. Notably, Healy recognized a settlement pattern shift from loosely structure settlements at sites such as the Selin Farm to highly organized settlements, post AD 1000, at sites such as Río Claro (Healy, 1975; Healy, 1978a). Río Claro is located in the Department of Colón and was the first site in the region to have radiocarbon dates, which placed the site in the Cocal Period (AD1000 to AD1530). Río Claro is one of the largest sites in the region, consisting of more than 50 rectangular, square, and irregular earthen mounds built of clay and stone boulders. Deep ditches surrounded the mound complex at Río Claro, possibly for defensive purposes (Healy, 1978b). In addition, Healy documented the Cuyamel Caves, which are the only systemically documented caves containing human remains other than Talgua Caves in northeast Honduras. Cuyamel Caves are discussed in detail in the Honduran mortuary section of this chapter.

Chris Begley's extensive archaeological investigation of northeast Honduras begins with his dissertation research (Begley, 1999), where he recorded 125 sites in the mid-to-late 1990s. His definition of a site was similar to eastern North American state regulations, and was defined as an area containing two or more artifacts recovered during pedestrian reconnaissance or subsurface testing. Sites containing visible architecture, such as earthen mounds, were contained to 75 m intervals, and mounds or groups of mounds separated by distances over 75 m were classified with separate site designations

15

(Begley, 1999). The sites Suyapita, Marañones, El Cafetal, Altas de Subirana, Buena Vista, El Garrapatero, and La Cooperativa were among some of the larger sites recorded and excavated during his research. Sites identified were dated using radiocarbon or ceramic sequencing, and dated to the Classic Period (AD500) or later. Begley's research provides evidence for interaction with Mesoamerican groups beginning around AD250 to AD600. The habitation sites identified in northeast Honduras date to at least the Classic Period, and do not relate to the interred at Talgua Caves. Only the Cuyamel Caves and the Talgua Cave sites have known Formative Period components.

Ceramic analysis, including ceramic figurines and musical flutes, is increasing in popularity in northeast Honduran archaeology (Dennett, 2008a; 2008b; Dennett and Healy, 2008; 2012; Healy et al., 2010; Healy et al., 2011). These types of analyses are important for interpreting regional chronology, identity, and perhaps spirituality. Although, these types of analyses are important for understanding northeast Honduran prehistory, additional bioarchaeological research is needed. By incorporating skeletal analysis into archaeology we gain insight into diet, nutrition, health and disease, demography, activity patterns, and human movement (Knudson and Stojanowski, 2008). The only bioarchaeological investigations conducted in the region are from Talgua Caves by Nicholas Herrmann and Derek Benedix (Benedix et al., 1999; Herrmann, 2002). Their research is detailed in the Sites and Samples chapter of this thesis.

2.3   Human movement

Studies of human movement have once again become a valid field of study in archaeology after many years of criticism (Hakenbeck, 2008). Human movement is influenced by social and political factors, kin alliances, economic benefits, and even

religious or spiritual perceptions. Individuals move across the landscape for many reasons, some being economic or political growth, personal gain, forced relocation, or religious perspectives. Sacred places, such as caves, were valued in Pre-Columbian Central America, and traveled to during 'religious pilgrimages.' For instance, Naj Tunich, a large Guatemalan cave containing architecture, interments, tombs, artifacts, and over 500 glyphs, is a documented pilgrimage site in Mesoamerica (Brady and Stone, 1986). This is an example of short-term movement, where the individual returns to their associated residence. Human movement in northeastern Honduras may also have resulted in permanent relocation, also termed migration or a change in residential history. The term migration must meet the minimum definition of a "one way residential relocation to a 'different environment' by at least one individual" (Cabana and Clark, 2011:4). This definition provides some interpretation of the environment. Environment can refer to any physical or cultural differences in the landscape. For this research project, the phrase 'geographic origin' will be used to refer to human movement, since human enamel apatite captures the early life signature during childhood and adolescence and aids in the interpretation of early residential history.

Advances in genetics and isotope analysis have opened avenues for scientific inquiries surrounding trade, identity, kinship, shared technology, marriage, political complexity, status, demography, and affiliation. Exactly how much human movement was occurring in northeast Honduras during the Formative Period is currently unknown. Since a static population, or a population closed to human movement, is very uncommon (Milner et al., 2008); it would be safe to assume some movement did occur in the

Olancho Valley. Although, the movement involved may not have required long-distance permanent relocation.

Since genetic, biodistance, or comparative skeletal data are not available for northeast Honduras, cultural goods may provide insight to movement in the region. Material goods are transported by individuals, and with the individuals, knowledge, traditions, and possibly genetic material are passed along (Murrieta-Flores, 2010). Long distance and domesticate exchange provides tangible evidence for regional interactions. Although it has been suggested that long-distance exchange in northeast Honduras prior to AD500 was rare (Healy, 1992), jadeite was identified at Talgua Cave in Formative Period components. Jadeite was used throughout Central America as a prestigious high status marker for material goods, such as beads, earplugs, dental inlays, and other forms of ornamentation, which may be indicative of social stratification (McCafferty and McCafferty, 2009; 2011). The closest primary jadeite deposits are located along the Motagua fault zone in Guatemala (Harlow et al., 2011).

Evidence from the paleobotanical record, such as cashew, maize, and cotton, has demonstrated intercontinental trade networks by as early as the Formative Period. For instance, the central Honduran site Yarumela is known for its exotic goods, including early evidence of cashew wood (Lentz et al., 2005). Cashew wood is native to the Amazon Basin, demonstrating that the possible range of movement of individuals extended to South America during the Formative Period. Cacao beans (*Theobronm cacao L.*), which were used in ritual beverages in Mesoamerica, may have also been exchanged as early as the Formative Period (Healy, 1974). This highly valued good may have been a sought after trade item that individuals traveled far distances to obtain.

2.4   Pre-Columbian cave practices

The Maya word for cave, *ch'en* or *ch'een*, has a broader meaning than does the Westernized version and refers to spring, waterhole, sinkhole, crevice or rock shelter (Moyes and Brady, 2012). The broad meaning of *ch'en* is associated with the important emphasis that Pre-Columbian societies, including eastern Honduras, had for caves. The Central American Pre-Columbian worldview of caves was powerful and caves were thought of as the source of clouds, rain, thunder and lightning, linked to life, fertility, and rebirth (Moyes and Brady, 2012). For instance, to the Maya, caves were not inanimate objects, but "living manifestations of spiritual power" for life and death cycles (McNatt, 1996: 81). These 'living manifestations' were spirits or deities that resided in the mountains and caves. Other cultures in Mesoamerica also associated caves with life and death cycles, creation myths, and the origin of deities. For instance, the Mixtec of Oaxaca connected the dripping in caves with rain, and the Maya, Zapotec, and Aztec rain deities, Chac, Cocijo, and Tlaloc respectively, were thought to reside in caves (Moyes and Brady, 2012).

An examination of Pre-Columbian caves provides an excellent opportunity to study social structure, ritual activities, political organization, and life histories of past populations (Prufer and Dunham, 2009). Caves in Central America had many different functions, which make them powerful archaeological resources. Thompson (1975) stated the Yucatan caves functioned as: (1) sources of drinking water; (2) sources of 'virgin' water; (3) venues of religious rites; (4) places for burials, ossuaries, and cremations; (5) art galleries; (6) deposition of ceremonially discarded utensils; (7) places of refuge; and (8) other uses (including mining). For instance, obsidian blades or wooden *duho*

19

(benches), are sometimes found within caves, and provide evidence for sacrificial, autosacrificial bloodletting or ancestor veneration (Philmon, 2012). These 'ceremonial' artifacts support Thompson's (1975) criteria for the third function, the venues of religious rites. The remainder of this section will focus on the function of caves as places for burials, ossuaries, and cremations.

Traditionally, Pre-Columbian cave research focused on Classic and Post-Classic Period burial practices of the elite. But elite cave interments were less common, and the majority of the ossuaries in Central America were used by non-elite individuals that were grouped according to kinship (Fitzsimmons, 2012). Ethnographic evidence of lineage caves from the Maya region showed that veneration of a cave was related to particular land holdings of patrilineal kin groups (Dixon et al., 1998). The work of Guiteras-Holmes (1947) demonstrated that caves functioned as kin markers of territory among the Maya of Guatemala. The location of the cave represented the origin of a particular lineage, where individuals were returned in death to complete the cycle of life and death (Moyes and Brady, 2012).

2.4.1 Honduran mortuary practices

Mortuary practices are influenced by social factors, such as rank, ideology, economics, and worldviews (Carr, 1995). Mortuary practice (i.e. interment) is an act performed by the living, and most aspects of cave mortuary practices must be interpreted as reflecting the living (Parker Pearson, 1999). Caves containing non-elite individuals provide a glimpse into the lives of everyday Central American individuals and their social influences. However, mortuary practices in Honduras are not well understood (Healy, 1978).

Different mortuary practices appear to occur across Honduras dependent upon the time period and region. Most of the accounts come from the Bay Islands, where a majority of the archaeology fieldwork was conducted in the early 20th century. On the Bay Island of Utila, three extended burials that dated to the Cocal Period were located by Kidder II, Strmsvik, and Ekholm (Healy, 1984). Urn burials or human remains placed in ceramic vessels were also reported by workmen on the same island (Epstein, 1957). In 1923, eight human remains were recorded by Spinden in a shell midden on the Bay Islands (Healy, 1984). Unfortunately, the Urn burials and shell midden remains were not associated with any chronology for the region, limiting the assessment of the Bay Island accounts.

Residential burials, or burials near or beneath residential structures, were the common mortuary practice in Central America after the Late Formative Period (Webster, 1997). During this period, residential burials were common at Puerto Escondido, located in the lower Ulúa Valley on the southern fringe of Mesoamerica, but no Early or Middle Formative Period burials have been recovered (Joyce, 2011). Other than these patchy, second-hand accounts no information exists for Honduras outside of the Formative Period Ossuaries: Talgua Caves, Gordon's Cave #3, and Cuyamel Cave.

Gordon's Cave #3 (GC3) is an ossuary containing partially cremated remains and secondary bundle burials located three kilometers from Copán. The site was originally documented by George B. Gordon in 1896 during a Peabody Museum survey of the mountains surrounding the Copán valley. Gordon's Cave #3 consists of three chambers, with chamber three containing the highest concentration of human remains. From a sample of skeletal material from the cave, Rue et al. (1989) determined that juveniles

accounted for a large portion of the skeletal assemblage (22 adults and 46 juveniles). A later reassessment of the Gordon's Cave #3 determined that the cave was used from the Formative Period through the Late Classic Period, and that the "crude figurines," were associated with non-elite ancestor veneration (Brady, 1995: 35).

The only published evidence (Healy, 1974) of an ossuary cave in northeast Honduras that is contemporary with Río Talgua comes from Cuyamel Cave, which is located in northeast Honduras in the Department of Colón. The interred individuals were disarticulated, secondary burials with evidence of cremation (Healy, 1974). Unfortunately, no skeletal, mortuary, or bioarchaeological analyses have been conducted at Cuyamel Cave. Vessels found at Cuyamel Cave with Olmec inspired designs that resemble the black-wares from Tlapacoya, an Olmec site in the Gulf region, suggest an Early to Middle Formative Period date (Healy, 1974). Importantly, these black-wares provide evidence that northeast Honduras had contact with the Olmec cultural tradition, either through trade or imitation. Even more interesting, no associated residential habitation site was ever identified for Cuyamel Caves, which is also the circumstance for the Talgua and Arañas caves (Evans, 2004). Although more evidence is needed, based on Gordon's Cave #3, Cuyamel Cave, and the Talgua caves (discussed in Chapter V), secondary bundle burials interred in ossuary caves may have been the common mortuary practice in Formative Period Honduras (Moyes and Brady, 2012).

2.5   Dental metrics

Tooth size is population specific, and the study of it contributes to the understanding of human variation. This variation includes relationships within and between populations, and between biological sex (i.e. sexual dimorphism) (Kieser, 1990;

Joseph et al., 2013). Variation in tooth size is considerably influenced by genetic factors, but it is also responsive to selection and/or environmental mechanisms (Scott and Turner, 1997). Groups that have metric features in common tend to be more closely related than groups that do not share commonalities. The size of the group can range from large regional populations to ancestral lineages, making studies within and between populations possible (Jacobi, 2000). Current dental anthropology research shows that there are 2% to 6% differences between males and females and up to 7.3% variation in sexual dimorphism for some archaeological sample populations (Scott and Turner, 1997; Hillson, 2005). Canines are typically the most sexually dimorphic teeth, followed by mandibular molars. Human deciduous dentition is also dimorphic, with molars and canines having up to 7% variation between males and females (White et al., 2012), and can be used to sex subadults (Vodanović et al., 2007). Therefore when a reference sample is available and multivariate observations are possible, dental metric analysis is a reliable method for sex estimation.

Unfortunately, no dental metric data is available for northeast Honduras during the Formative Period. Although certain dental metric studies have been done in areas of Mesoamerica, the measurement data is quite different from the Talgua Caves assemblage (Rhoads, 2002; Wrobel, 2003; Scherer, 2007). For instance, based on Scherer's (2007) dental analysis of the Classic Period Maya, size of dentition (i.e. mesial-distal and buccal-lingual measurements) from the Talgua Caves is large in comparison to Classic Period Copán male and females.

2.5.1   Gender

Since the 1970's, biocultural bioarchaeology emphasized interactions between humans and their physical and cultural environments (Zuckerman and Armelagos, 2011). In essence, biology and culture both play essential roles in the human condition. A holistic perspective is typically applied to these studies, using cultural, biological, and archaeological concepts, to enhance the picture of past populations. Social identity is a common social construct examined using biocultural theory. Identities may reflect the group, which are multidimensional and dynamic, thus constructed and reaffirmed through social behaviors and practices deemed acceptable (Paul et al., 2013). Researchers address social, political, and economic ramifications of identities using gender. When bioarchaeologists study biological sex relative to cultural or social context, gender roles, gender behavior, and gender identity can be elucidated (Knudson and Stojanowski, 2008). For this research the ideology of gender is defined as a society's perspectives and ideas regarding the behaviors and actions of that particular social role (Cohodas, 2002:16).

Interpretations of gendered behaviors or ideologies in archaeology "tend to rely on binary reconstructions" applying Western ideologies of gender roles (Stockett, 2005:566). The Western division of sex as 'male' and 'female' does not accurately reflect northeast Honduran Pre-Columbian society. For instance, in parts of Mesoamerica, such as the Basin of Mexico at Tlatilco, and Western Honduras at Playa de los Muertos gender was more complex than the binary male/female division (Joyce, 2003). Figurines documented at Tlatilo and Playa de los Muertos have been considered direct evidence for diverse gender roles. For example, some figurines recovered from Tlatilco are depicted in

a loincloth, a costume identified with 'maleness', with exposed breasts, while other figurines lack gentiles altogether (Joyce, 2000). The lack of genitalia may represent a possible third gender or the combinations of costumes and exposed breasts may represent a gender spectrum.

Gender identity or gendered activities are unknown for the Formative Period in eastern Honduras (Hoopes, 2001). Ethnographic sources were not consulted due to the problematic biases encountered and the limited time to conduct this portion of the research. One important bias typically encountered in these ethnographic Spanish accounts is the fact that they are documented by Colonial men who may have had certain prejudices regarding sex and gender (Stephens, 2002). Although there is available information for gender in the Middle Formative Period of Western Honduras, as discussed above, this region was involved in different cultural practices, such as residential burial practices. Therefore, there is not enough information to know whether gender identities were fluid or bimodal for northeast Honduras during the Formative Period and was not factored into the dental metric analysis.

2.6   Summary

Northeast Honduras "remains one of the least studied and least understood regions in Lower Central America" (Dennett and McCafferty, 2012: 52). Traditionally, research conducted in the region focused on connecting the Lower Central America with Mesoamerica and South America, inhibiting a distinct cultural identity and local affiliation for northeast Honduras. Although some linguistic, biological, and cultural similarities are apparent between northeast Honduras and surrounding regions, distinctions remain. For this research project the theoretical approach used by Healy and

Begley was applied. This research will enter into the discussion of the linkages between northeast Honduras and Mesoamerica and South America. Exactly how much human movement was occurring in northeast Honduras during the Formative Period is currently unknown. The advances in isotope analysis have opened avenues for scientific inquiries surrounding human movement, and aid in understanding affiliation for northeast Honduras.

Although more evidence is needed, based on Gordon's Cave #3, Cuyamel Cave, and the Talgua caves (discussed in Chapter V), secondary bundle burials interred in ossuary caves may have been the common mortuary practice in Formative Period Honduras (Moyes and Brady, 2012). The location of these caves may represent the origin of a particular kin lineage, where individuals were returned in death. Isotope analysis may demonstrate that individuals were local to northeast Honduras, (i.e. no change in residential history occurred), which may indicate low human movement for the sample population. This would provide additional evidence that the Talgua Caves functioned as local lineage caves.

CHAPTER III

BIOGEOCHEMISTRY

3.1   The discovery of isotopes

An isotope is an atom or nuclide with the same number of protons and electrons

with different numbers of neutrons. Isotopes of an element have the same properties as

their counterpart, except for the size of their atomic masses. Isotopes can be either stable

or radiogenic, where stable isotope variation results from physiochemical processes and

radiogenic isotope compositions are from nuclear processes (White, 2013). The history of

radiogenic isotopes begins with the discovery of radioactive elements from the

experiments of Henri Becquerel (1896). Through chemical experiments by Becquerel and

the famous Curies, radioactivity and nuclear decay were identified. The changes in the

nucleus of the atom were not completely understood at this time because the existence of

the neutron was not identified until 1932. Natural physiochemical processes for stable

isotopes were determined later with the publication of "*The Thermodynamic Properties*

of Isotopic Substances" in 1947 (Faure and Mensing, 2005). Harold C. Urey is

considered a pioneer in the field of isotope chemistry for his experiments with hydrogen

(H) and the discovery of deuterium (^{2}H). His work was vital to stable isotope chemistry

and the introduction of temperature dependence fractionation with oxygen. This early

work paved the way for the use of stable and radiogenic isotope biogeochemistry in the

physical sciences and the later anthropology.

3.2   Radiogenic strontium isotopes

Strontium, derived from the Scottish town *Strontian*, is an alkaline earth element belonging to the group IIA (strontium, calcium, magnesium, barium, beryllium, and radium) (Attendorn and Bowen, 1997). Strontium (Sr) is a reactive metal with a relative atomic mass of 87.62 that resembles Calcium (Ca). Since the ionic radius of Sr is comparable in mass (1.13 Å) to Ca (0.99 Å), Sr^{2+} can replace Ca^{2+} in many materials, including apatite and calcium carbonates. One restriction of Sr^{2+} when replacing Ca^{2+} is that strontium ions only fit in eightfold coordinate sites, whereas calcium ions may occupy either the eightfold or sixfold sites in the crystal lattice. In mineralogy, Sr occurs as the mineral celestine ($SrSO_4$), or strontium sulfate, and strontianite ($SrCO_3$), a rare carbonate mineral (cite). Strontium has 23 total isotopes, where four isotopes, ^{88}Sr, ^{87}Sr, ^{86}Sr, and ^{85}Sr, are naturally occurring with the isotopic abundances of 82.53, 7.04, 9.87, and 0.56 percent, respectively. Of these isotopes, ^{87}Sr is both stable and radiogenic, whereas ^{88}Sr, ^{86}Sr, ^{85}Sr are all stable isotopes of strontium. Radiogenic strontium isotope measurements are expressed as $^{87}Sr/^{86}Sr$ and are reported to five decimal places.

Strontium isotopes were initially identified for the purposes of radioactivity and dating geologic materials from the radioactive decay of rubidium (Rb). Campbell and Wood (1906) first demonstrated the natural radioactive decay of Rb in the early twentieth century, but its use in geology was not popularized until mid-1950 with the invention of mass spectrometry (Faure and Mensing, 2005). The Sr-Rb dating method was derived based upon the law of radioactivity using ^{87}Rb and ^{87}Sr and detailed by Faure and Powell (1972).

Rubidium (comes from Latin *Rubidus*) belongs to the alkali metal group IA (lithium, rubidium, sodium, potassium, cesium, and francium), and is a soft, highly reactive white metal (Attendorn and Bowen, 1997). Rb does not form any minerals, but has a similar mass to potassium, which allows for substitution of K in rocks with K-bearing minerals (micas, K-feldspars, sylvite, carnallite, and certain clays). Rubidium has 27 isotopes, two that are naturally occurring isotopes (^{85}Rb and ^{87}Rb). The isotope ^{87}Rb decays into ^{87}Sr by electron emission of negative beta particle (Faure, 1977). The ratio of ^{87}Sr to the stable isotope ^{86}Sr increases with time as a function of the original bedrock Rb/Sr ratio (Bataille and Bowen, 2012). At nucleosynthesis, or the origin of chemical elements in the cosmos or on Earth, the ^{87}Sr/^{86}Sr value of the proto-Earth is assumed to have had a similar value to the primordial value 0.699 (Capo et al., 1998). It is not completely certain if the primordial Sr composition of the Earth was homogeneous or heterogonous upon formation, but the study of meteorites, more specifically basaltic achondrites, has given geologists the most accurate estimations because meteorites have crystallized silicates that resemble the terrestrial ground surface (Faure, 1986). Current differential Sr ratio values on Earth vary from the initial abundance of the isotope, the amount of time passed, and geologic processes (Pye, 2004).

Strontium has been demonstrated to be heterogeneous over time and continues to change with contributions from both the lithosphere and hydrosphere. The parent material of the bedrock (igneous, metamorphic, or sedimentary, such as carbonate rich bedrock) is a major contributor to the Sr ratio variation. For instance, most young volcanic rocks that are thought to have originated in the mantle have Sr ratios approximately 0.704 (±0.002), where old metamorphic rock have ^{87}Sr/^{86}Sr ratios near 0.715 (Faure, 1998). Age of

bedrock is a factor, but there are also variations within igneous rocks depending on the original environment. There are distinguishing differences in the continental crust versus the Earth's upper mantle, where the ratio is typically greater in the continental crust than the upper mantle. For instance, ocean tholeiites are lower (0.70280) compared to continental igneous rocks (0.70577) (Faure and Powell, 1972). Sedimentary rocks in a region tend to give an overall homogenous picture of the strontium ratio of the area, due to the weathering of sedimentary rocks and their interaction with the hydrosphere. Chemically weathered minerals are released into the water system of that particular region, which become homogenized during transport and mixing, then they re-enter the lithosphere via calcium carbonate (Faure, 1986). Strontium in water systems is associated with the bedrock type in the region, which may be elevated in particular regions especially where there are marine carbonate rocks, such as strontianite. Overall the parent material is more enriched than the sediment released during chemical weathering, and the minerals are more enriched than the water in the environmental system. Enrichment of the bedrock occurs in response to the Rb-bearing minerals, such as micas and feldspars, which are more resistant than Sr-bearing minerals, such as calcite and plagioclase. Therefore, chemical weathering of the parent material is more enriched, and the Sr ratios ($^{87}Sr/^{86}Sr$) will be depleted.

Variations in the underlying bedrock, due to time, type of parent material, and chemical weathering contribute to specific geographic strontium signatures. When parent material erodes it transfers the geologic Sr signature into soils, plants, and water systems that are then passed through the food chain. Humans consume plant and animal tissues from that particular region and their skeletons retain the geographic signature in the form

of a bioavailable Sr signature. The bioavailable signature is the average of all Sr in the sample from that region (Bentley, 2006). The theoretical principles of isotopes enable anthropologists to use these bioavailable signatures from skeletal samples to provenance individuals.

3.2.1   Complications of strontium

Strontium isotope analysis is a beneficial method used in anthropology. One reason, as discussed above, relates to the ionic bonds of heavy metals which make strontium isotopes less susceptible to fractionation. Despite such advantages, there are a number of complicating factors. Geologic processes, such as weathering and erosion, mixing, and anthropogenic activities all have the ability to cause variations in geologic strontium isotope ratios and thus the bioavailable human signature.

Alterations in the 'expected' range of Sr signatures are dependent on the parent material and the interaction of the bedrock with the environmental system. Sedimentary, igneous, and metamorphic rock all respond differently due to the mineralogy of the structure and the hydrological system of the environment. Water plays an important role in chemical sediment transport, deposition, and mixing of the sediment and corresponding Sr signatures in the water. Sedimentary rocks contain more Sr-bearing minerals that erode at a faster pace than igneous and metamorphic rocks that contain greater Rb-bearing minerals, which are more tolerant of chemical weathering (Faure, 1998). This produces an isotopic disequilibrium with the surrounding groundwater because of subsurface water flow and time (Faure and Mensing, 2005). Igneous and metamorphic strontium signatures are further complicated by the creation and destruction of rock formations during new magma flows, folding, and thermoactivity (Faure, 1986).

31

Human activity further complicates the bioavailable signatures of strontium isotopes. Certain foodstuff have been imported into regions for religious, economic, and sociopolitical reasons that retain the geologic signature of where the food was grown or harvested. This may generate homogenous ratios, not as extreme, but comparable to the globalization of the modern food market in the United States. In parts of Central America and North America lime was used to processes maize for consumption. For instance, lime processing raises the Ca and Sr concentrations, which bias the $^{87}Sr/^{86}Sr$ ratios towards the enrichment of lime (Burton and Wright, 1995). Sea salt was another imported good exploited by the Maya, which has been inferred as the reason for enriched $^{87}Sr/^{86}Sr$ signatures at Tikal (Wright, 2005). This explanation is based from the known ratio of seawater (0.7092) and the elevated human signatures compared to the geologic signatures. Imported goods and processing minerals have been demonstrated to enrich the biologically available signature and complicate human Sr ratios.

3.3   Stable oxygen isotopes

Oxygen (O) is the most abundant chemical element in the mantle and is involved in almost all geochemical and biochemical processes on Earth (Faure and Mensing, 2005). Oxygen is a highly reactive nonmetal element with three stable isotopes: ^{16}O, ^{17}O, and ^{18}O. A stable isotope is a nuclide that does not decay over time and whose relative abundances fractionate in nature. Principle characteristics of stable isotopes are a generally low atomic mass, relative mass difference between their isotopes are large, a high degree of covalent bond formation, the abundance of the rare isotope is sufficiently high, and in the case of O, form a wide variety of compounds (White, 2013). The natural abundances of ^{16}O, ^{17}O, and ^{18}O are 99.76, 0.035, and 0.2 respectively, making the

32

measurements of ^{18}O and ^{16}O more accurate indicators. Since O isotopes fractionate (discussed in detail below), the ratio of ^{18}O to ^{16}O is expressed using the delta notation (δ). The final notation for $^{18}O/^{16}O$ is δ^{18}O, which is an important stable isotope ratio used in many scientific fields, is defined by equation (3.1):

$$\delta^{18}O = \left[\frac{\left(^{18}_8O\big|^{16}_8O\right)\,spl - \left(^{18}_8O\big|^{16}_8O\right)\,std}{\left(^{18}_8O\big|^{16}_8O\right)std} \right] x\ 10^3\ ‰ \qquad (3.1)$$

spl is the measured value of the sample, std is the measured value of the standard, and ‰ is expressed in terms of *permil* deviations or parts per thousand. Standards are measured in order to reduce systematic errors when measuring samples on different mass spectrometers (Hoefs, 2009). Two standards are commonly measured, VSMOW (standard mean ocean water) and VPDB (Pee Dee Belemnite), where VSNOW is used for phosphates and VPDB is used for carbonates.

3.3.1   Oxygen fractionation

Oxygen is one of the most abundant elements on Earth associated with the biosphere, lithosphere, and the hydrosphere (Faure, 1977). The isotopic composition of oxygen is highly susceptible to fractionation. Light isotopes, or elements with low atomic masses, are variable in terms of fractionation because of their low atomic masses and covalent bonds. Isotope fractionation occurs when the relative abundance of isotopes of a specific element differs in mass relative to the mass of that element and results in differences in the physiochemical properties from kinetic or equilibrium effects (Hoefs, 2009). The effects of fractionation can be understood through quantum mechanics, which focus on the molecular forces and behaviors of molecules. Equilibrium fractionations

arise from the energy of a molecule in gases, liquids, atoms in crystals based on electron interactions, plus translational, rotational and vibrational motions (White, 2013). The energy of molecules, and thus fractionation effects, is dependent on mass differences and zero point energy. Zero-point energy is the finite value of a molecule at absolute zero (Faure, 1986). The energy of the molecule decreases with decreasing temperature. Therefore, light isotopes in a molecule have higher zero point values and higher vibrational frequencies that break weaker bonds within molecules (Brand and Copeland, 2012). These types of molecules are more reactive, and fractionate easily. Kinetic fractionation is associated with processes like evaporation, diffusion, dissociation and biologically facilitated reactions (White, 2013). When reactions do not achieve equilibrium the lighter isotope is typically preferred in the reaction products. Fractionation can be used on two different levels when analyzing isotopes, at the level of the chemical reaction or for environmental processes, such as evaporation, that result in enrichment or depletion of the isotopic composition (Attendorn and Bowen, 1997). The later use is beneficial for examining the hydrologic cycle and understanding the isotopic variation in nature for geolocation studies.

3.3.2   Oxygen isotope variation

Oxygen's ability to combine with hydrogen to form water (H_2O) is essential for human $\delta^{18}O$ provenance studies. Variations in the hydrologic cycle result in distinct regional $\delta^{18}O$ values due to seawater, precipitation, surface water, and climatic variations (Mook, 2006). Environmental systems vary in terms of elevation, rainfall, and aridity, which generate distinct meteoric $\delta^{18}O_{(water)}$ signatures. This distinction occurs because of temperature and humidity, explained by the Rayleigh distillation, wherein light isotopes

evaporate faster than the heavy isotopes (Hoefs, 2009). The regional $\delta^{18}O_{(water)}$ variations are in turn observed in the $\delta^{18}O$ hydroxyapatite of organisms, which may be derived from multiple drinking water sources (Luz et al., 1984). This bioavailable $\delta^{18}O$ signature reflects the $\delta^{18}O$ of body water when local water sources are ingested (Martin et al., 2008). There are three potential $\delta^{18}O$ sources for body water and include dietary inputs, drinking water, and atmospheric inhalation (Ehleringer et al., 2008). For instance, atmospheric diatomic molecules (O_2) contribute >20% of the oxygen atoms in body water (Podlesak et al., 2009). Therefore, the human body water signature is enriched compared to the $\delta^{18}O$ value of the source water due to the source inputs and biological processes, such as the circulatory system (Ehleringer et al., 2010).

White and colleagues (1998) suggest that $\delta^{18}O$ signatures in archaeological populations are highly reflective of a region's hydrology, varying only ±1‰. This variation is attributed to the reservoir effect, or the evaporation of lighter isotopes that enrich $\delta^{18}O$ signatures, and may occur in water catchments or storage vessels (Knudson et al., 2009; Bowen, 2010). The $\delta^{18}O$ of enamel apatite is a useful measure of human mobility and early residential history of individuals in archaeological populations. Stable oxygen isotopes are complementary to $^{87}Sr/^{86}Sr$, and can be used to corroborate or reject evidence for past residential histories. Whereas human $^{87}Sr/^{86}Sr$ signatures reflect the bedrock $^{87}Sr/^{86}Sr$ signature, human $\delta^{18}O$ signatures reflect the hydrology (water sources) $\delta^{18}O$ signature of the region. Isotopic measurements of both $^{87}Sr/^{86}Sr$ and $\delta^{18}O$ from the same sample are therefore a more effective approach for interpreting and cross-checking isotope results.

3.4   Stable carbon isotopes

Carbon (C), derived from the Latin word *carbo*, is the fourth most abundant element in the solar system (Faure and Mensing, 2005). Carbon, having nonmetallic and tetravalent characteristics, is a member of group 14 on the periodic table. Carbon forms covalent bonds due to the four electrons occupying the outer orbit, and has three naturally occurring isotopes. Two of the three isotopes are stable, ^{12}C and ^{13}C with natural abundances of 98.90% and 1.10%, respectively. One isotope is radioactive, ^{14}C, which is commonly used for dating carbon compounds in archaeology. The final notation for ^{13}C/^{12}C is expressed as δ^{13}C, and is defined in equation (3.2):

$$\delta^{13}C = \left[\frac{\left(^{13}_{6}C \big| ^{12}_{6}C\right) spl - \left(^{13}_{6}C \big| ^{12}_{6}C\right) std}{\left(^{13}_{6}C \big| ^{12}_{6}C\right) std} \right] x\ 10^3 ‰ \qquad (3.2)$$

spl is the measured value of the sample, std is the measured value of the standard, and ‰ is expressed in terms of *permil* deviations or parts per thousand. The VPDB (Pee Dee Belemnite) standard is used to measure δ^{13}C ratios, which is typically more negative for bone and teeth carbonate when compared to the PDB limestone fossil standard (Craig, 1957).

3.4.1   Carbon isotope variation

The principles of fractionation, as discussed above, also apply to stable carbon isotopes. An additional fractionation process observed in the carbon system occurs primarily in terms of photosynthesis reactions in green plants:

$$6CO2 + 6H2O \rightarrow C6H12O6 + 6O2 \qquad (3.3)$$

36
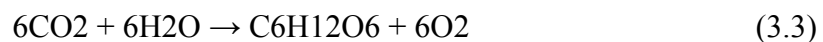
Photosynthesis reactions enable $\delta^{13}C$ bioavailable signatures to be used in paleodietary analysis to determine whether the consumer subsisted on C_3, C_4, CAM, or mixed amounts of terrestrial plants. C_3 plants are found in temperate geographic regions and typically include wheat, rice, root crops, legumes, tree crops (fruits and nuts), and vegetables. Common economically used C_4 plants include maize, sugarcane, millet, and sorghum, which grow in tropical environments. C_4 plants have an evolutionary advantage over C_3 plants due to their Kranz anatomy (Cerling, 1999). Kranz anatomy is a combination of mesophyll and bundle-sheath cells that allow C_4 plants to tolerate certain stressors, such as high temperature and low CO_2, which can be harmful to C_3 plants (Brugnoli et al., 1998). This evolutionary feature minimizes the amount of time the leaf pores are open, to limit water loss of plants inhabiting tropic or arid environments, which metabolically restricts the amount of the heavy C isotope (^{13}C) incorporated by C_4 plants. Thus, the ratio of ^{13}C to ^{12}C ($\delta^{13}C$) in C_3 plants is greater than C_4 plant $\delta^{13}C$ signatures. For instance, the $\delta^{13}C$ of C_3 plants range from -23‰ to -34‰ and the $\delta^{13}C$ values of C_4 plants range from -6‰ to -23‰ (Faure and Mensing, 2005). CAM plants, or plants that use the Crassulacean acid metabolism, can fix CO_2 in either daylight or darkness, resulting in $\delta^{13}C$ values that overlap the C_3 and C_4 signatures, ranging from -11‰ to -33‰ (Norr, 1991; Faure and Mensing, 2005). Some common CAM plants include pineapples, nopal cactus, maguey, vanilla, and aloe (Bender, 1968). Climatic factors, as seen with oxygen isotopes, also affect the stable carbon isotopic distribution. For instance, $\delta^{13}C$ values in C_3 plants may vary depending on temperature and rainfall fluctuations, which may alter the $\delta^{13}C$ signature (Tieszen, 1991).

Stable carbon isotope ratios are preserved in human tissues, such as bone collagen and tooth apatite, and are used in paleodiet reconstructions. This concept is based on the principle that "you are what you eat" or that the bioavailable signature of an animal reflects the isotopic composition of their diet (DeNiro and Epstein, 1978). Although this is generally the case, factors such as metabolic processes, respiration and transport, prohibit equilibrium between the organism and its diet. For instance, bone apatite is enriched up to 12‰ when compared to the diet carbon sources (van der Merwe et al., 2000). The $\delta^{13}C$ of bone and tooth apatite is a proxy for carbon in the whole diet, which includes carbohydrates, proteins and fats (Turner, 2008). Traditionally, the $\delta^{13}C$ of bone collagen is thought to represent the protein portion of the diet, but research by Kellner and Schoeninger (2007) demonstrated that the difference between $\delta^{13}C_{apitite}$ and $\delta^{13}C_{collagen}$ is not an absolute measure of diet constituents. Since, the value of $\delta^{13}C_{apitie}$ is not specific to any particular combination of protein or whole diet, the predictive power for diet reconstruction is limited (Kellner and Schoeninger, 2007). The $\delta^{13}C_{apitite}$ can be an accurate measure of whole diet carbon, if the difference between $\delta^{13}C_{apitite}$ and $\delta^{13}C_{collagen}$ is known for all the diet sources (Schwarcz, 2000). Therefore, $\delta^{13}C$ for this research project will be used as a qualitative marker for individual differences in diet, not for a quantitative biomass paleodiet reconstruction.

3.5   Human tissue biochemistry

The biomineralization process is an important concept for understanding chemical crystalline structures, such as apatite, in biogeochemistry. This is the process by which living organisms produce minerals to harden or model tissues, such as bone (Skinner and Jahren, 2005). Biomineralization is presented here to explain how $\delta^{18}O$, $\delta^{13}C$, and

$^{87}Sr/^{86}Sr$ are obtained from archaeological human tissues, specifically enamel. Types of human tissues that are used for isotope analysis in anthropology include bone, hair, fingernails and toenails, and teeth. There are different advantages to analyzing each type of tissue as well as multiple tissues depending on the research question being asked. Bone, fingernails, toenails, or hair may be used (if available) for research related to late life history. For instance, bone remodels over time, revealing the isotopic signature incorporated late in life, approximately over the last 10 years (Katzenberg, 2008). In contrast, enamel captures the early life signature during childhood and adolescence as no remodeling of dental tissue occurs (Wright and Schwarcz, 1998). Furthermore, an advantage of using enamel over tooth dentine or bone is the composition of enamel, and its resistance to diagenetic alterations from soil and other surrounding materials.

Bone, tooth dentin, and enamel are all composed of minerals, proteins, and lipids (Ambrose, 1993). Enamel is a non-porous, highly crystalline hexagonal structure mainly composed of inorganic material. Mature enamel is a cell free tissue with no vascular supply containing less than 2% organic material (Ortner, 2003; Skinner and Jahren, 2005). These features lock in the isotopic signature, since no new enamel is produced after formation. Hydroxylapatite ($Ca_{10}[PO_4]_6[OH]_2$) is the mineral component of these tissues, where carbonate-hydroxyapatites [$Ca_9((PO_4)_{4.5}(CO_3)_{1.5})OH_{1.5}$] are used for $\delta^{18}O$ and $\delta^{13}C$ analyses (Koch et al., 1997). Phosphate (PO_4) or carbonate (CO_3) are extracted from the carbonate-hydroxyapatite to obtain $\delta^{18}O_P$ (phosphate) and $\delta^{18}O_c$ (carbonate) /$\delta^{13}C$, respectively. The $\delta^{18}O_P$ measurement is preferred in archaeology, since it is less susceptible to diagenetic changes due to the stronger P-O bonds (Martin et al., 2008). Carbonate extracted can generate $\delta^{18}O_c$ (carbonate) and $\delta^{13}C$ congruently. The $\delta^{18}O_c$

39

values tend to be more enriched due to the O and C4+ bound (White, 2013). Radiogenic strontium can also be analyzed from tooth enamel due to the fact that Sr ions replace Ca ions during mineralization (need several more sentences to detail process). All bioavaible isotope signatures from enamel apatite aid in the interpretation of early residential history and diet.

3.6   Biogeochemistry in Anthropology

Biogeochemistry combines the study of chemical, geological, and biological processes within the environment by analyzing chemical elements and their isotopes to measure and interpret biological and environmental systems (Schlesinger, 2005). The interpretation of isotope compositions is a powerful tool commonly used in the Earth Sciences, and later adopted in anthropology (Attendorn and Bowen, 1997). Isotopes were first used by archaeologists in the 1960's to provenance metal artifacts, such as lead, and paleoenvironmental reconstructions through analyzing peat cores, lake sediments, and tree rings (Pollard, 1998). In bioarchaeology, biogeochemical methods provide broad applications to test questions for individuals or skeletal lineages. The light stable isotopes of $\delta^{13}C$ and $\delta^{15}N$ were the first isotopes used to study archaeological populations for investigating paleodiet (Katzenberg, 2008). For instance, the early publications of Vogel and van der Merwe (1977) and van der Merwe and Vogel (1978) demonstrated the spread of maize into the North American lower Illinois Valley by the Late Woodland Period (c. 1000AD) through the use of $\delta^{13}C$ isotopes. Since the 1980's, the use of light stable isotope analysis expanded to include $\delta^{18}O$ with the help of the geochemist, Longinelli. He found positive correlations between blood and bone phosphate with $\delta^{18}O$ local meteoric water (Longinelli, 1984; Longinelli, 1995). This early research, along with the use of

^{87}Sr/^{86}Sr ratios, has facilitated mobility reconstructions in archaeology. Although, the measurement of Sr/Ca was initially used for paleodiet reconstruction (Schoeninger, 1979; Bisel, 1980; Sillen, 1981), this purpose was later debated due to the metabolic function of Sr in the system (Burton, 2008; Darrah, 2009).

In recent years, Mesoamerican sites from Teotihuacan to Copán have received a great deal of attention in the application of isotope analysis. Biogeochemistry has been used for ethnic identity (White et al., 2004a), status (Somerville et al., 2013), diet (Ambrose and Norr, 1992; van der Merwe et al. 2002; Wright et al., 2010), gender (White, 2005), weaning (Wright and Schwarcz, 1998; Wright and Schwarcz, 1999; Williams et al., 2005), and residential history (White et al., 1998; Price et al., 2000; White et al., 2000; Hodell et al., 2004; Wright, 2005; White et al., 2007; Price et al., 2008; Price et al., 2010; Wright et al., 2010; Wright, 2012). Isotope analysis, such as δ^{13}C, has also been applied to examine crop residue in the humic component of soil organic matter, in Belize, to determine if the soil was used for maize agriculture (Webb et al., 2004).

Only a single isotope study was found during the literature review for the Intermediate Area of Central America, which reconstructed pre-Columbian subsistence for areas in Panama and Costa Rica. For her dissertation project, Norr (1991) measured δ^{13}C and δ^{15}N for 500 individuals recovered from over twenty archaeological sites in the region. Her results demonstrated that a peak in maize consumption was seen during 200BC to AD 500 in Central Panama and maize subsistence gradually increased after 500BC for northwest Costa Rica. No biogeochemistry studies testing residential histories for archaeological individuals of Lower Central America are currently known. Isotope

data and interpretation from Río Talgua will be an excellent addition for understanding

residential history and mortuary practices in this understudied region.

3.7   Isoscapes

Isoscapes (termed in 2005) are predictive models that are used to interpret isotope

patterns across time and space (Bowen, 2010). Also called "isotopic landscapes,"

isoscapes are maps created to visualize large-scale geographic distributions of isotopes in

environmental systems (Bowen and West, 2008). In past isotope archaeological research,

when faunal remains were unavailable or modern samples from the region unobtainable,

geologic maps were used for comparison (Price et al., 2002; Bentley, 2006). This

approach is useful for assigning archaeological $^{87}Sr/^{86}Sr$ ratios to region-of-origin, but

sometimes these $^{87}Sr/^{86}Sr$ maps are incomplete where bedrock or soil samples were not

collected. Isoscapes are a useful resource for interpolating continuous isotope values or

fill in the gaps where incomplete isotope records exist. Baseline isoscapes are generated

from the collection of stable or radiogenic isotope data, and are modeled for large-scale

regions using geo-statistical programs. Geostatistics provide ways to relate and compare

spatial data, through spatial autocorrelation, where isotope values are predicted for

unknown locations (Cressie, 2015).

Isoscapes were first used by geologists interested in the anthropogenic effects of

pollutants, and ecologists monitoring the migrations of organisms. In the mid-twentieth

century, the International Atomic Energy Agency (IAEA), in cooperation with the World

Meteorological Organization, launched a global survey to measure the isotopic

composition of precipitation to monitor climate change. This project was known as the

Global Network of Isotopes Project (GNIP), which later inspired the collection of large

climate and hydrology datasets of groundwater isotopes throughout the globe. These early

isotope maps pioneered the way for isoscapes used in many scientific disciplines today,

including anthropology.

In archaeology there is a movement away from the use of the faunal baseline

towards the isoscape (Makarewicz and Sealy, 2015). Isotope baselines based on faunal

signatures are not always reliable indicators for human archaeological samples. Many

baselines are created from a minimum number of faunal samples, and are used to

interpret isotope values of large regions or local foodwebs (Makarewicz and Sealy,

2015). This approach is limiting, and may not reflect the complexities of the

biogeochemical environment. While faunal baselines may help interpret non-locals in the

sample population, they lack the assignment power to detect small-scale human

movement, which is historically more common than long-distance permanent relocation

or migration (Murrieta-Flores, 2010).

Isoscape models can replicate many environmental systems, including precipitation

and bedrock weathering. For instance, precipitation generally follows the basic principle that

the further away from the equator, the more depleted (or more negative) $\delta^{18}O$ values become

(continental effect). Additionally, with increasing altitude $\delta^{18}O$ becomes depleted, during the

winter $\delta^{18}O$ values are depleted (seasonal effect), and heavy rain depletes $\delta^{18}O$ (amount

effect) (Mook, 2006). For human tissue isotope values, the water or bedrock isoscape models

must be calibrated for comparison. There are a number of ways to calibrate an isoscape,

which range in complexity. One possibility is to convert the human $\delta^{18}O$ values into drinking

water $\delta^{18}O$ values using already developed equations. The calibration techniques used in this

research project are detailed in the Methods and Procedures Chapter of this document.

3.8   Summary

Early research in the fields of chemistry, physics, geology, and biology paved the way for the use of biogeochemistry in anthropology. Biogeochemistry combines the study of chemical, geological, and biological processes within the environment by analyzing chemical elements and their isotopes to measure and interpret biological and environmental systems (Schlesinger, 2005). An understanding of biogeochemistry and its principles are relevant to this thesis project to interpret residential history, specifically geographic origin, and the mortuary arrangement of the individuals in the Talgua and Arañas ossuaries using their isotopic values. The radiogenic strontium ($^{87}Sr/^{86}Sr$) and stable oxygen ($\delta^{18}O$) isotopic values measured from the Río Talgua dentition will be used to test the geographic origin of the interred individuals by incorporating isoscapes into the assignment models. There are several incentives for using isoscapes as baseline faunal replacements. Isoscapes provide cost-effective comparisons, no destructive analyses are needed, and bioavailable faunal signatures may incorrectly represent the geographical $^{87}Sr/^{86}Sr$ and $\delta^{18}O$ signatures (Bentley, 2006). Isoscapes also provide finer scale resolution for assignment models and spatially link isotope measurements on the landscape (Makarewicz and Sealy, 2015). The spatial distribution of $\delta^{13}C$, $\delta^{18}O$, and $^{87}Sr/^{86}Sr$ isotopes within the Río Talgua Cave will also be used to examine mortuary arrangement patterns. Since limited biogeochemistry studies have been conducted in Lower Central America, this research aids in the understanding of early Honduran prehistory, and create foundational baseline data for the region.

CHAPTER IV

SITES AND SAMPLES

4.1   The Río Talgua drainage

The Río Talgua drainage was virtually unexplored by archaeologists until the

mid-1990s with the discovery of Cueva del Río Talgua (Talgua). The crystalline calcite

deposits in Talgua made the skulls appear to "sparkle", giving rise to the name, the *Cave*

of the Glowing Skulls (Brady et al., 1995a). This anomaly led to a large amount of

publicity, including a headline feature in *Archaeology*, which increased looting activities

in the area Brady et al., 1995b). The Talgua Archaeological Project (TAP) was initiated

the following summer under the direction of James Brady with the cooperation of the

Instituto Hondureño de Antropología e Historia (IHAH) to systematically document

Talgua, and survey the drainage for an affiliated Formative Period habitation site.

During the following two field seasons (1995 and 1996), three additional caves

were documented and two were re-evaluated: Cueva de las Arañas, Cueva de Piedra

Blanca, Cueva Grande, Cueva Boquerón, and Cueva Jamasquire. Cueva Boquerón and

Jamasquire were previously recorded by Doris Stone (1957), and contained artifacts

associated with ritual activities, but no ossuary deposits. Cueva Grande featured a large,

heavily looted chamber with fragments of jade and shell. Researchers speculated that

pilgrimages were once made to Grande (Dixon et al., 1998). The ossuary caves, Cueva de

Piedra Blanca and Cueva de las Arañas, both contained deposits of poorly preserved

commingled human remains (Brady et al., 2000). TAP research efforts focused on Arañas, due to location and size, during the 1996 field season.

A total of 39 additional archaeological sites were identified on terraces above the floodplain during the TAP (Dixon et al., 1998). The Talgua Village site (OL-33) located approximately one Km downstream from the Talgua and Arañas caves, was investigated using a combination of shovel tests, trenching, excavation units, and resistivity. Site OL-33 consists of at least 80 visible mounds arranged around several plazas, the largest of the mounds reaching 2.5 meters in height (Dixon et al., 1998). The ceramics recovered at the Talgua Village Site include 'Chalky' group Polychromes, and Ulúa Polychromes that date to the Late Classic Period (Brady et al., 2000). Two radiocarbon dates retrieved from fire hearths identified the occupation of the site from AD625 to AD1160 (Hasemann, 1995). Although Site OL-33 is the largest nucleated settlement along the Talgua River, the radiocarbon dates and the relative ceramic dates do not correspond to the interred Formative Period Talgua cave population. The lack of a Formative Period occupation may relate to the limited investigations at OL-33. Eight excavation units, two trenches, and 111 shovel tests (40 cmbs) were tested based on prior geophysical data (Luke et al., 1997). The possibility remains that the individuals interred at Talgua and Arañas occupied another habitation site in the area.

4.2   Environmental Setting

Central America is the ideal region for distinguishing geologic $^{87}Sr/^{86}Sr$ signatures, due to its remarkable geomorphic diversity. There are few other regions on the globe that exhibit comparable diversity (Marshall, 2007). Honduras is comprised of this same geomorphic diversity, with various environmental ranges and heterogeneous

geologic formations that are ideal for distinguishing human bioavailable $^{87}Sr/^{86}Sr$

signatures. The continental basement formation of Honduras is located on the Chortis

Block, which is overlain by Mesozoic schists, gneisses, plutonic rocks, followed by

marine carbonates, and fluvial deposits (Harp et al., 1981; Viland and Henry, 1996).

Specific geologic isotope dates and lithology of the region are still understudied (Rogers

et al., 2007), but the physiographic provinces of Central America have been defined

(Marshall, 2007). Honduras is located mostly in the Chortis Highlands Province, with a

small northern section of the country located in the Mosquito Coast Lowlands Province.

The Chortis Highland Province consists of a broad, dissected, highland plateau that

extends across Honduras, where the elevation reaches over one km that extends up to 400

km near the active volcanic front (Marshall, 2007).

The Olancho Department of Honduras, and thus the Talgua Caves, is situated in

the Eastern Dissected Plateau and the Central Chortis Plateau geomorphic sub-regions

(Figure 4.1). The Central Chortis Plateau is the main sub-region of the Chortis Highlands,

consisting of Paleozoic metamorphic basement rocks and an overlying sequence of

folded Cretaceous sediment with elevations reaching 700-1000 m, where the major rivers

cut deep canyons into the bedrock (Marshall, 2007). The Eastern dissected highlands

encompass a rugged mountain landscape dissected by drainage network, traversed by the

Patuca, Coco, and Matagalpa rivers. The large rivers create intense erosion and

weathering in the Eastern Dissected Highlands, causing lower-elevation terrain around

500 m, with steep ridges and valleys (Marshall, 2007). The lithology of the Upper Talgua

Drainage consists of limestone, marl, dolomite, and calcareous shale bedrock from the

Cretaceous Period Yojoa Group, overlain by shallow dark brown Rendzina (SU) clay

47

(Dixon et al., 1998). The lower Olancho Valley consists of Quarternary-period continental and marine sediments.

The Talgua Caves are situated in the Patuca watershed, above the northeast bank of the Talgua River, seven Km from the modern town of Catacamas in the Olancho Valley of northeast Honduras. Río Talgua's headwaters start in the cloud forests of the Sierra de Agalta (2,174 m) and they drain into the Río Guayape and flow directly into the Olancho Valley, which eventually flows into the Caribbean from the Río Patuca system (Dixon et al., 1998). This area is located in the Eastern Dissected Highlands (discussed above), in close proximity to the Caribbean lowlands of the Mosquito Coast, where there is a sharp climatic gradient towards the coast. This location receives significantly greater rainfall, twice the precipitation than the Eastern Chortis Highlands, for instance (Marshall, 2007). The rainy season in the Mosquito region tends to last eight months out of the year, which demonstrates the gradient in higher precipitation towards the Caribbean coastal region (Harborne et al., 2001). This variation in precipitation will make this region ideal for distinguishing δ^{18}O signatures, since δ^{18}O values are enriched towards the coast and depleted with increased latitude.

Figure 4.1   Physiographic Regions of Honduras

4.2.1 Cueva del Río Talgua

Cueva del Río Talgua was originally mapped in 1986 by a team of speleologists under the direction of Larry Cohen, and investigated during the Talgua Archaeological Project (Brady, 1994). Talgua is one of the few ossuary caves with evidence of multiple-episode interments identified along the Río Talgua drainage in northeast Honduras. Human remains were documented in niches along passages of the cave and on the floor within flowstone pools (Herrmann, 2002). These burials appeared bundled and ranged from a single individual to multiple individuals occupying a single niche (Brady, 1994). Although the complete mortuary program of northeast Honduras is not well understood, these remains most likely were disarticulated or allowed to decompose outside of the cave, coated with red ochre/hematite, then bundled and placed in the cave (Brady et al., 2000). The red pigment was copiously applied to the remains, which even stained the cave wall. During the TAC investigations, Talgua was subdivided by the three levels of the ossuary into Operation I, II, and III, and each burial niche was designated a lot number (Brady, 1994). Temporal assignment of Talgua was based on pottery sequencing and five calibrated radiocarbon dates (Table 4.1). These dates suggest the use of Talgua was extensive throughout the Formative Period, but also utilized up until the Classic Period.

Table 4.1   Radiocarbon Dates for Talgua Caves

Site	Provenience	Context	Sample ID	Radiocarbon Date	OxCal 4.2 Date	Component
Talgua	Second passage	Human bone	WG285	3110±85 B.P.	1125-1605 BC	Early Formative
Talgua	III-2	N/A	Beta-77105	2830±60 B.P.	837-1192 BC	Middle Formative
Arañas	Passage to ossuary	Charcoal	Beta-95367	2790±100 B.P.	796-1221 BC	Middle Formative
Talgua	III-3	N/A	Beta-77106	2620±80 B.P.	510-975 BC	Middle Formative
Talgua	III-4	Charcoal	Beta-85276	2510±60 B.P.	430-799 BC	Middle Formative
Talgua	N/A	Human bone	WG286	1385±75 B.P.	AD 432-852	Classic

(Brady et al., 2000)

Due to the poor preservation of human remains at Talgua, the majority of the skeletal analysis was conducted *in situ* (Herrmann, 2002). A tributary of the Río Talgua runs through the cave that causes fluctuations in water levels that resulted in the deposition of calcite, a common polymorph of calcium carbonate ($CaCO_3$), on the skeletal elements, which encased and embedded them to the cave floor (Brady, 1994). Taphonomic damage to the skeletal material, due to exposure above the water line and looting activities, reduced some skeletal elements to bone meal (Brady et al., 2000). A total of 1707 skeletal elements, along with 446 teeth were assessed in Talgua. From the combined skeletal and dental inventory, and GIS queries, the minimum number of individuals (MNI) for Talgua was estimated at 73 individuals, 15 being subadults under the age of 15 at death (Herrmann, 2002).

The findings from the preliminary survey in 1994 suggested the individuals interred in Talgua belonged to an egalitarian society, where grave goods were associated with multiple human remains (Brady, 1994). Talgua was extensively vandalized between field seasons of TAP, and some of the skulls were chipped from the calcite matrix and removed by the looters. A skull from III-4 was removed by looters exposing a ceramic vessel above the bundle of long bones. The ceramic vessel had a modeled face, and a radiocarbon date from the charcoal inside provided a date for the other vessels with similar style to the Middle Formative Period (Brady et al., 2000). This discovery may support the argument that grave goods were associated with particular individuals rather than multiple individuals in the lot, and may suggest a degree of social stratification, or differences in wealth.

4.2.2   Cueva de las Arañas

Cueva de las Arañas, a small cave only about 85-m deep, is located only a few hundred yards from the entrance of Cueva del Río Talgua. Arañas was documented in 1996 during the second field season of the TAP. There are several isolated deposits of human remains in Arañas that are consistent with a secondary bundle burial practice (Brady et al., 2000). Provenience of the remains was subdivided into three operations (II, III, and IV), and 16 lots, with the largest lot located at the rear of the cave. Talgua and Arañas are most likely contemporaneous of a single population due to their temporal and mortuary practice similarities (Herrmann, 2002). The passage to the ossuary chamber was radiocarbon dated to 1211 BC to 796 BC (Beta-95367, calibrated one sigma) (Brady et al., 2000).

The human remains were cemented in calcite requiring the bioarchaeological

assessment to be conducted *in situ*, which eliminated certain analyses, such as the

documentation of skeletal pathologies (Herrmann, 2002). From the 615 skeletal elements,

118 teeth, and GIS queries, the MNI for Arañas was estimated at 22 individuals, three of

which were subadults (Benedix et al., 1999). The dental analysis of *in situ* and loose teeth

(n=718) from Talgua and Arañas demonstrated that 16% of the sample had at least one

carious lesion (n=89), and 19 teeth had multiple carious lesions (Benedix et al., 1999). A

total of 17% of the sample exhibited hypoplastic defects (n=98), consisting primarily of

linear enamel hypoplasia (Benedix et al., 1999).

A high density of artifacts associated with ritual activity was observed in the

vestibule of Arañas, along with a single modified left lateral mandibular incisor. The

intentionally modified tooth exhibited filing of the incisal, mesial, and distal margins,

consistent with Romero's (1958) C-6 category (Herrmann et al., 1999). A large range of

artifacts, possibly associated with ritual activity, were documented in the vestibule,

including ceramics, a small burnt corn cob, and snail shells. For instance, *Pachychilus*

sp., termed *jute* or *tutu* in Maya, are snail shells associated with Maya ritual meals (Healy

et al., 1990), and were documented in large quantities in the cave entrance. Remnants of

red and black cave paintings are also present in the entrance chamber, and in the passage

to the ossuary a ladder-like painting remains (Brady et al., 2000). Just inside the vestibule

three well-preserved images remain, two depict non-human faces and another is a ladder

like geometric design (Brady et al., 2000). In the burial chamber, only a few shell beads

and a fragment of a marble vessel were observed in association with the interments

(Brady et al., 20000). The ritual activities in the vestibule appear to date to the Late

Classic Period, which is later than the individuals interred in the chamber (Brady et al.,

2000).

4.3   Isotope sample selection

Dentition collected from Cueva del Río Talgua and Cueva de las Arañas in 1996

by Dr. Nicholas Herrmann was used for the research project. The Instituto Hondureño de

Antropología e Historia (IHAH) generously granted permission to collect loose dental

remains throughout Talgua and Arañas that totaled 564 teeth (Benedix et al., 1999). Any

human remains, such as skulls with associated dentition, adhered to the calcite matrix of

the cave were left *in situ*. Preservation of dentition ranged from good to poor, with

portions of the assemblage showing post-mortem taphonomic damage (Herrmann, 2002).

Since the assemblages are commingled, MNI was determined to ensure only single

individuals were represented in the isotope analysis. A Talgua Osteological Database was

previously created in Corel Paradox 8 and it was transferred to Microsoft Access for this

study. This database was queried by Operation, Lot, and tooth number to determine the

tooth number of highest frequency for each lot. For example, Operation II, Lot 2 (II-2)

had five right upper M2 teeth (2) and two lower left M2 teeth (18), then the right upper

M2 or tooth 2 was sampled from II-2. Preferably, second or third molars, where crown

initiation occurs 2.5-3 (M2) and 7-10 (M3) years of age (Hillson, 1996), were sampled to

avoid the effects of weaning. Biogeochemistry studies have demonstrated that

breastfeeding enriches the $\delta^{18}O$ signature of the infant compared to the imbibed signature

of the mother (Eerkens and Bartelink, 2013). Therefore, teeth formed during infancy have

higher $\delta^{18}O$ signatures than teeth formed during the juvenile stage (Wright and Schwarcz,

1996). A total of 37 individuals were sampled from across the lots at Talgua and Arañas

for $\delta^{13}C$, $\delta^{18}O_p$, and $\delta^{18}O_c$. Due to budgetary constraints, the samples for $^{87}Sr/^{86}Sr$ were limited to 14 individuals, and were sub-sampled from the original 37 individuals based on spatial location within the caves. The provenience descriptions of where the samples originated are discussed below.

4.3.1   Talgua Cave lot descriptions

Twenty-three distinct deposits, or lots, of human remains were identified in Talgua. Of these 23 lots, 20 contained multiple commingled individuals, and three contained a single individual per lot (Brady, 1994). Due to budgetary limitations, only 13 lots were sampled throughout Talgua (Figure 4.2). A total of eight individuals were sampled from Operation I, three individuals from I-1 and five individuals from I-2 (Table 4.2). Operation I is located in the lowest passage of the cave, and contains two distinct lots (Brady, 1994). This area is highly disturbed, evident by graffiti on the walls and displaced or crushed human remains (Brady, 1994). A total of six individuals were sampled from Operation II, one individual from II-1 and five individuals from II-2. Operation II is located on the second passage of Talgua and contains two distinct lots. Multiple individuals covered in red pigment are represented in each lot. Five intact vessels, along with 20 ceramic sherds, were recovered from this area of the cave (Brady, 1994). One effigy vessel in the shape of a bird, three anthropomorphic vessels, and one orange-slipped vessel were recovered from II-2 (Brady, 1994). Operation III was the most densely concentrated area of human remains, and a total of eighteen individuals were sampled. Operation III is located in the highest passage of Talgua, and contained 19 lots, nine of which were sampled for this research project. Three lots in Operation III are thought to contain a single individual, whereas the remaining lots all contained multiple

55

individuals (Brady, 1994). All of the human remains are poorly preserved, excluding the elements cemented in calcite, which were left in the cave. Red pigment was also observed on or associated with the interments in Operation III (Brady, 1994). Artifacts were recovered from this area of the cave, and included: jade fragments, a single bead, six ceramic vessels, and two marble vessels. A total of 20 intact or restorable vessels were recovered from Talgua, and the two marble vessels do not resemble any variations found in studied parts of Honduras (Brady, 1994).

Table 4.2   Cueva del Río Talgua Lot Descriptions

	$^{87}Sr/^{86}Sr$ Samples	$\delta^{18}O$ Samples	$\delta^{13}C$ Samples	Lot Description
Operation I				
Lot 1	1	3	3	I-1 is restricted to an area of 70 cm by 1 m on top of a small earthen hill of light brown soil. This area was extensively vandalized. Red ochre is present on the poorly preserved skeletal material. Multiple individuals represented.
Lot 2	1	5	5	I-2 is located in an alcove at the end of the chamber. The deposit of human remains is 3.6 m in length. Red ochre is present on the poorly preserved skeletal material. A small ulna, fragments of long bones, a humerus head, and juvenile vertebra were documented. Multiple individuals represented.
Operation II				
Lot 1	1	1	1	II-1 is located in a 'C' shaped 60-cm by 40-cm niche in the cave wall. The human remains were vandalized, and some were found on the cave floor. Red ochre is present on the skeletal material. Multiple individuals represented.
Lot 2	2	5	5	II-2 is located in a small side tunnel behind a rim stone dam. The human remains were compact down by vandals. Artifacts were documented in the deposit and included: three vessels with modeled faces, one bird-shaped vessel, and an orange slipped vessel. Approximately 20 sherds were collected behind the dam, leading to the tunnel. Multiple individuals represented and date to the Middle Formative Period.
Operation III				
Lot 2		2	2	III-2 is located in a 110 cm by 36 cm depression surrounded by limestone formations. No skulls are present, but multiple teeth remain. Red ochre is present on the skeletal material. Multiple individuals represented. Radiocarbon dated to the Middle Formative Period.
Lot 3	1	2	2	III-3 is located in a small depression three to four meters above the floor of the chamber. No skull is present, but multiple teeth remain. Red ochre is present on the skeletal material. Artifacts included one broken vessel and two small pieces of jade. Multiple individuals represented. Radiocarbon dated to the Middle Formative Period.

(extracted from Brady, 1994)

Table 4.2 (continued)

	$^{87}Sr/^{86}Sr$ Samples	**$\delta^{18}O$ Samples**	**$\delta^{13}C$ Samples**	**Lot Description**
Operation III				
Lot 6		3	3	III-6 is 90 cm long, 80 cm wide, and 82 cm high, and is located on a ledge of the cave 2 m above III-5. Red ochre is present on the poorly preserved skeletal material. Multiple individuals represented.
Lot 7		3	3	III-7 is 120 cm by 55 cm and 70 cm high at the entrance, and is located in an alcove surrounded by limestone formations. Human remains may have been stacked very high in this chamber because the red pigment is high on the wall. Red ochre is present on the poorly preserved skeletal material. Artifacts included two ceramic vessels near the entrance, one vessel contained a small bead and both contained red pigment. Multiple individuals represented.
Lot 8	1	1	1	III-8 is an extension of III-7, and is 55 cm by 64 cm and 40 cm deep. Most of the deposit is below the water line, but some elements, such as a single skull was encased in calcite. Multiple individuals represented.
Lot 9	1	1	1	III-9 is 30 cm by 40 cm, and is located in a niche along the north wall. The long bones are stacked parallel with a poorly preserved skull placed on top. Red ochre is present. A ceramic vessel with an orange slipped rim was recovered 10 cm from the remains. A single individual is
Lot 10		2	2	III-10 is 25 cm by 40 cm, and is located in a niche in the wall below III-9. Red ochre is present on the poorly preserved skeletal material. Human remains were placed in parallel stacks. Multiple individuals represented.
Lot 17	1	4	4	III-17 is located in a circular depression 120 cm in diameter and 25 cm deep. Artifacts include two marble vessels, one has a "kill hole" in the bottom, one dichrome jar with red-on-orange geometric designs and one modeled face vessel. Multiple individuals represented and date to the Middle Formative Period.
Lot 19	1	1	1	III-19 is 90 cm by 90 cm, and is located in a large niche in a huge stalagmite column. Red ochre is present on the skeletal material. Multiple individuals represented.
Total	**11**	**32**	**32**	

Figure 4.2   Plan map of Cueva del Río Talgua

4.3.2　Arañas Cave lot descriptions

Sixteen distinct deposits, or lots, of human remains were identified in Arañas (Brady et al., 2000). All 16 lots contained multiple commingled individuals (Brady et al., 2000). Due to collection limitations of loose dentition, only the vestibule and two lots from Operation II were sampled from Arañas. A total of two individuals were sampled from Operation I (vestibule), at proveniences I-1 and I-5 (Table 4.3). Operation I is located in the vestibule of the cave, and is thought to contain artifacts associated with ritual or ancestor veneration (Brady et al., 2000). A total of three individuals were sampled from Operation II (II-1 and II-4). Operation II was highly disturbed by natural phenomena, evident by the state of preservation of the remains (i.e. bone meal) (field notes). No artifacts were observed in this area, possibly from looting activities.

Table 4.3   Cueva de las Aranas Lot Descriptions

	$^{87}Sr/^{86}Sr$ Samples	$\delta^{18}O$ Samples	$\delta^{13}C$ Samples	Lot Description
Operation I (Vestibule)				
Lot 1	1	1	1	A high density of artifacts were documented in the vestibule, and included ceramics, a small burnt corn cob, snail shells, and a single modified left lateral mandibular incisor.
Lot 5	1	1	1	A high density of artifacts were documented in the vestibule, and included ceramics, a small burnt corn cob, snail shells, and a single modified left lateral mandibular incisor.
Operation II				
Lot 1		1	1	II-1 is located in the northeastern end of the chamber. Red ochre is present on the poorly preserved skeletal material. A total of four teeth were collected. Multiple individuals represented.
Lot 4	1	2	2	II-4 is located in the northeastern end of the chamber. Red ochre is present on the poorly preserved skeletal material. A total of 18 teeth were collected. Multiple individuals represented; possibly a 6-10 year old and an older adult.
Total	**3**	**5**	**5**	

(extracted from field notes)
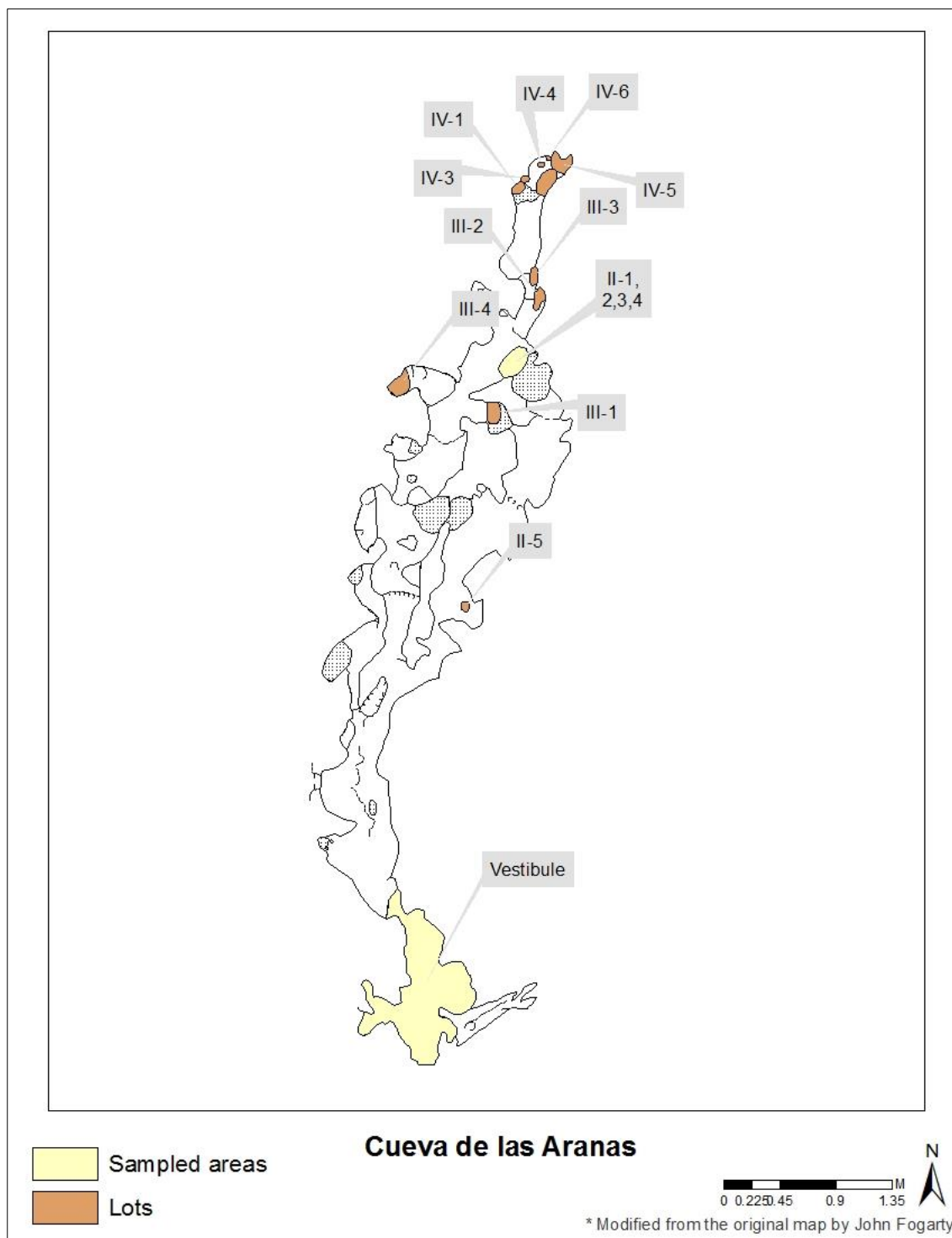
Figure 4.3   Plan map of Cueva de las Arañas

4.4   Summary

Doris Stone (1957) originally suggested that cave burials were the common mortuary program for prehistoric Honduras. The discovery of skeletal remains in Cueva del Río Talgua, Cueva de las Arañas, and Cueva de Piedra Blanca provides evidence for Stone's assumption. Talgua and Arañas were extensively documented during the Talgua Archaeological project, and the collection of loose dentition made this thesis research project possible. Since no associated Formative Period habitation could be identified during the survey portion of the TAP project, stable and radiogenic isotope analysis will aid in determination of the geographic affiliation of the interred individuals. A total of 37 individuals were sampled for the research project from spatially distinct locations throughout the caves. Based on the MNI of 73 individuals interred at Talgua, 44% of the sample was measured for $\delta^{13}C$, $\delta^{18}O_p$, and $\delta^{18}O_c$, which increases the odds for determining their affiliation. Since northeast Honduras continues to be a neglected region of study (Dennett and McCafferty, 2012), this research will add to the prehistory of the Río Talgua drainage and the Cuevas de Talgua National Park.

CHAPTER V

METHODS AND PROCEDURES

In this chapter, the isotope analyses, data analyses, and the dental metrics are discussed. Preparations, diagenetic tests, and laboratory procedures for $\delta^{13}C$, $\delta^{18}O_c$, $\delta^{18}O_p$, and $^{87}Sr/^{86}Sr$ isotope analyses are described in the isotope analysis component of this chapter. The data analysis section details the qualitative and quantitative techniques used to interpret the primary and secondary research objectives of the project. Specifically, the ArcGIS protocols developed for the likelihood assignment models to determine the probability of geographic origin and the intra-ossuary spatial analyses to examine mortuary arrangement are discussed in the data analysis section. The sample selection for the dental metrics and data analysis is detailed separately in the last component of Chapter V. The statistical software, JMP and R studio, the mapping platform, ArcGIS, and the online resources, IsoMAP and GME, were used to analyze the isotope and dental metric data for this research project.

5.1   Isotope analysis

Mississippi State University (MSU) does not have the necessary isotope ratio mass spectrometers to analyze bioapatite (i.e. bones and teeth) for either the stable or radiogenic isotopes required for this research project. Thus, the samples that were selected for isotope analysis, discussed in Chapter IV, were cleaned and powdered in the

Forensic Anthropology and Bioarchaeology Laboratory (FABLab) at MSU, and sent to certified facilities to measure the $\delta^{13}C$, $\delta^{18}O_c$, $\delta^{18}O_p$, and $^{87}Sr/^{86}Sr$ isotopes. The $\delta^{13}C$, $\delta^{18}O_c$, and $\delta^{18}O_p$ isotopes (n=37) were measured at the University of California's Santa Cruz Stable Isotope Laboratory and the $^{87}Sr/^{86}Sr$ isotopes (n=14) were measured at IsoForensics, Inc.

5.1.1   Sample preparation

Sample preparation is a crucial step in the isotope analytical process and the quality of results depends on strictly enforced protocols (Meier-Augustine, 2004). Samples were prepared in the FABLab at MSU. Protocols for isotope sample preparation were based on Turner et al. (2009) with slight modification. Enamel samples were sonicated in 50ml deionized (DI) water, dried in the fume hood for 24 hours, and then the enamel surfaces were abraded using a Dremel™ to remove any surface contamination. Quartered enamel sections were saved at this stage of the sample preparation for $^{87}Sr/^{86}Sr$, since a clean laboratory is required for the radiogenic preparation and analysis. Drill bits were cleaned with HCl between samples, and then dried with acetone. Once the enamel surface was cleaned, the sample was soaked in 10ml of acetone for 10 minutes, then rinsed with DI water, and sonicated in 50ml of DI for 15 minutes. Limited pre-treatment of the enamel surface was needed, due to the fact that enamel is a reliable reservoir of biogenic Sr, O, and C, unlike dentine or bone (Budd et al., 2000). After the enamel was treated, it was dried in the fume hood for 24 hours. Lastly, the enamel was powdered, using an agate mortar and pestle until finely ground. The mortar and pestle were cleaned with HCL between samples, rinsed with DI, and then dried with acetone.

65

Enamel powder (5-20mg) was placed into separate micro-centrifuge tubes for $\delta^{13}C$ and $\delta^{18}O_c$ (carbonate), and $\delta^{18}O_p$ (phosphate), then shipped to the Santa Cruz laboratory.

5.1.2   Oxygen and carbon isotope analyses

The $\delta^{13}C$, $\delta^{18}O_c$, and $\delta^{18}O_p$ isotopes were processed at the University of California's Santa Cruz Stable Isotope Laboratory (SOPs in Appendices A.1, A.2, and A.3). The Santa Cruz isotope lab dissolved the powdered enamel in acid solutions to remove any contaminates and extracted the phosphate and carbonate. The $\delta^{13}C$ and $\delta^{18}O_c$ samples (n=37) were measured using a ThermoScientific MAT-253 dual-inlet isotope ratio mass spectrometer (IRMS). The Carbonate Device and dual-inlet system allow for generation and cryogenic distillation of carbon dioxide gas from calcium carbonate and other inorganic materials (e.g., bone apatite) under vacuum conditions. The $\delta^{13}C$ and $\delta^{18}O_c$ measurements were corrected using three standards (LSVEC, NBS18, and NBS19) and reported relative to the VPDB (Pee Dee Belemnite) carbonate standard and expressed using standard notation (Gröning, 2004). Analytical precision of internationally calibrated in-house standards was approximately 0.2‰. Values were corrected for size, drift and source stretching effects with precision approximately 1%.

The $\delta^{18}O_p$ samples (n=37) were chemically wet converted as silver phosphate and barite and analyzed using a Finnigan high temperature conversion elemental analyzer (TCEA) interfaced to a ThermoFinningan Delta Plus XP isotope ratio mass spectrometer (IRMS) (see Appendix A for Standard Operating Procedures). Stephan (2000) is typically referenced as the standard for isolating phosphate Ag_3PO_4 from apatite. Briefly, this procedure begins with silver encapsulated samples undergoing pyrolysis in an oxygen free environment at around 1350-1450°C. The products then pass through an

ascarite/magnesium perchlorate trap to remove water and contaminants before the column before the introduction into the IRMS. Calibrated in-house standards are measured between samples to correct for size effects, source stretching, and drift (calibrated against NIST Standard Reference Materials: IAEA-601, IAEA-602 Benzoic Acid). The $\delta^{18}O_p$ measurements are reported relative to the VSMOW (standard mean ocean water).

5.1.3   Strontium analysis

The $^{87}Sr/^{86}Sr$ isotope samples (n=14) were measured using a Neptune *Plus* High-Performance Multicollector inductively-coupled plasma mass spectrometer (ICP-MS) for the measurement in liquid matrix via self-aspiration in a clean room at IsoForensics (SOP in Appendix A.4). Prior to measurement, the strontium was purified and concentrated in at least 1 ml 2.4% HNO_3 using an automated off-line column chemistry system. Specifically, the powdered tooth enamel is dissolved using 500 µl of 3N HNO_3, evaporated, then redissolved in 500 µl of 3N HNO_3, and purified through cation exchange columns filled with Sr exchange resin. Dissolved samples are then loaded in the column, and rinsed with 300 µl of 3N HNO_3. Purified samples are dried, redissolved in 2 µl of 0.3N H_3PO_4 and 2 µl of $TaCl_5$, and then loaded onto degassed Re filaments for analysis. Samples were analyzed in order of lowest to highest concentration The Standard Reference Material (SRM® 987) was used and measured every three samples. Additionally, reference material (TORT-2) was used to determine the quality (QC) and precision of the instrument.

5.1.4   Diagenesis

Chemical postmortem alteration of human remains has been demonstrated to change the isotopic composition of certain skeletal elements, especially bone, in certain burial environments (Lee-Thorp and van der Merwe, 1987). Techniques such as XRD, ion and electron microprobe, transmission electron microscopy, small-angle X-ray scattering, and ratios of F/P or Ca/P have been used to observe any alterations to the crystalline structure of skeletal elements (Pellegrini et al., 2011). Unfortunately, none of these processes listed above ensure stable oxygen modifications.

The relationship between the phosphate and carbonate fractions in specimens has been used to quantify any adverse effects on the CO3 structure, based on the premise that bioapatite precipitates simultaneously from body water. This technique calculates the offset or the difference between the $\delta^{18}O_P$ and $\delta^{18}O_C$ values (ΔC-P). The basic premise is that the carbonate-fluorapatite mineral phase of apatite fossils may replace the original hydroxylapatite during dissolution and precipitation (Iacumin et al., 1996). This mineral phase during deposition tends not to alter the $\delta^{18}O_p$ due to the strong P-O bond with the phosphate ion, and thus a linear correlation should be present between $\delta^{18}O_c$ and $\delta^{18}O_p$ (Genoni et al., 1998). The ΔC-P offset has been documented with a wide range of variability between species and even within individual teeth, up to 12‰ (Pellegrini et al., 2011). This variability may even be attributed to enamel mineralization, since it is not fully understood for the rate of incorporation of $\delta^{18}O_P$ and $\delta^{18}O_C$ (Pellegrini et al., 2011).

The ΔC-P offset was determined from converting the $\delta^{18}O_C$ (VPDB) values into $\delta^{18}O_C$ (VSMOW) values then taking the difference between the $\delta^{18}O_P$ (SMOW) and the

$\delta^{18}O_C$ (VSMOW) values (ΔC-P). The Coplen et al. (1983) equation was used to convert the VPDB values into VSMOW:

$$\delta^{18}O \text{ (VSMOW)} = 1.03091 * \delta^{18}O \text{ (VPDB)} + 30.91 \qquad (5.1)$$

Samples with values greater than 10.6‰ will be regarded with great caution, following this common threshold in the literature (Martin et al., 2008).

5.2   Data analysis

The second component of this chapter discusses the methods and techniques that were used to test the research questions and interpret the isotope results. Prior to the spatial analysis and development of the likelihood assignment models, the isotope results were explored using a combination of statistical techniques. Descriptive summary statistics were used to visualize the isotope distributions (i.e. scatter plots, histograms) for each isotope ($\delta^{13}C$, $\delta^{18}O_c$, $\delta^{18}O_p$, and $^{87}Sr/^{86}Sr$). Intra-site (i.e. Arañas and Talgua), and intra-tooth (i.e. M1s and M2s) variation were also examined for isotope patterns before the quantitative assessment. Additionally, principle component analysis (PCA) was used to qualitatively explore the variance of the four isotope variables. In the following two sections, the likelihood assignment models for $\delta^{18}O$ and $^{87}Sr/^{86}Sr$ are described, along with the intra-ossuary techniques used to analyze the mortuary arrangement in Río Talgua.

5.2.1   Likelihood assignment models for geographic origin

To test the first hypothesis, $\delta^{18}O$ and $^{87}Sr/^{86}Sr$ isoscapes were used to assign the bioavailable $^{87}Sr/^{86}Sr$ and $\delta^{18}O$ Talgua Cave signatures to their geographic origin. An isoscape approach utilizes the variation from the underlying bedrock geology and water

hydrology to predict or quantify geographic origin (discussed in Chapter III). Assignment methods based on likelihoods, or probabilities, are common statistical techniques used for estimating origin with isoscape models (Wunder, 2012). Unlike common linear regression, assignment methods based on probability are more accurate, and may incorporate prior probability using Bayes' rule to directly estimate origin based on previous data (Wunder and Norris, 2008). Three ^{87}Sr/^{86}Sr isoscapes created by Bataille et al. (2012) for the circum-Caribbean region were used as the isoscape models to assign the Talgua Cave ^{87}Sr/^{86}Sr values. A δ^{18}O precipitation isoscape modeled using IsoMAP was used as the prediction map to assign the δ^{18}O Talgua Cave values. The models are described in detail below.

5.2.1.1   Geographic ^{87}Sr/^{86}Sr assignment model

Prior to the assignment model, other techniques used to determine outliers (i.e. "non-locals") in bioarchaeology were explored, including the Price et al. (1994) technique, Wright's (2005) trimming technique, and Grubb's outlier test. The Price et al. (1998) approach is an exploratory technique that identifies ^{87}Sr/^{86}Sr outliers that fall two standard deviations from the mean. Furthermore, the Wright (2005) technique trims the outliers first, and then estimates the normality of the ^{87}Sr/^{86}Sr measurements in the remaining dataset using the technique discussed above. Grubb's test, which is used to detect outliers in a normally distributed dataset, was the third preliminary technique used to determine outliers in the ^{87}Sr/^{86}Sr dataset. The results from these tests were later compared to the likelihood assignment model results.

Three ^{87}Sr/^{86}Sr isoscape models (Bedrock, Catchment, and Soil) developed by Bataille et al. (2012) were used for the Talgua Cave likelihood assignments. The

bedrock-only model was developed from known bedrock ^{87}Sr/^{86}Sr values for the circum-Caribbean and interpolated throughout the region. The bedrock model has limitations that cause carbonate rocks to be the dominant source of Sr into a system, attributed to high weathering ability, when only trace amounts of carbonate rocks may be present in certain areas of the region. The catchment and soil ^{87}Sr/^{86}Sr isoscapes account for multiple ^{87}Sr/^{86}Sr inputs that tend to more accurately reflect the geographic ^{87}Sr/^{86}Sr in a region. The catchment water isoscape is a two source mixing model that accounts for sea salt and bedrock weathering (Figure 5.1). The soil water isoscape is a three-source mixing model that accounts for mineral dust, bedrock weathering, and sea-salt accumulation.
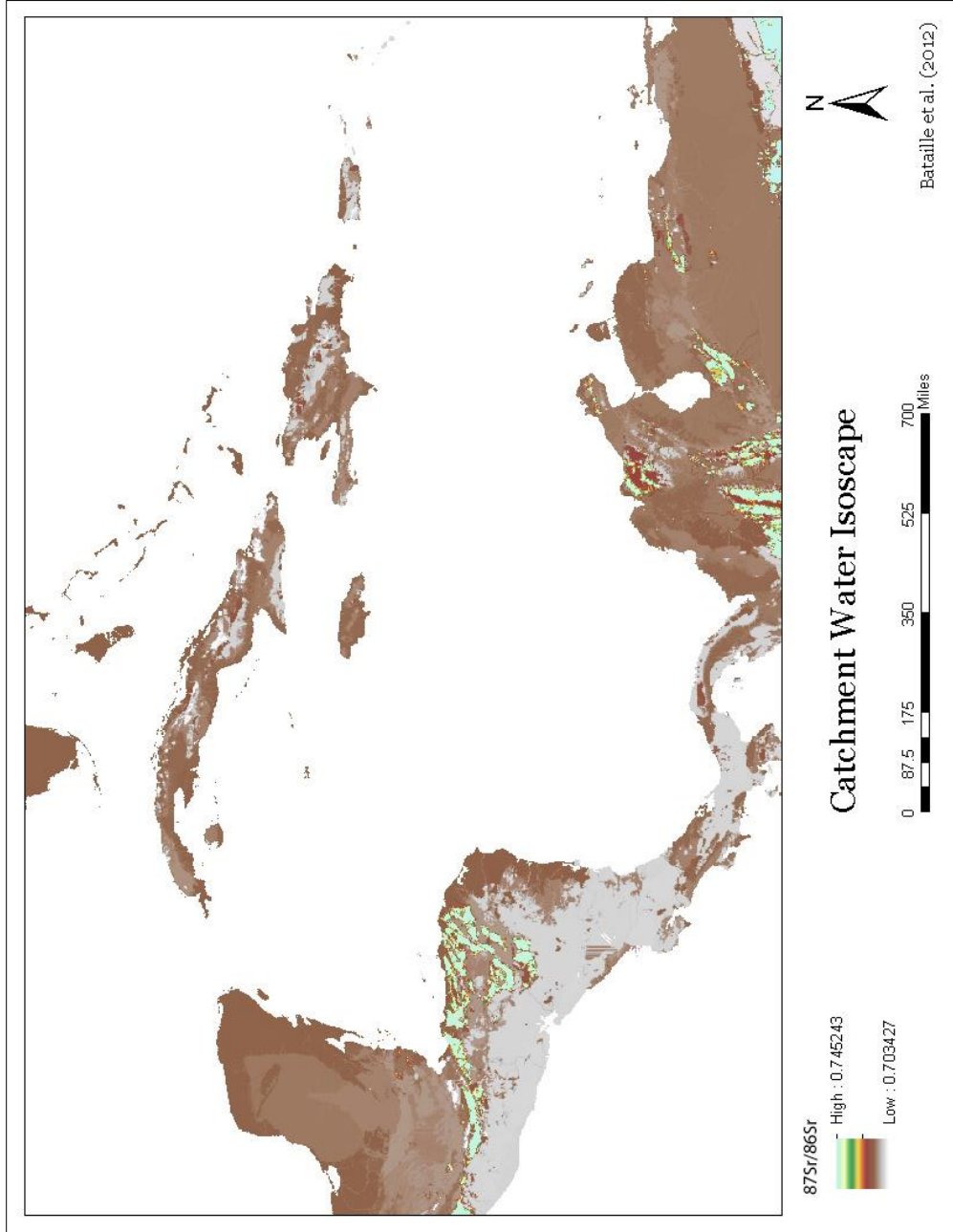
Figure 5.1   Catchment Isoscape used for ^{87}Sr/^{86}Sr Assignments

Since the Bataille et al. (2012) isoscapes reflect the geographic $^{87}Sr/^{86}Sr$ distribution for the circum-Caribbean, these models were calibrated using archaeological human and faunal $^{87}Sr/^{86}Sr$ values previously published sources to determine the bioavailable $^{87}Sr/^{86}Sr$ values for the region. Table C.1 in Appendix C lists the archaeological sites (n=60), $^{87}Sr/^{86}Sr$ value, latitude, longitude, publication source, and species (if known) information that was incorporated in to the Bataille et al. (2012) models. The majority of the archaeological $^{87}Sr/^{86}Sr$ data is from the Mesoamerican and island regions (i.e. Cuba, Puerto Rico), and, unfortunately, Lower Central America lacks any previously recorded $^{87}Sr/^{86}Sr$ data. To determine which of the three geographic $^{87}Sr/^{86}Sr$ models was the best fit for the region, the bioavailable $^{87}Sr/^{86}Sr$ data was plotted in ArcGIS, and the geographic $^{87}Sr/^{86}Sr$ values were extracted from those coordinate locations. Linear regressions of the geographic to bioavailable $^{87}Sr/^{86}Sr$ data was determined for each model and are listed below:

1. Catchment model: $y = 0.987x + 0.010$ ($R^2=0.751$)
2. Bedrock model: $y = 0.880x + 0.085$ ($R^2=0.677$)
3. Soil model: $y = 0.856x + 0.102$ ($R^2=0.583$)

Based on these regressions, the catchment isoscape model was the best-fit for bioavailable $^{87}Sr/^{86}Sr$ in the circum-Caribbean region. The linear function $y = 0.987x + 0.010$ was added to the catchment model using raster math in ArcGIS to create the bioavailable $^{87}Sr/^{86}Sr$ isoscape for the circum-Caribbean region that was used for the Talgua Cave likelihood assignments.

The likelihood assignment model was developed in ArcGIS, using a Bayesian framework that has been applied in many recent animal migration studies (see Wunder,

73

2005; Wunder, 2010; Vander Zanden et al., 2001). The application applies Bayes

Theorem, where probability A_i is the geographic origin for a measured sample value δ_s,

and was adjusted by Bowen et al. (2014) for IsoMAP (discussed below) to assign

observed isotope values to probable geographic expected isotope values. The expression

used is listed below in equation (5.2):

$$P(\delta s | Ai) = \frac{1}{\sqrt{2\pi(\sigma_p i^2 + \sigma_\varepsilon p^2)}} e^{\frac{-(\delta sp - \delta pi)^2}{2(\sigma_p i^2 + \sigma_\varepsilon p^2)}} \qquad (5.2)$$

Where, variable $\sigma_{p,i}$ is the estimated variance for the calibrated $^{87}Sr/^{86}Sr$ isoscape model

(spatial error), $\sigma_{\varepsilon,p}$ is the variance of the $^{87}Sr/^{86}Sr$ sample value (sample error), and $\delta_{p,i}$ is

the calibrated $^{87}Sr/^{86}Sr$ isoscape predicted value. The $\sigma_{p,i}$ was determined by estimating

the standard deviation of the original catchment $^{87}Sr/^{86}Sr$ raster and the calibrated

$^{87}Sr/^{86}Sr$ raster. The $\sigma_{\varepsilon,p}$ is the measurement error that was determined by IsoForensics for

each sample and is discussed in the following chapter. Equation (5.1) was input into

ArcGIS using the raster calculator, and the assignment model was developed using model

builder (Figure 5.2). The likelihood probability surfaces were ran using the assignment

model for each Talgua Cave sample, and is discussed in Chapter VI (Results).

75
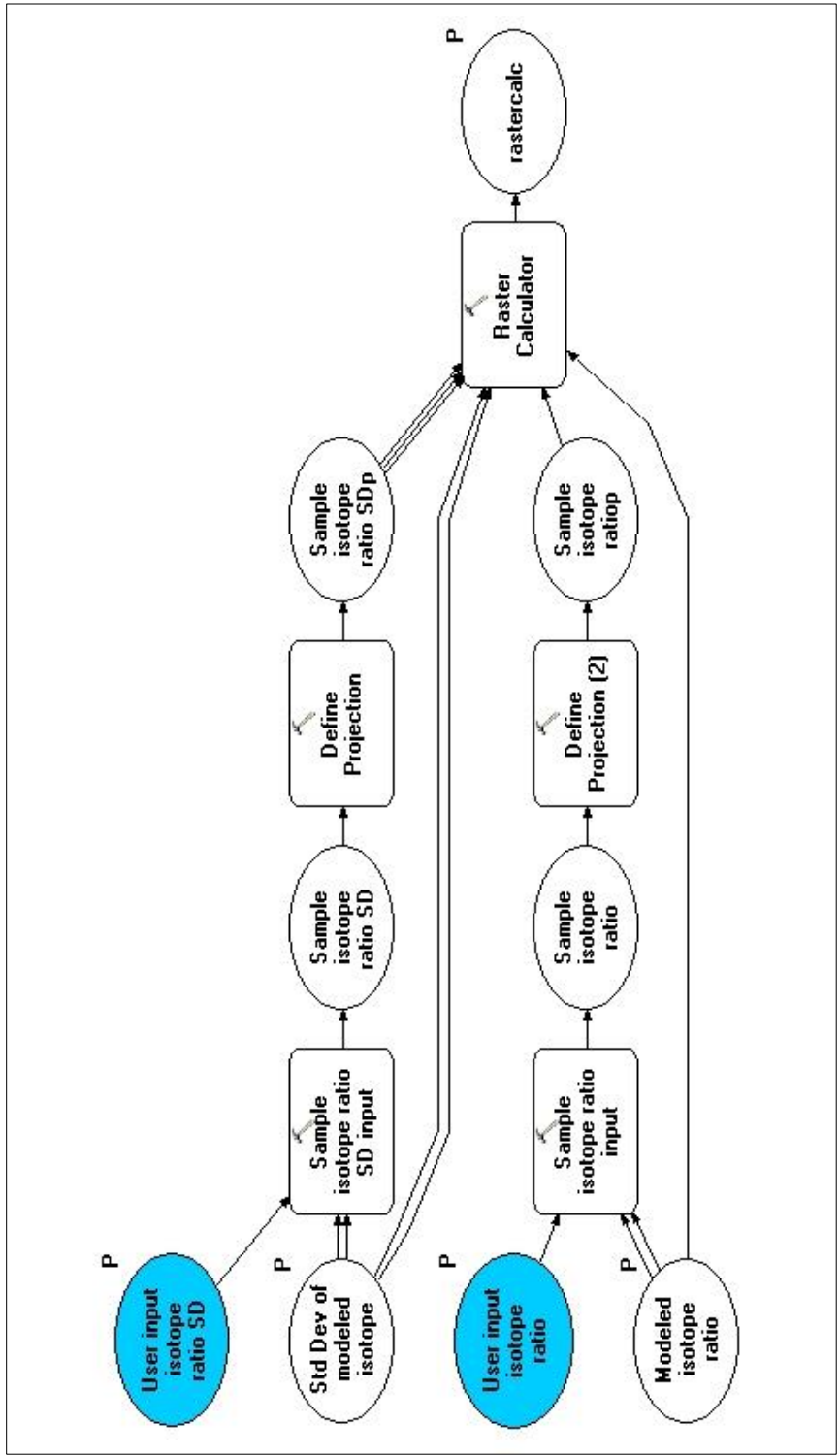
Figure 5.2   Model Builder Steps for ^{87}Sr/^{86}Sr Assignments within ArcMap

5.2.1.2 Geographic $\delta^{18}O$ assignment model

Prior to the assignment model, the techniques discussed above to determine outliers (i.e. "non-locals") were also explored for the $\delta^{18}O$ measurements (both carbonate and phosphate). Unlike $^{87}Sr/^{86}Sr$, $\delta^{18}O$ values from Mesoamerica do not always follow expected patterns, and may vary more within a site than between sites (Price et al. 2010). Due to these complications, $\delta^{18}O$ was used as the secondary indicator for geographic origin in this research.

An IsoMAP $\delta^{18}O$ precipitation model was used for the Talgua Cave $\delta^{18}O_p$ likelihood assignments. IsoMAP is an interactive, online resource (http://isomap.org) for isoscape modeling and geographic assignments using modern precipitation data (1960-2010). A precipitation $\delta^{18}O$ isoscape (job key 49183) was developed within IsoMAP with elevation and latitude as the independent variables for the circum-Caribbean region (Figure 5.3). Both the regression model (R^2=0.657) and the geostatistical model (Moran's I=0.636, p=0) were statistically significant for the model, based on the dependent and independent variables. No paleoclimate data for northeast Honduras could be located to calibrate the modern precipitation $\delta^{18}O$ values to paleo $\delta^{18}O$ values. Therefore, the geographic assignments for Talgua Caves were determined using the isoscape with no alterations. From a brief examination of paleoclimate data available through the National Oceanic and Atmospheric Administration (NOAA), $\delta^{18}O$ slightly fluctuates during the Formative Period for areas in Mesoamerica. For instance, sediment cores extracted from Lake Chichancanab, Mexico showed small differences in $\delta^{18}O$ between 2394 BP to 3278 BP, which ranged up to 2‰ (Hodell et al., 1995).

Precipitation Map for the circum-Caribbean

IsoMAP (Job Key 49183)

18O Value
High : -1.85681
Low : -13.0368
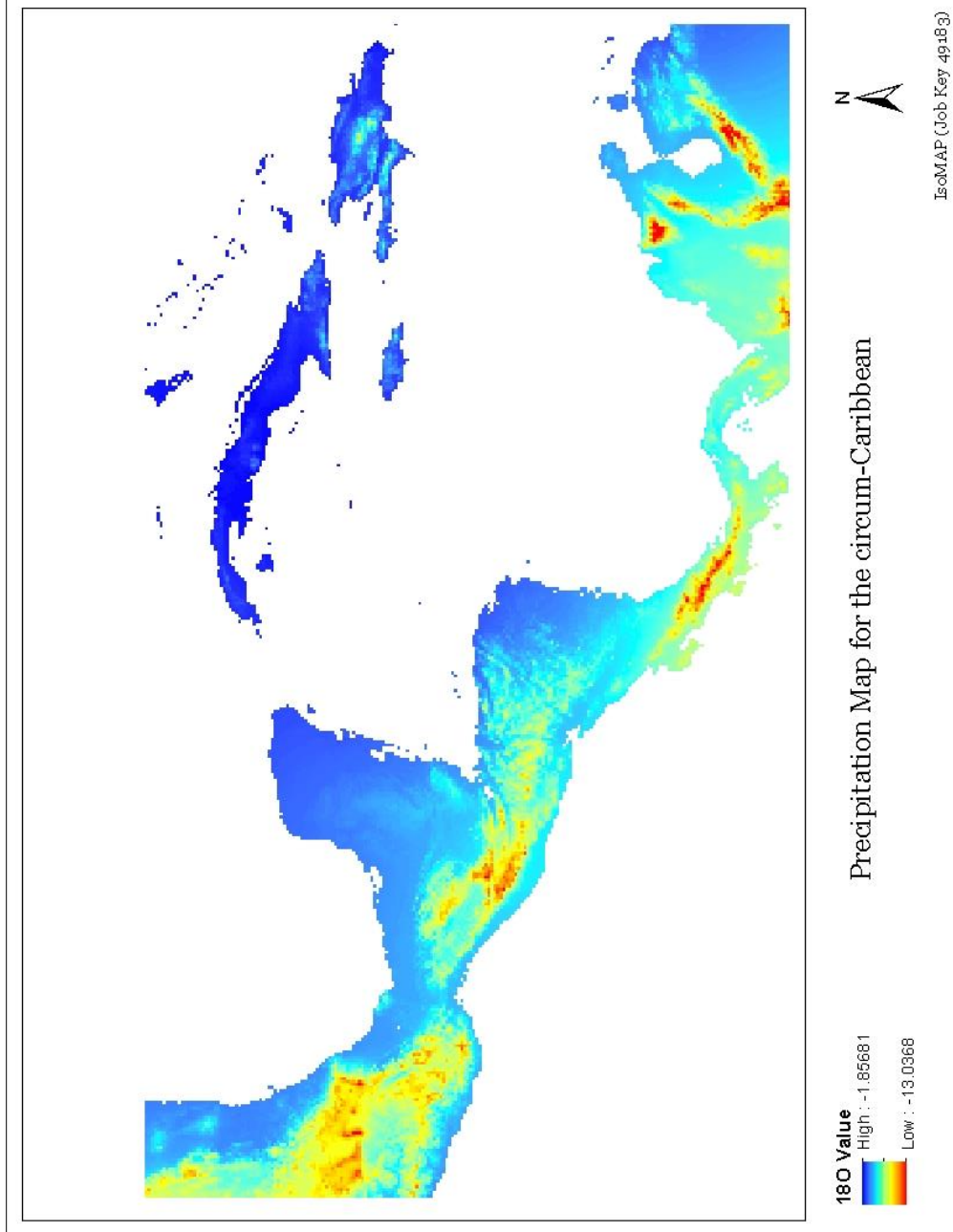
Figure 5.3   Precipitation Isoscape used for δ18Odw Assignment

77

The Talgua Cave $\delta^{18}O$ values were converted to modern drinking water values in order to compare the bioavailable $\delta^{18}O$ values to $\delta^{18}O$ precipitation values. The equation below was used to convert the $\delta^{18}O_p$ to $\delta^{18}O_{dw}$ values (Luz et al., 1984):

$$\delta^{18}Odw \ (VSMOW) = (\delta^{18}Op \ (VSMOW) - 22.70)/ \ 0.78 \qquad (5.3)$$

After $\delta^{18}O_p$ was converted to $\delta^{18}O_{dw,}$ the samples were separated into unique groups, or bins, to decrease the processing time. The means and standard deviations of the binned values were entered into the IsoMAP assignment model to explore the range of geographic $\delta^{18}O$ variation (Bowen et al., 2015). Since there was a ~4.08‰ range in the $\delta^{18}O_p$ values, the samples were grouped by their 1‰ difference and the corresponding samples were placed in one of the four bins. The assignment model applies the Bayesian framework that was discussed in the previous section. Details of the model can be found in Bowen et al. (2014). Once the single assignments were generated in IsoMAP, the ASCII files were imported into ArcGIS, then clipped to define the continental boundaries and a new raster was created so the probability surface of the assignment would equal one. Lastly, the online ecology resource, geospatial modeling environment (GME) was used to develop isopleths, or contours, to visualize the 90% probability assignment surface areas.

5.2.2   Mortuary arrangement

To test the second hypothesis, or determine if there are random patterns of $\delta^{13}C$, $\delta^{18}O$, and $^{87}Sr/^{86}Sr$ values between the lots in the Río Talgua Cave ossuary, a combination of exploratory and deterministic GIS spatial techniques was used for the intra-ossuary analysis of the Río Talgua cave ossuary. A spatial analysis was not

performed for the Arañas cave ossuary due to the small sample size and limited samples available between lots in the cave. Preliminary exploration of the isotope data was performed prior to the spatial analysis to identify any patterns in the data. The $\delta^{13}C$, $\delta^{18}O_p$, $\delta^{18}O_c$, and $^{87}Sr/^{86}Sr$ datasets were examined by the three Operations (I, II, and III) using a series of Welch's t-tests. Welch's t-tests (or unequal variances t-tests) were used when the two samples had unequal variances or different sample sizes. This exploration also included identifying qualitative relationships between lots containing artifacts and isotopic value. Certain lots containing contextual artifacts in Cueva del Río Talgua may relate to distinct $^{87}Sr/^{86}Sr$, $\delta^{18}O$, and/or $\delta^{13}C$ bioavailable signatures.

Quantitative GIS spatial techniques were used to visualize the isotopic distribution between the lots in the Río Talgua cave ossuary. The $^{87}Sr/^{86}Sr$, $\delta^{18}O_p$, and $\delta^{13}C$ datasets were examined between the lots in the Río Talgua cave ossuary using inverse distance weighting (IDW). Inverse distance weighting is a type of interpolation, or procedure that predicts values across grid cells based on the observed values. Interpolation was briefly touched upon in Chapter III in the Isoscape section. The IDW interpolation is a spatially dependent technique that estimates the unknown values using distance and common relationships (i.e. neighborhood) (Lu and Wong, 2008). Generally, the predicted values are determined from the weighted averages of the observed values within the neighborhood, which are inversely related as a function of distance from the observed value (Lu and Wong, 2008). The IDW interpolation is based on the general equation:

$$\hat{v} = \frac{\sum_{i=1}^{n} \frac{1}{d^{p_i}} v_i}{\sum_{i=1}^{n} \frac{1}{d^{p_i}}} \qquad (5.4)$$

Where $\hat{v}$ is the expected value, v_i is the observed value, and $d^{p}i$ is the distance from the observed values.

The IDW was performed on each isotope dataset ($^{87}Sr/^{86}Sr$, $\delta^{18}O_p$, $\delta^{18}O_c$, and $\delta^{13}C$) for the Río Talgua ossuary cave using the spatial analyst extension package in ArcGIS 10.2. The IDW interpolated raster datasets were based on the mean isotopic values of each lot in the ossuary. Since the means values were used in the IDW, lots were also compared using the Kruskal-Wallis test as a secondary technique to ensure that the mean values accurately represent the spatial distribution. The Kruskal-Wallis one-way analysis of variance is a non-parametric test (i.e. data that is not normally distributed) equivalent to the ANOVA, which compares the means to determine if they are from the same population. If there was a single isotopic value that represented a lot, it was combined with the nearest lot. For the $\delta^{13}C$ isotopes, lot II1 was combined with II2, III7 with III8, III9 with III10, and III17 with III19.

5.3 Dental metric analysis

Dental metric data were previously collected by Dr. Nicholas Herrmann, which followed procedures outlined in *Standards for Data Collection from Human Skeletal Remains* (Buikstra et al., 1994). Two measurements, mesiodistal diameter and buccolingual diameter, were collected on the majority of the Talgua Caves dentition. Mesiodistal diameter (MD), refers to the maximum crown length, and is taken as the maximum width of the tooth crown in the mesiodistal plane (Hillson, 1996).

Buccolingual diameter (BL), refers to crown width or crown breadth, and is taken at the maximum width or perpendicular to the MD plane. Measurements are dependent on the type of attrition or wear present on the crown, whether occlusal, interproximal, or a combination of both. Not only is tooth wear related to mastication, but also age (Miles, 2001). Therefore, MD data was used in the analysis, but the results were interpreted with caution. Dental calculus and taphonomic damage also affect dental measurements, calculus adding up to 5mm in buccolingual diameter (Kieser, 1990).

Incorporation of the complete Talgua Caves dental metric assemblage totaled 425 BL and MD measurements that included all tooth types and numbers. The dental metric data was combined from both of the caves to maximize sample size. This combination should not be a factor for the sex estimation, since the mortuary practices, vicinity of the locations of the caves, same temporal component, and isotopic values (discussed in the results chapter) are all similar for both ossuaries. But, the sample size was significantly reduced when extracting the first and second molar data (upper molars, n=58; lower molars= 51). Specific tooth types selected for the analysis and associated dental metric data were determined by querying the Talgua Osteological Database. Since lower canines and mandibular molars are typically the most sexually dimorphic teeth in human populations, molars from the Talgua Caves were used in the analysis. All of the dental metric data used in this study is listed in Appendix C.2. The majority of the teeth sampled for isotopic analyses were molars, therefore molars were selected for the analysis. Both upper and lower molars were selected, and data from the left and right quadrants of the mandible and maxilla were combined to maximize sample size. Available data for the upper first molars (UM1) included tooth numbers 3 and 14 (n=26), and for the upper

second molars (UM2) included tooth numbers 2 and 15 (n=31). Available data for the

lower first molars (LM1) included tooth numbers 19 and 30 (n=33), and for the lower

second molars (LM2) included tooth numbers 18 and 31 (n=17). These IM1, UM2, LM1,

and LM2 subgroups were used in the models to estimate biological sex, which is

discussed in detail below.

5.3.1   Finite mixture models

Finite mixture models were used for the secondary research objective and to test

the third hypothesis, or determine any significant relationships between isotopic value

and tooth size. There are a variety of types of mixture models including likelihood,

Bayesian, univariate, and multivariate. A Bayesian approach would require some known

dental metric data from the region for the Formative Period to set the points for sex

estimation. The closest available data for comparison comes from Late Classic period

Copán (Scherer, 2004). Therefore, multivariate and univariate normal mixtures were used

for the analysis. The multivariate analysis included both the MD and BL variables in the

models, and the univariate analysis classified the MD and BL independently of each other

to observe any differences between MD and BL subgroup classification. Additionally, no

skeletal indicators for the assemblage are available, which will bias sex estimation for the

Talgua Cave samples (Larsen, 1997). Due to time constraints, the influence of age on the

tooth dimensions using dental wear was not factored into the dental metric analysis. This

analysis to estimate biological sex for the Talgua Caves samples was performed in a

qualitative manner and is considered to be preliminary.

A normal finite mixture model provides the framework to estimate the probability of sub-populations within the sample population. These models use probability density functions to determine unknown distributions or mixtures from the known distributions (McLachlan and Peel, 2004). The finite mixture models were performed in JMP®, which uses the following general equation:

$$F(t) = \sum_{i=1}^{k} w_i * F_i\ (t) \tag{5.5}$$

Where k is a known constant, w_i are the weights, and F_i are the distribution functions. The weights all sum up to one and are based on normal distributions. Prior to performing the mixture models, all of the data subgroup (UM1s, UM2s, LM1s, LM2s) were explored to determine normality of the datasets. If any of the datasets were determined to have skewed distributions, the F_i was changed to a lognormal distribution, which was done in JMP® simply by selecting a distribution type for the data.

When the probabilities from the mixture models contained subgroups, the probability for each sample belonging to which subgroup was determined. Samples with probabilities $\geq 96\%$ were classified into either possible female or possible male. Based on sexual dimorphism of the teeth, samples with $\geq 96\%$ probabilities that had high BL or MD measurements were classified as possible male, and samples with $\geq 96\%$ probabilities that had low BL or MD measurements were classified as possible female. Any samples that had probabilities $< 96\%$ were classified as indeterminate individuals. Once the samples were separated into either possible male, possible female, or indeterminate, the samples with possible sex estimations were compared to their corresponding isotopic values ($\delta^{13}C$, $\delta^{18}O_p$, $\delta^{18}O_c$, and $^{87}Sr/^{86}Sr$).

5.4   Summary

Prior to testing any of the primary or secondary hypotheses, exploratory analysis of the $\delta^{13}C$, $\delta^{18}O_p$, $\delta^{18}O_c$, and $^{87}Sr/^{86}Sr$ datasets were performed, which included testing for diagenesis. There are two primary research objectives for this research project and one secondary objective. The first primary research objective was to assign geographic origin to the $\delta^{18}O_{dw}$ and $^{87}Sr/^{86}Sr$ bioavailable signatures using calibrated likelihood assignment models. The second primary research objective was to perform a spatial analysis using inverse distance weighting to visualize the distribution of isotopic values by mortuary arrangement in the Río Talgua Cave. The final research objective for this project was to examine tooth size by isotopic value using finite mixture models to estimate preliminary biological sex of the individuals interred in the Talgua Caves.

CHAPTER VI

RESULTS

In this chapter, the Talgua Caves isotope data are presented, along with the dental metric data. The $\delta^{13}C$, $\delta^{18}O_c$, $\delta^{18}O_p$, and $^{87}Sr/^{86}Sr$ isotope results are summarized in their corresponding isotope sections, while the test for diagenesis is discussed in the Oxygen isotope data section (6.2). Preliminary geographic origin of the individual samples is also touched upon in these summary sections. The thesis research objectives (geographic origin, mortuary arrangement, and dental metric analysis) are sectioned by topic and discussed individually. Statistical results from the data analyses are detailed in each section for the individual components, and the findings from the hypothesis testing are stated in the form of rejection or acceptance.

6.1   Strontium isotope data

The statistical summary of the $^{87}Sr/^{86}Sr$ data (n=14) is presented below, along with the results from several different outlier methods. The outlier methods discussed here are a preliminary approach to determining if any "non-locals" are represented in the Talgua Caves dataset. A further discussion of potential geographic origins for the individuals' is detailed in the Research question section (6.4). Fourteen samples were analyzed for $^{87}Sr/^{86}Sr$ isotopes and strontium concentrations ($\mu g/g$) (Table 6.1). Two duplicate samples (9023 and 9344) were measured for $^{87}Sr/^{86}Sr$ to determine the precision

of the analysis. Using the Student's t-test, the precision of the ^{87}Sr/^{86}Sr measurements

was high (t=0.010, p=0.993). Once the duplicate samples were averaged together, the

Talgua Caves ^{87}Sr/^{86}Sr values range from 0.70719 to 0.71338 with a mean of 0.71014 for

the dataset. Based on the Price et al. (1998) technique to identify outliers in the dataset,

using two standard deviations from the mean, no outliers are present in the ^{87}Sr/^{86}Sr

Talgua Caves data (s.d.=0.002). Additionally, Wright's (2005) "trimming" technique

could not be applied to the dataset, since the ^{87}Sr/^{86}Sr distribution was fairly normal,

demonstrated by the Shapiro-Wilk normality test results (w=0.929, p=0.294). Grubb's

test, or the extreme studentized deviate (ESD) method for outliers, identified sample 9425

as an outlier (G=1.623, U=0.781), but is not significant (p=0.634) (Figure 6.1).

Table 6.1   Strontium Concentration and ^{87}Sr/^{86}Sr Isotope Results

Site	Sample	Sr	^{87}Sr/^{86}Sr	std. error
Arañas	573	744	0.70831	0.000014
Arañas	592	178	0.70761	0.000015
Talgua	9004	345	0.70723	0.000012
Talgua	9023	134	0.70907	0.000013
Talgua	9023		0.70907	0.000015
Talgua	9132	431	0.71162	0.000016
Talgua	9153	529	0.71089	0.000015
Talgua	9230	545	0.71156	0.000013
Talgua	9318	602	0.71147	0.000012
Talgua	9344	584	0.71197	0.000012
Talgua	9344		0.71201	0.000014
Talgua	9375	451	0.70966	0.000013
Talgua	9397	623	0.71184	0.000015
Talgua	9415	276	0.70719	0.000013
Talgua	9425	219	0.71338	0.000014
Arañas	9440	378	0.71008	0.000016
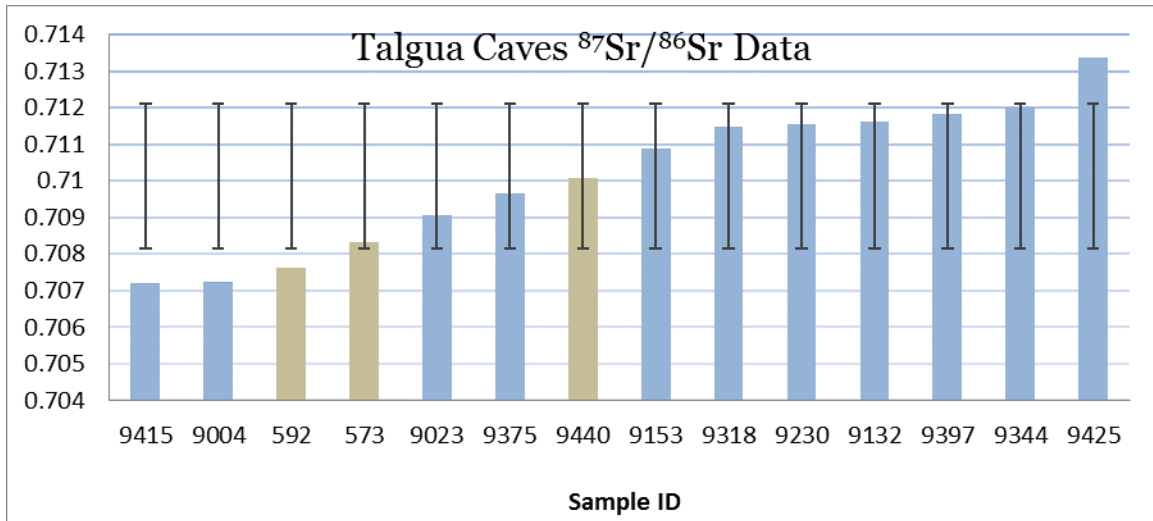
Figure 6.1   Distribution of ^{87}Sr/^{86}Sr Data

Arañas Cave   Talgua Cave

When the ^{87}Sr/^{86}Sr data was separated by site, the Cueva del Río Talgua dataset

(n=11) range from 0.70719 to 0.71338 with a mean of 0.71054. The ^{87}Sr/^{86}Sr mean for

Talgua is only slightly elevated from the ^{87}Sr/^{86}Sr mean of the dataset as a whole, but

Grubb's test identified a different outlier. Sample 9415 was identified as a possible

outlier (G=1.670, U=0.693), but not at a significant level (p=0.424). Once the possible

outliers (samples 9415 and 9425) were removed, the mean for the complete Talgua Caves

dataset is 0.71011. Cueva de las Arañas ^{87}Sr/^{86}Sr (n=3) data range from 0.70761 to

0.71008 with a mean of 0.70867. No outlier techniques were performed on Arañas due to

the small sample size.

The Talgua Caves ^{87}Sr/^{86}Sr dataset was initially compared to ^{87}Sr/^{86}Sr data from

Mesoamerica, since archaeological bioavailable data is unavailable for Lower Central

America. The mean ^{87}Sr/^{86}Sr value for Talgua Caves (0.71011) does not correspond to

any mean bioavailable signatures in the Mesoamerican Region, indicating that the mean

87

value (0.71011) is unique to the northeastern Honduran region. Additionally, imported products do not appear to alter or skew the data. Sea salt, for instance, enriches $^{87}Sr/^{86}Sr$ signatures, skewing bioavailable signatures towards the ratio of seawater (0.70920). Only sample 9023 (0.70907) has an $^{87}Sr/^{86}Sr$ value near the seawater ratio. The two possible sample outliers (9425 and 9415) were compared to the Mesoamerican bioavailable data (Appendix C.1). Sample 9425 (0.71338) does not correspond to any of the mean signatures available for the Mesoamerican region. This individual may have originated near an area of old metamorphic rock or even the Maya Mountains (0.71200-0.71800). Sample 9415 (0.70719), may have originated from the Maya Lowlands, possibly near Quiriguá (0.70730) located in southeast Guatemala. Other low $^{87}Sr/^{86}Sr$ sample values from the Talgua dataset (9004=0.70723 and 592=0.70761) fall outside of the one standard deviation range (0.002) may have possible Mesoamerican geographic origins. For instance, sample 592 (0.70761) from Arañas has a similar bioavailable signature to the Cerro de las Mesas (0.70760) mean. This discussion of the geographic origins for the Talgua Cave individuals using $^{87}Sr/^{86}Sr$ is preliminary and is further evaluated in section 6.4.1.

6.2   Oxygen isotope data

The statistical summary for the $\delta^{18}O_c$ and $\delta^{18}O_p$ data (n=37) is presented below, along with the diagenetic test for CO_3. Further discussion of the $\delta^{18}O$ data is detailed in the research question section (6.3). Thirty-eight samples were analyzed for $\delta^{18}O_c$ (Table 6.2). A duplicate $\delta^{18}O_c$ sample (9266) was measured to determine the precision of the analysis, which was not significantly different between the values, -3.11‰ and -3.34‰ (s.d.=0.163). The Talgua Caves $\delta^{18}O_c$ values range from -4.54‰ to -2.94‰ with a mean

of -3.68‰ for the dataset. The Shapiro-Wilk normality test results demonstrate that the $\delta^{18}O_c$ data is not normally distributed (w=0.923, p=0.014) at the 0.02 level. Based on two standard deviations from the mean two samples (9023=-4.53‰ and 9191=-4.54‰) are outliers in the $\delta^{18}O_c$ dataset (s.d.=0.832). When separating the $\delta^{18}O_c$ data by site, Cueva del Río Talgua $\delta^{18}O_c$ data (n=32) range from -4.54‰ to -2.94‰ with a mean of -3.70‰. Cueva de las Arañas $\delta^{18}O_c$ (n=5) data range from -4.01‰ to -3.11‰ with a mean of -3.54‰. No outliers are present in the $\delta^{18}O_c$ data when separated by site.

Table 6.2   Oxygen Isotope Results

Site	Sample	δ¹⁸O_c (VPDB)	δ¹⁸O_c (VSMOW)	δ¹⁸O_p (VSMOW)	Δδ¹⁸O_c-δ¹⁸O_p (VSMOW)
Arañas	573	-3.92	26.87	16.93	9.94
Arañas	592	-3.31	27.50	18.07	9.43
Arañas	695	-4.01	26.77	16.62	10.15
Talgua	9004	-2.98	27.84	16.32	11.53
Talgua	9021	-3.95	26.84	18.26	8.58
Talgua	9023	-4.53	26.24	15.50	10.74
Talgua	9108	-3.71	27.09	16.21	10.88
Talgua	9109	-3.97	26.82	16.61	10.21
Talgua	9110	-3.43	27.37	16.44	10.94
Talgua	9111	-3.18	27.64	16.86	10.77
Talgua	9132	-3.78	27.02	16.72	10.30
Talgua	9153	-3.33	27.48	16.56	10.92
Talgua	9154	-3.46	27.34	16.77	10.57
Talgua	9155	-4.11	26.67	15.18	11.50
Talgua	9188	-3.81	26.99	16.82	10.17
Talgua	9190	-3.64	27.15	17.03	10.12
Talgua	9191	-4.54	26.23	16.64	9.59
Talgua	9230	-3.66	27.14	17.46	9.69
Talgua	9240	-4.45	26.32	16.08	10.24
Talgua	9265	-3.97	26.82	17.10	9.73
Talgua	9266	-3.23	27.58	16.92	10.66
Talgua	9275	-3.90	26.89	16.93	9.96
Talgua	9288	-3.29	27.52	17.03	10.49
Talgua	9303	-3.53	27.27	16.73	10.54
Talgua	9304	-3.76	27.04	16.31	10.72
Talgua	9318	-3.59	27.21	18.20	9.01
Talgua	9344	-3.21	27.60	17.19	10.41
Talgua	9352	-3.57	27.23	16.75	10.48
Talgua	9364	-3.61	27.19	16.92	10.27
Talgua	9368	-3.72	27.07	16.96	10.12
Talgua	9375	-3.32	27.48	17.65	9.84
Talgua	9397	-2.94	27.88	17.31	10.58
Talgua	9399	-4.30	26.47	16.96	9.52
Talgua	9415	-3.65	27.15	17.73	9.41
Talgua	9425	-4.18	26.60	16.71	9.89
Arañas	9440	-3.11	27.71	16.95	10.76
Arañas	9442	-3.37	27.43	18.36	9.07

High ΔC-P offsets in red

Thirty-nine samples were measured for $\delta^{18}O_p$, two of which were duplicates. Duplicate samples (9191 and 9415) were measured for $\delta^{18}O_p$ to determine the precision of the analysis. Using the Student's t-test, the precision of the $\delta^{18}O_p$ measurements was high (t=0.296, p=0.994). Once the duplicate samples were averaged together, the Talgua Caves $\delta^{18}O_p$ values range from 15.18‰ to 18.36‰ with a mean of 16.88‰ for the dataset. The Shapiro-Wilk normality test results demonstrate that the $\delta^{18}O_p$ data was not normally distributed (w=0.936, p=0.035) at the 0.05 level. This larger distribution increased the number of outliers, and included four samples (9021=18.26‰, 9023= 15.50‰, 9155=15.18‰, and 9442=18.36‰), which were two standard deviations from the mean (s.d.=1.361). Sample 9023 is the only common outlier between the $\delta^{18}O_p$ and $\delta^{18}O_c$ datasets, along with being one of the possible $^{87}Sr/^{86}Sr$ outliers. Sample 9023 is explored in detail in the discussion of this research.

When separating the $\delta^{18}O_p$ data by site, Cueva del Río Talgua $\delta^{18}O_p$ data (n=32) range from 15.18‰ to 18.26‰ with a mean of 16.84‰. Cueva de las Arañas $\delta^{18}O_p$ (n=5) data range from 16.62‰ to 18.36‰ with a mean of 17.39‰. The inter-site comparison showed no outliers for Arañas, and four outliers for Talgua. The same samples (9021, 9023, and 9155) were present when Talgua was separated, along with sample 9318 (18.20‰). Outlier 9442, discussed above for the complete $\delta^{18}O_p$ dataset was no longer included in the inter-site outlier comparison.

Using the Coplan et al. (1983) equation to convert the $\delta^{18}O_c$ (VPDB) to $\delta^{18}O_c$ (VSMOW) values, ten Talgua Cave samples exhibited high ΔC-P offsets. Samples with offsets greater than 10.6‰ were regarded with caution during remaining analysis, especially for the $\delta^{13}C$ and $\delta^{18}O_c$ datasets, and are highlighted in red in Figure 6.2.

Diagenesis "affected" a combination of tooth types, including first molars, second

molars, and premolars. Keeping in mind the advantage of both $\delta^{18}O_c$ and $\delta^{18}O_p$ (i.e.

carbonate analysis is more accurate, but considerably more vulnerable to alteration than

phosphate, which is significantly resistant to diagenetic alteration), the results from the

diagenetic test will not hinder the interpretation of the $\delta^{18}O_p$ dataset. As mentioned

previously, the high offset may not be attributed to alteration in CO_3 but due to

differences in $\delta^{18}O$ uptake during mineralization. Additionally, the removal of the

possibly affected samples does not appear to alter the interpretation of results in this
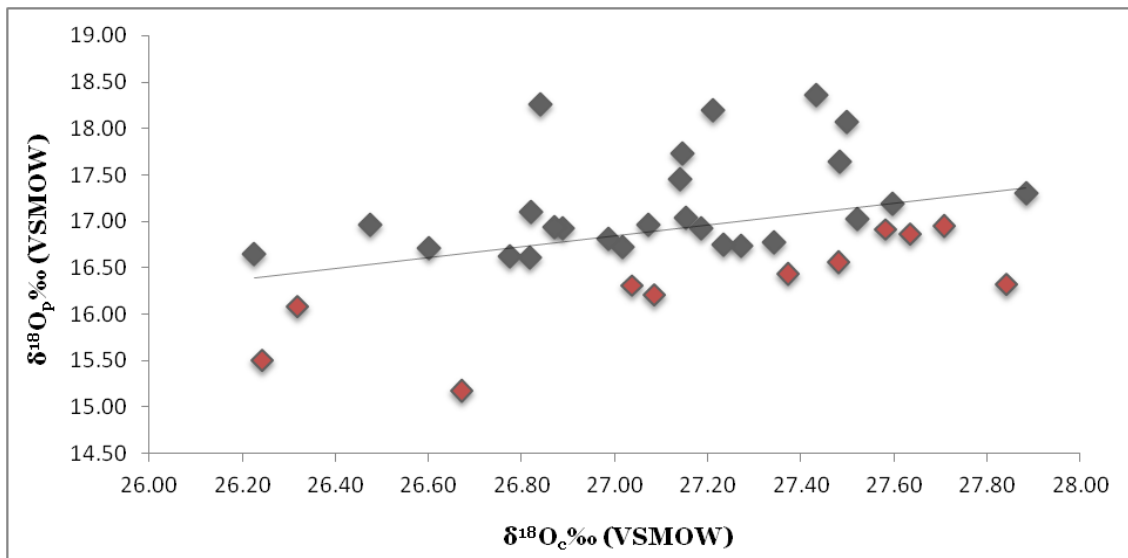
research (see PCA discussion).

Figure 6.2   Possibly Altered $\delta^{18}O_c$ Samples (in red)

Since a combination of tooth types was used for this research project, inter-tooth

differences were explored for both $\delta^{18}O_p$ and $\delta^{18}O_c$. The possibly altered $\delta^{18}O_c$ were

removed for this portion of exploratory analysis. A total of 15 M1s, 19 M2s, and a single

I1, P1, and P2 were sampled for isotope measurements. The specific tooth number for each sample is detailed in the oxygen table above. Scatter plots did not show any notable relationships between δ18O value and tooth type for either the $\delta^{18}O_c$ or $\delta^{18}O_p$. The mean $\delta^{18}O_c$ and $\delta^{18}O_p$ values for M1s were -3.82‰, 16.72‰ (respectively) and -3.67‰, 16.99‰ (respectively) for M2s. There was no significant difference between M1s and M2s for $\delta^{18}O_p$ (ANOVA: F=2.157, p=0.153). Inter-tooth isotope differences are further discussed below in the Carbon isotope data section (6.3).

6.3   Carbon isotope data

The statistical summary for the $\delta^{13}C$ data (n=37) is presented below, along with the results from the PCA. A further discussion of the $\delta^{13}C$ analysis is detailed below in the Research question section. Thirty-eight samples were analyzed for $\delta^{13}C$, which included one duplicate sample (Table 6.3). The duplicate was measured to determine the precision of the $\delta^{13}C$ results, and was high (s.d.=0.070). The Talgua Cave $\delta^{13}C$ values exhibit a large range of variation, ranging from -11.71‰ to -5.95‰ with a mean of -8.02‰ for the dataset. When the possible diagenetic samples were removed, the range of $\delta^{13}C$ values changes slightly (-11.71‰ to -6.02‰, mean=-8.07‰, s.d.=1.335). This mean reflects a diet high in C_3 species consumption. For instance, during the PreClassic Period at the Maya site, Kaminaljuyu, the $\delta^{13}C$ mean for M1s is around -2.7‰ and -1.8‰ for M3s, demonstrating a diet high in C_4 plant consumption. Although the Talgua Cave individuals exhibit $\delta^{13}C$ signatures high in C_3 plant consumption, some samples are enriched, such as sample 9109 (-6.02‰), and relates to a mixed diet of C_3 and C_4 foods. The Shapiro-Wilk normality test results demonstrated that the $\delta^{13}C$ data was normally distributed (w=0.923, p=0.552). When separating the $\delta^{13}C$ data by site, Cueva del Río

Talgua $\delta^{13}C$ data (n=32) range from -11.71‰ to -5.95‰ with a mean of -8.11‰

(s.d.=1.508). Cueva de las Arañas $\delta^{13}C$ (n=6) data range from -8.67‰ to -6.41‰ with a

mean of -7.45‰ (s.d.=0.987). This difference in $\delta^{13}C$ variation between the two cave

sites suggests slight differences in diet, certain individuals in Talgua having higher C_3

diets, but the sample size for Arañas is not large enough for this interpretation.

Table 6.3   Carbon Isotope Results

Site	Sample	Tooth	$\delta^{13}C$ (‰)
Arañas	573	31	-8.12
Arañas	592	15	-8.67
Arañas	695	31	-6.41
Talgua	9004	9	-11.58
Talgua	9021	18	-6.67
Talgua	9023	18	-6.69
Talgua	9108	15	-7.37
Talgua	9109	15	-6.02
Talgua	9110	15	-7.56
Talgua	9111	15	-10.46
Talgua	9132	19	-7.11
Talgua	9153	3	-8.24
Talgua	9154	3	-8.30
Talgua	9155	3	-6.49
Talgua	9188	14	-9.68
Talgua	9190	14	-8.30
Talgua	9191	14	-6.73
Talgua	9230	2	-8.93
Talgua	9240	3	-8.00
Talgua	9265	30	-7.88
Talgua	9266	30	-8.02
Talgua	9266 *	30	-7.97
Talgua	9275	19	-8.57
Talgua	9288	19	-8.14
Talgua	9303	2	-10.31
Talgua	9304	2	-5.95
Talgua	9318	15	-9.63
Talgua	9344	2	-6.96
Talgua	9352	2	-7.09
Talgua	9364	19	-7.86
Talgua	9368	19	-11.71
Talgua	9375	2	-8.13
Talgua	9397	2	-10.05
Talgua	9399	2	-7.25
Talgua	9415	19	-6.94
Talgua	9425	15	-6.83
Arañas	9440	11	-6.52
Arañas	9442	4	-7.54

* Duplicate sample measurement
Possibly altered samples in red

Since a combination of tooth types was used for this research project, inter-tooth differences were also explored for the δ^{13}C dataset. The relationship between M1s (n=15) and M2s (n=19) was examined, since only single values were measured for C, I1, and P2. The mean for M1s was -8.13‰ (s.d.=1.274) and -7.85‰ (s.d.=1.447) for M2s. Using a one-way ANOVA, no significant differences between the means for M1s and M2s (F=0.348, p=0.559) were observed. Since the mean value for these two groups do not explain significant variation, a scatter plot was used to explore any variation. The M1s grouped together, where the M2s vary in both δ^{13}C and δ^{18}O$_p$ (Figure 6.3). Initially the range for M1s was -11.71‰ to 6.49‰, but after sample 9368 (-11.71‰) was removed the range drops from -8.57‰ to -6.49‰ (mean=-7.74, s.d.=0.677). Sample 9368 may have been incorrectly identified as a M2 due to the fragmented condition of the tooth. Both the original scatterplot and the scatter plot with sample 9368 removed show the M1s clustering approximately around -8.5‰ to -6.5‰ (2‰ difference). The difference between the M1s and M2s for δ^{13}C may demonstrate stricter childhood feeding practices before the age of three (approximate), and the diet is diversified after this possible weaning period.
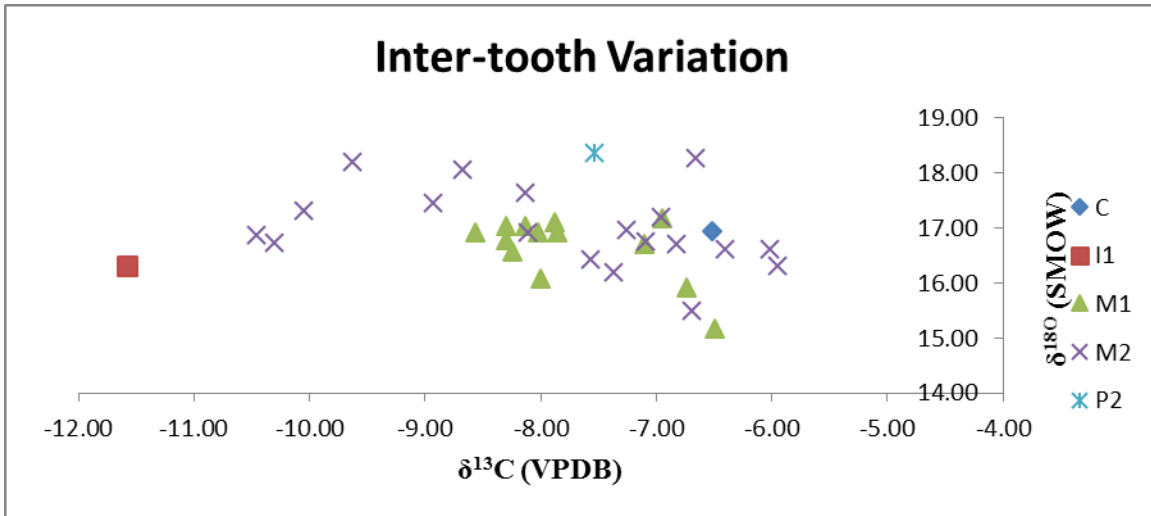
Figure 6.3   Carbon and Oxygen Inter-tooth Variation

A principle component analysis (PCA) is presented in this section, since all of the
isotope summary information has been introduced. A PCA analysis was conducted using
all four isotope variables ($\delta^{13}C$, $\delta^{18}O_c$, $\delta^{18}O_p$, and $^{87}Sr/^{86}Sr$), therefore a limited number of
samples were explored with this technique (n=14). Most of the variance (loadings) was
observed in compartments 1 and 2 of the PCA (cumulative proportion, 0.729).
Component 1 is strongly correlated with three variables ($\delta^{13}C$, -0.583; $\delta^{18}O_c$, 0.633;
$\delta^{18}O_p$, 0.482) and Component 2 is strongly correlated with two of the isotope variables
($^{87}Sr/^{86}Sr$, 0.850; $\delta^{18}O_p$, 0.476). Some relationships are observed in the loadings and on
the PCA graph (Table 6.4; Figure 6.4). There is a negative relationship between $\delta^{13}C$ and
both the $\delta^{18}O_c$ and $\delta^{18}O_p$ isotopes. The $^{87}Sr/^{86}Sr$ data has a relationship with $\delta^{13}C$ (0.219),
and $\delta^{18}O_p$ (0.476), but they are not significant. Two separate groups of samples cluster
together, showing similar relationships for all isotope variables. Samples 573 and 9415 (1
and 12 on the graph) are especially close in $\delta^{18}O_p$ (16.93‰ and 17.19‰) and somewhat

97

similar in $^{87}Sr/^{86}Sr$ (0.70831 and 0.70719) values. Samples 9153 and 9440 (6 and 14 on

the graph) have strong $\delta^{18}O_p$ (16.95‰, 16.56‰), and somewhat similar $^{87}Sr/^{86}Sr$

(0.71008, 0.71162) and $\delta^{18}O_c$ (-3.11‰, -3.33‰) relationships. These four samples also

represent both caves (Arañas and Talgua), where samples 573 and 9440 were recovered

from Arañas and samples 9153 and 9415 were recovered from Talgua. Individuals

interred in the two separate ossuaries have very similar isotopic signatures, which

supports the mortuary interpretation that the samples are from the same or similar

population.

Table 6.4   PCA Samples and Loadings

Graph ID	Sample	Cave	Component 1	Component 2	Component 3	Component 4
1	573	Arañas	-0.504	-0.938	-0.495	0.560
2	592	Arañas	1.464	-0.451	-1.396	0.254
3	9004	Talgua	1.903	-2.248	1.413	0.018
4	9023	Talgua	-3.041	-1.468	0.378	0.383
5	9132	Talgua	-1.143	0.552	0.241	-0.141
6	9153	Talgua	-0.092	0.003	0.773	-0.550
7	9230	Talgua	0.299	0.783	0.217	0.718
8	9318	Talgua	1.217	1.166	-0.248	1.219
9	9344	Talgua	-0.084	1.144	0.001	-0.956
10	9375	Talgua	0.758	0.243	-0.655	-0.115
11	9397	Talgua	1.654	0.726	1.084	-0.142
12	9415	Talgua	-0.316	-1.036	-1.396	-0.262
13	9425	Talgua	-1.987	1.314	0.478	0.450
14	9440	Arañas	-0.129	0.210	-0.394	-1.435
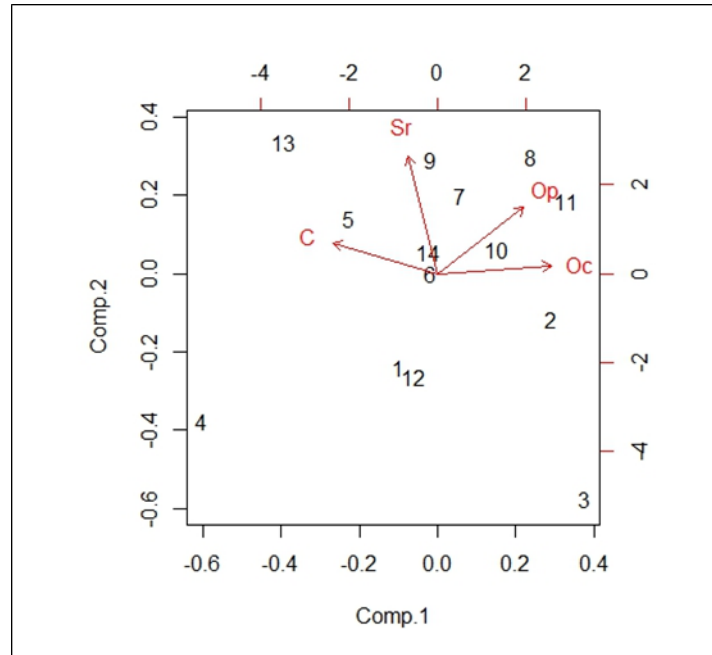
Figure 6.4   PCA Graph

It is also important to note the negative relationships observed for certain samples on the graph. For instance samples 9004, 9023, and 9425 (3, 4, and 13 on the graph) fall towards the edges of the central PCA cluster. Sample 9004 has the most depleted δ^{13}C signature (-11.58‰). Samples 9023 and 9425 are the possible "non-locals" to the Olancho Valley. Sample 9023 is the only common outlier between the δ^{18}O$_p$ and δ^{18}O$_c$ datasets, along with being one of the possible ^{87}Sr/^{86}Sr outliers. Sample 9425 is a possible ^{87}Sr/^{86}Sr outlier with the highest value (0.71338). The PCA was also conducted after the possibly altered samples were removed, four in total, limiting the sample size to 10 individuals. The PCA shows the same correlations that were discussed above, without the groupings of samples 9153 and 9440, since those samples were removed due to the possible diagenetic alteration of the δ^{18}O$_c$ (i.e. CO$_3$ molecule).

99

6.4 Research questions

This half of the chapter focuses on the primary and secondary research objectives of this project, which are divided into geographic origin, mortuary arrangement, and dental metric analysis. Each of these sections discusses the research questions and hypotheses. The hypotheses and/or research questions were explored and tested using the $\delta^{13}C$, $\delta^{18}O_c$, $\delta^{18}O_p$, and $^{87}Sr/^{86}Sr$ isotope datasets and the methods and techniques discussed in Chapter V.

6.4.1 Geographic origin

Primary research question 1 of this project was addressed using the exploratory outlier data presented at the beginning of this chapter and the likelihood assignments run in the ArcGIS model. The likelihood assignments were used as a quantitative approach for determining geographic origin from the $^{87}Sr/^{86}Sr$ and $\delta^{18}O_p$ Talgua Cave isotope data. To reiterate, the primary research objective and supporting questions and hypotheses, they are stated below:

- Research objective 1: To determine the geographic origins of the individuals interred at Talgua Caves.

- Question 1: Do the individuals sampled from the Talgua Caves have a high probability of originating from northeast Honduras?

- H_0: The Talgua Cave $^{87}Sr/^{86}Sr$ or $\delta^{18}O$ bioavailable signatures are assigned to northeast Honduras at 90% probability.

The above hypothesis was tested by assigning all of the $^{87}Sr/^{86}Sr$ samples (n=14) using the calibrated catchment model, and assigning the $\delta^{18}O_p$ by bin (n=4) using the $\delta^{18}O$ precipitation model developed in IsoMAP. Additionally, the $\delta^{18}O_p$ outliers (samples

9021, 9023, 9155, and 9442), and PCA "outliers" (9004, 9023, and 9425) that were determined through the exploratory techniques were also assigned using the δ^{18}O precipitation IsoMAP as secondary indicators for the ^{87}Sr/^{86}Sr assignments.

The likelihood assignment models with 90% probability surfaces generated broad geographical likelihood surfaces that encompassed areas within the circum-Caribbean region (Figure 6.5). These high probability areas are depicted in the maps below using isopleths, or polylines surrounding the 90% probability areas, for the δ^{18}O$_{dw}$ assignments. There is a general enrichment of the δ^{18}O$_{dw}$ towards the coastlines. Therefore the higher the δ^{18}O$_{dw}$ sample value, the larger the geographic extent of the probability surface. The δ^{18}O$_{dw}$ assignments have coarse resolution and adjusting the cell size of the δ^{18}O rasters did not decrease the pixel resolution. Bin 1 (-9.44‰, s.d.=0.292) shows the high probability areas inland that increase towards the 'Mesoamerican' zone, with small 90% probability zones throughout northeast Honduras. Bin 2 (-7.91‰, s.d.=0.287) and Bin 3 (-7.28‰, s.d.=0.223) have similar likelihood surfaces. These bins show high probability areas inland that increase towards the "Mesoamerican" zone and modern day Costa Rica, with linear 90% probability zones that encompass the Talgua Caves and Olancho Valley. High probability areas for Bin 4 (-5.97‰, s.d.=0.374) include the majority of the inland, only excluding the coastal areas and portions of the Olancho Valley from the likelihood origins. Unlike the δ^{18}O model, the ^{87}Sr/^{86}Sr likelihood assignments had higher resolution and could be used to determine if individuals originated from different locations, possibly even within the Olancho Valley. All of the likelihood assignment maps that were generated from the models are shown in Appendix B.
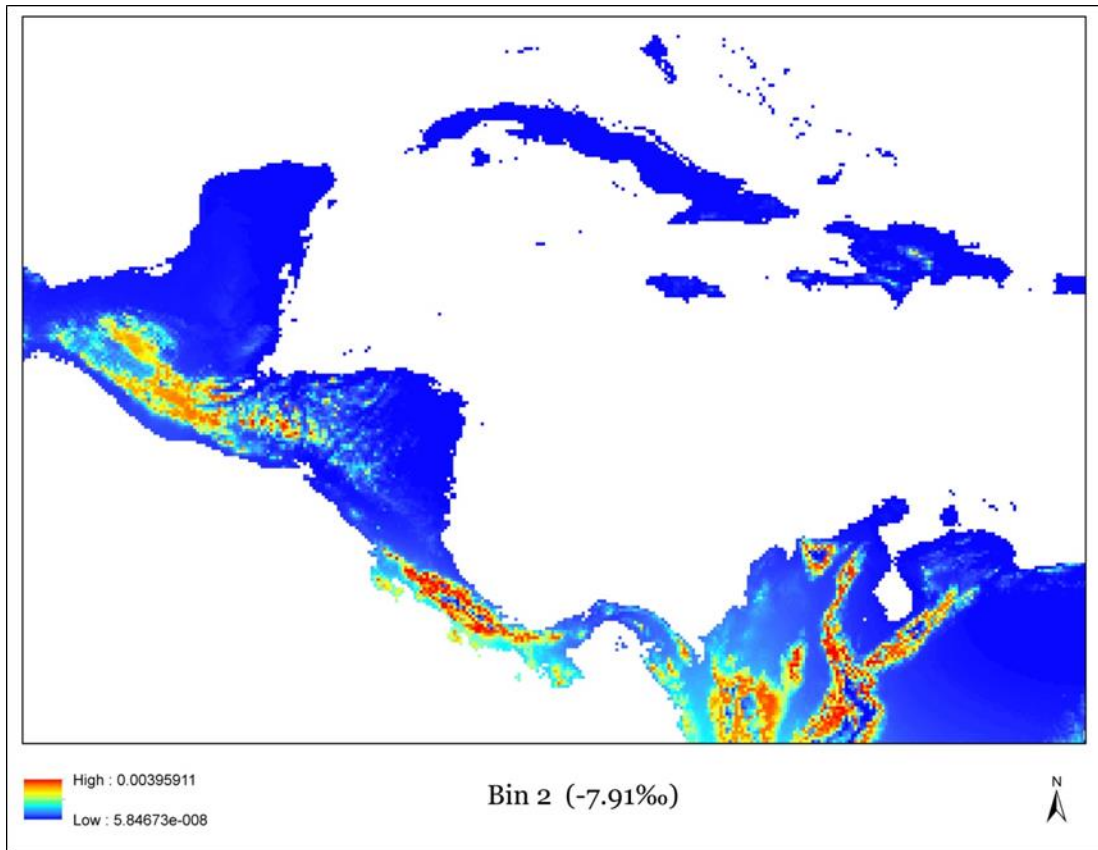
Figure 6.5   Geographic Extent of the Likelihood Assignment Model Output

The ^{87}Sr/^{86}Sr sample values and their corresponding measurement error were input into the calibrated ^{87}Sr/^{86}Sr catchment model. After these assignment probability surfaces were generated, the Talgua Cave ^{87}Sr/^{86}Sr values were separated into six bins and input into the calibrated soil and bedrock geographic ^{87}Sr/^{86}Sr models to compare the Talgua Cave ^{87}Sr/^{86}Sr assignments. All of the ^{87}Sr/^{86}Sr assignments generated high probability areas that encompassed portions of northeast Honduras. Bin 1 (samples 592, 9004, and 9415) had ^{87}Sr/^{86}Sr ratios ranging from 0.70719 to 0.70761, and were assigned in the Olancho valley (Figure 6.6). The likelihood assignment for this Bin generated a high probability surface that includes areas in Mesoamerica, South America, Lower

Central America, and Cuba, but it is probable that the individuals interred at Talgua Caves originated in the Olancho Valley. A 30 mile buffer was positioned around the Talgua Caves to determine if individuals were "non-local" to the Olancho Valley. All individuals had high probability origins near the Talgua Caves, Talgua Village Site, and other areas within the Olancho Valley (refer to Appendix B). This Bin is also most representative of the geographic $^{87}Sr/^{86}Sr$ ratios for the areas near the Talgua Caves and Talgua Village Site. Sample 9004 was a possible "outlier" in the PCA analysis, based on the individual's depleted $\delta^{13}C$ signature (-11.58‰). It is possible that this individual originated from the Olancho Valley, near the Talgua Sites, but consumed a diet high in C_3 plants at an early age (i.e. sample 9004 is an I1).

Bin 1

0.70719 to 0.70761

Probability
<50%
50-75%
75-90%
90-100%
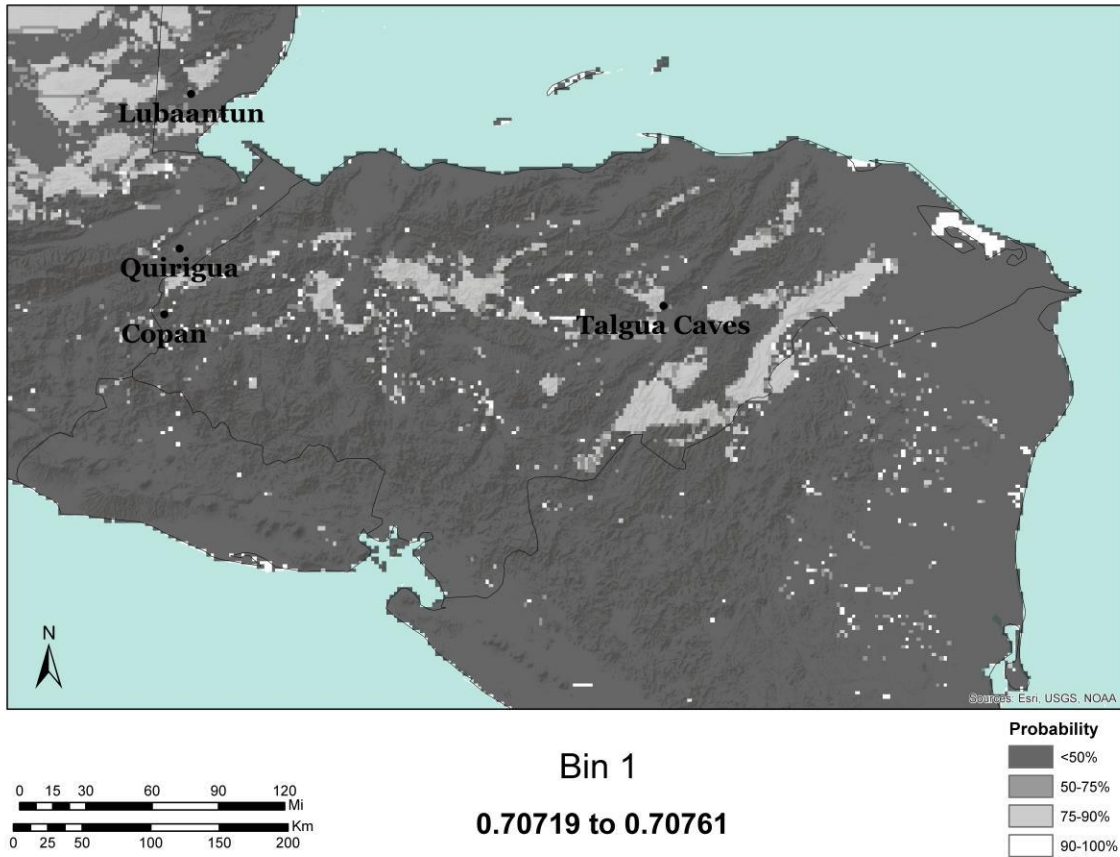
Figure 6.6   Bin 1 Assignment

Bin 2 (sample 573) or $^{87}Sr/^{86}Sr$ value 0.70831 was best assigned using the

calibrated catchment model. The high probability areas for this bin encompass much of

the visible extent of the circum-Caribbean region, including the entire Olancho Valley

(Figure 6.7). The calibrated catchment model for Bin 2 generated spotty probability

surfaces, but still included high probability zones, approximately 6.8 mi to 13.8 mi from

the Talgua Cave site. This is depicted in the buffer-zone map located in Appendix (B).

104

Bin 2

0.70831

Probability
<50%
50-75%
75-90%
90-100%
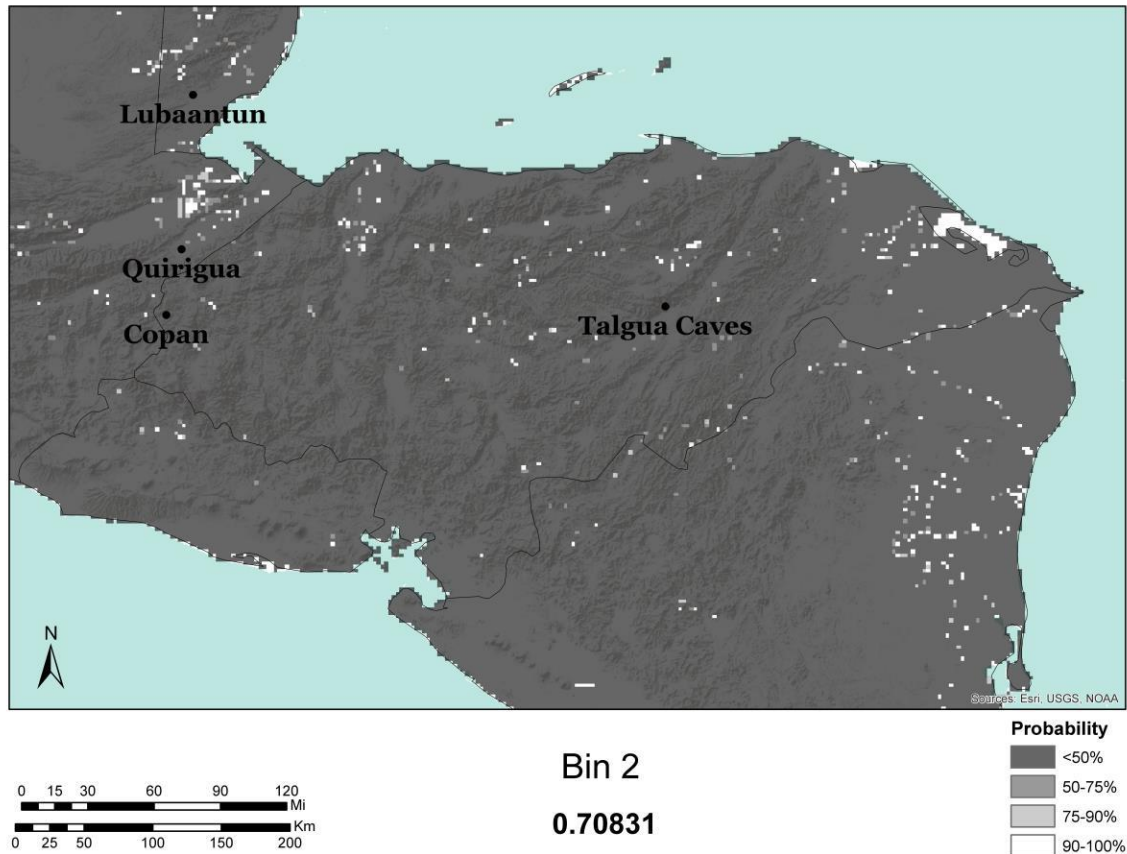
Figure 6.7   Bin 2 Assignment

Bin 3 (samples 9023 and 9375) $^{87}Sr/^{86}Sr$ values range from 0.70907 to 0.70966,

and were assigned by the catchment model to the coastal areas, such as the Mosquito

Coast in Honduras and eastern Nicaragua (Figure 6.8). The likelihood model also

generated spotty high probability areas throughout Honduras and into the Mesoamerican

region. In addition, areas within the Olancho Valley less than 20 mi from the Talgua

Caves site were observed. Although there were high concentrated probability areas near

the coast, the individuals most likely originated from the areas in the valley, based on the

$\delta^{18}O_{dw}$ likelihood assignments. The $\delta^{18}O$ likelihood assignments for the corresponding

samples (i.e. 9023=Bin 1; 9375=Bin 4) show the highest probability areas in the continental interior (Appendix B). Sample 9023 was suggested as a possible "non-local" to the Olancho valley based on the outlier techniques discussed above. The $^{87}Sr/^{86}Sr$ and $\delta^{18}O$ assignment results support this interpretation, but conflict with each other on possible region of origin. The $^{87}Sr/^{86}Sr$ assignment suggests a possible origin near the coast and the $\delta^{18}O$ assignment suggests a continental origin. Assuming the $\delta^{18}O$ assignment results are correct, than the individual may have originated outside of the Olancho Valley, since the only $^{87}Sr/^{86}Sr$ high probability areas in the valley are within the 50% probability range (B: Sample 9023). Where exactly the individual originated from in the interior is unknown.

Bin 3

0.70907 to 0.70966

Probability
<50%
50-75%
75-90%
90-100%
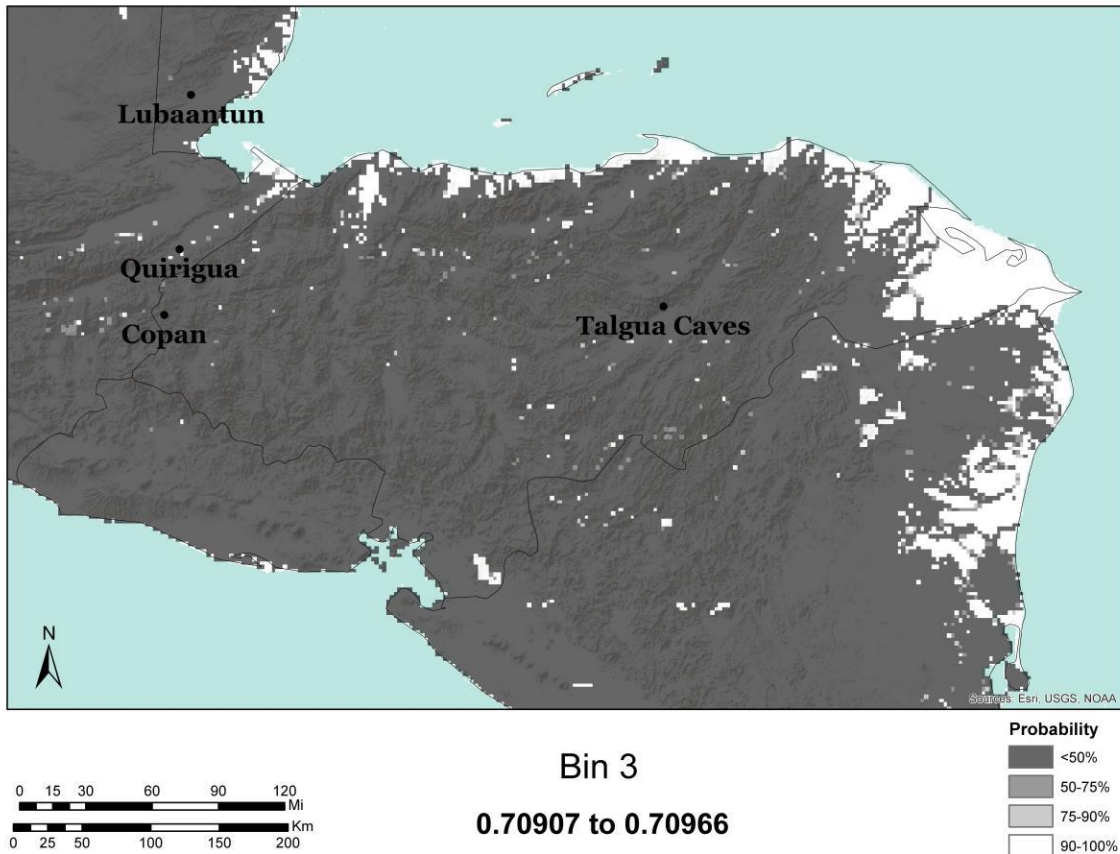
Figure 6.8   Bin 3 Assignment

Bin 4 (samples 9153 and 9440) ^{87}Sr/^{86}Sr range from 0.71008 to 0.71089, and were

best assigned by the calibrated catchment ^{87}Sr/^{86}Sr model. Areas of high probability

included the Mosquito Coast and eastern Nicaragua, similar to the probability surfaces

generated with the Bin 3 assignment (Figure 6.9). Bin 4 geographic assignment also

included the Olancho Valley with high probability (90%). These zones did not include

the geographic location of the Talgua Village, but were within approximately 20 mi of

the Talgua Caves (Appendix B). Neither of these samples was determined as possible

outliers from the exploratory techniques.
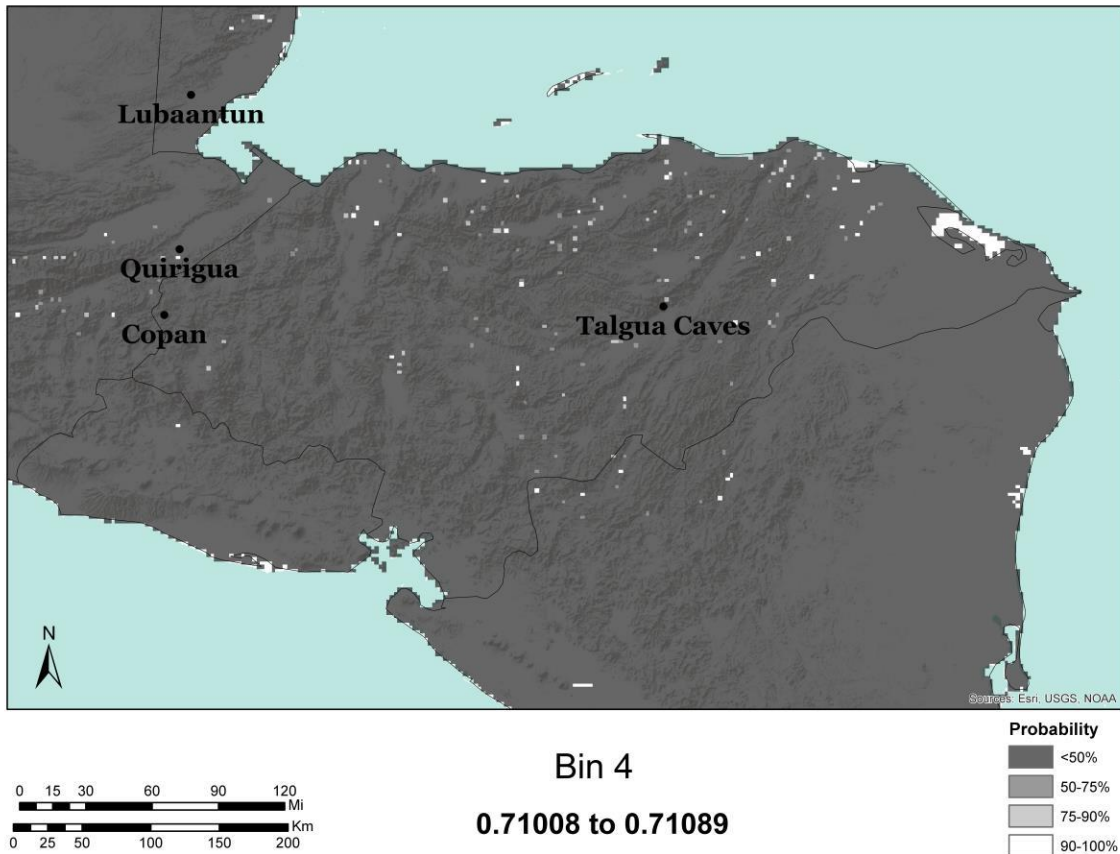
Figure 6.9   Bin 4 Assignment

Bin 5 (samples 9132, 9230, 9318, 9344, and 9397) had $^{87}Sr/^{86}Sr$ values ranging

from 0.71147 to 0.71199, and assigned all of the individuals to the Olancho Valley

(Figure 6.10). The calibrated catchment $^{87}Sr/^{86}Sr$ isoscape was the best fit for assigning

samples 9344 and 9397 and the soil $^{87}Sr/^{86}Sr$ isoscape was the best fit for the remaining

samples in Bin 5. The likelihood surfaces generated for samples 9132, 9230 and 9318

were spotty, but assigned the individuals within the southwest portion of the valley,

approximately 21.6 to 25.9 mi, and north in the adjacent valley, 12.8 mi north from the

Talgua Cave location (Appendix B). None of these samples were determined as possible

outliers from the exploratory techniques discussed above.
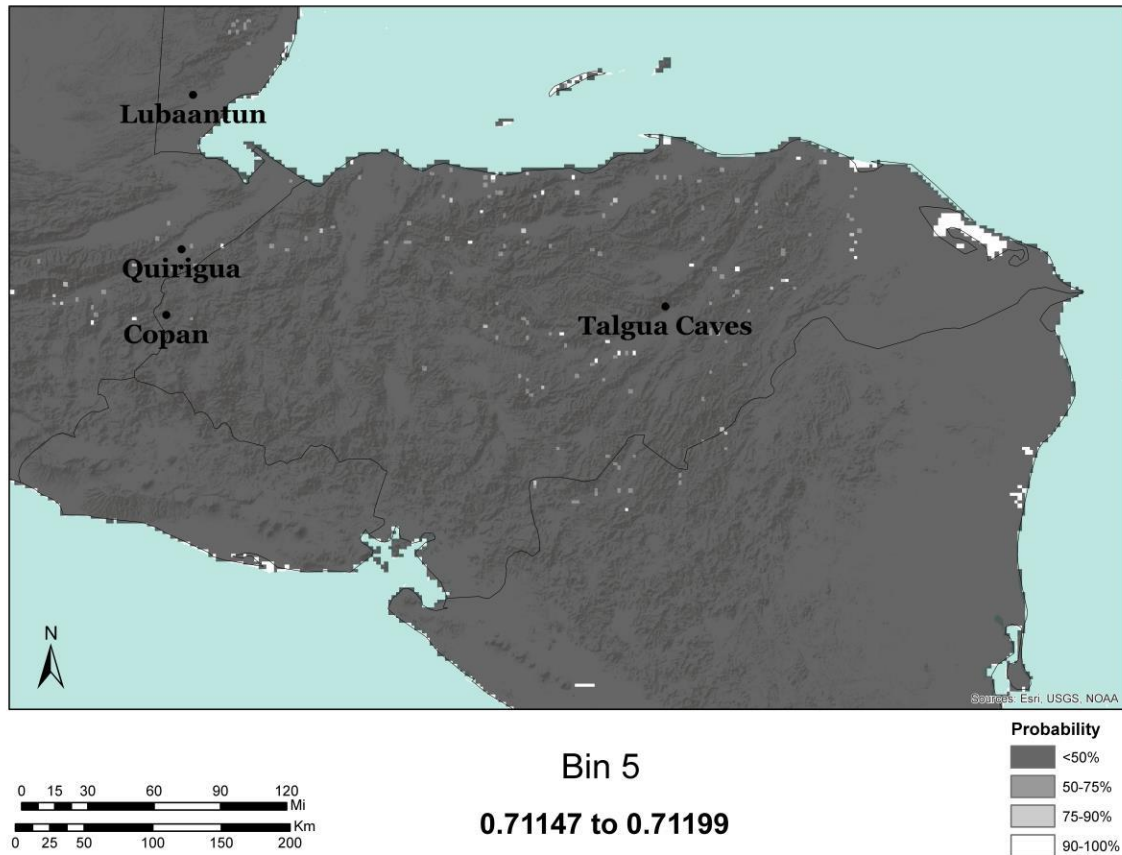
Figure 6.10   Bin 5 Assignment

The final bin, Bin 6 (sample 9425), had one $^{87}Sr/^{86}Sr$ value of 0.71338, which was

determined to be a possible outlier in the $^{87}Sr/^{86}Sr$ dataset, although not significant. The

calibrated bedrock $^{87}Sr/^{86}Sr$ model generated the best likelihood probability surface,

which assigned the individual to portions of the valley, approximately 15.8 mi to the

southwest and/or 8.2 mi to the northeast mountainous region (Figure 6.11). Therefore, in

this case, the assignment model result conflicted with the exploratory outlier techniques

performed on the isotope datasets. One possibility is that the individual had a childhood origin within or near the Olancho Valley, but this location differed from the other individuals sampled for analyses.
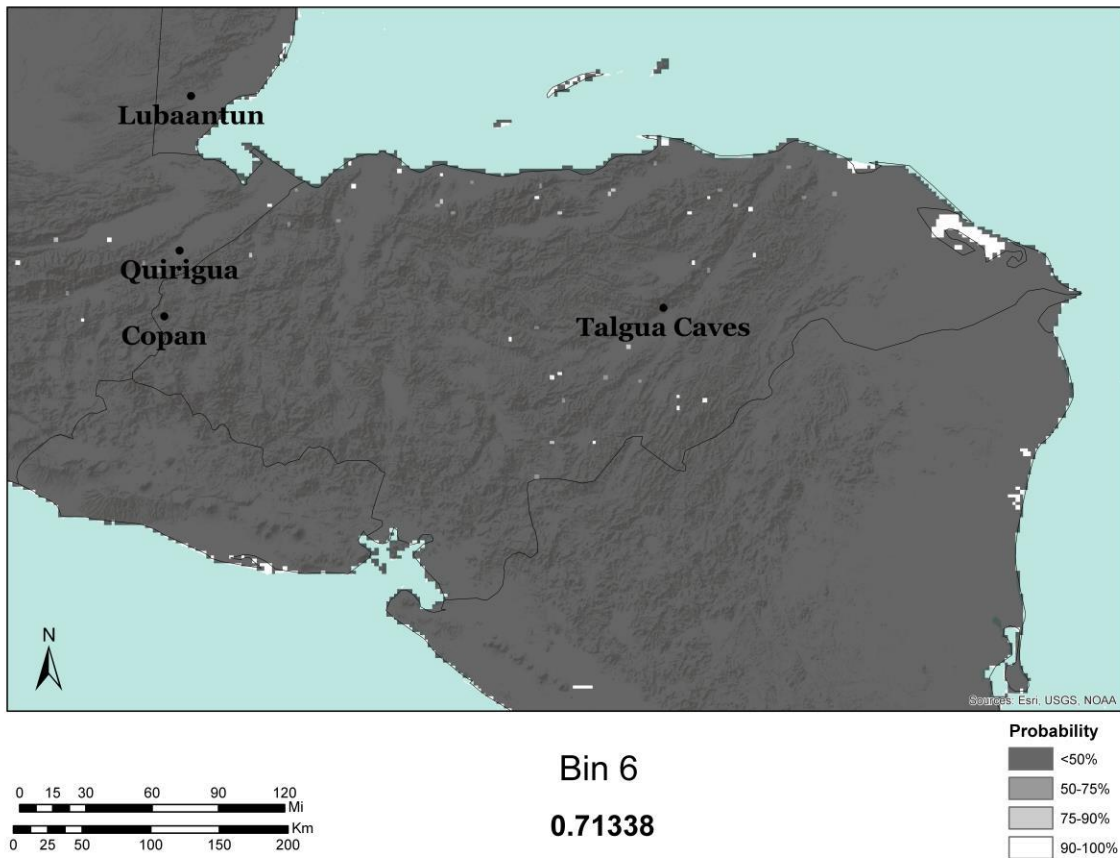
Figure 6.11   Bin 6 Assignment

Based on the $^{87}Sr/^{86}Sr$ and $\delta^{18}O_{dw}$ likelihood assignments, all of the Talgua Cave individuals tested in this research have a 90% probability of geographically originating from northeast Honduras, therefore the null hypothesis is accepted for Question 1. Although the null hypothesis was accepted, all of the individuals interred at the Talgua Caves did not have the same childhood geographic origins based on the $^{87}Sr/^{86}Sr$

assignments discussed above. For instance, Bins 1 and 2 had high probability likelihoods of originating from the Talgua Village site, and three of the samples in Bin 5 were either from the southwest portion of the valley (~21 to 25 mi away) or the adjacent valley. Sample 9023 was the only $^{87}Sr/^{86}Sr$ sample that did not have a high probability of originating from the Olancho Valley or within the 30 mile buffer zone (see images in Appendix B). In conclusion, it appears that there may be two separate groups, one based on the lower $^{87}Sr/^{86}Sr$ values (i.e. 0.70761) and one based on the higher $^{87}Sr/^{86}Sr$ values, such as 0.71156, that are interred in both the Arañas and Talgua Caves. From these two possible groups, sample 9023 may be "non-local" to the Olancho Valley.

6.4.2   Mortuary arrangement

- Research objective 2: To understand the mortuary arrangement in Cueva del Río Talgua through isotope values.

- Question 2: Are there distinct isotopic patterns between the spatially structured subdivisions (lots) in the Talgua Cave ossuary?

- H_0: There are random patterns of $\delta^{13}C$, $\delta^{18}O$, and $^{87}Sr/^{86}Sr$ values between the lots in the Talgua Cave ossuary.

A mortuary analysis of the individuals interred in the Talgua Caves assists in understanding the social organization and cultural practices of the Formative Period. Exploration of the isotope data ($\delta^{13}C$, $\delta^{18}O_p$, $\delta^{18}O_c$, and $^{87}Sr/^{86}Sr$) was performed prior to the spatial analysis to identify any patterns in the data at the operation level. In addition, any relationships between burial goods and isotope values were explored for Talgua. Spatial analyses of the isotope datasets were then conducted at the Lot level for Talgua using inverse distance weighting (IDW). Spatial analyses were not performed on Arañas

due to the small sample size and limited lots available for comparison across the cave. Differences that were observed in the IDW interpolation maps were examined for significance using summary statistics and a Kruskal-Wallis test.

There was limited isotope variability between the operations in Cueva del Río Talgua. From the samples (n=8) measured for Operation I, the $\delta^{18}O_p$ data range from 16.21‰ to 18.20‰, the $\delta^{18}O_c$ range from -3.97‰ to -3.18‰, the $\delta^{13}C$ range from -10.46‰ to -6.02‰, and the $^{87}Sr/^{86}Sr$ (n=2) range from 0.70933 to 0.70719. In Operation II (n= 6), the $\delta^{18}O_p$ data range from 16.31‰ to 17.46‰, the $\delta^{18}O_c$ range from -3.76‰ to -2.98‰, the $\delta^{13}C$ range from -11.58‰ to -5.95‰, and the $^{87}Sr/^{86}Sr$ (n=3) range from 0.70723 to 0.71199. In Operation III (n=18), $\delta^{18}O_p$ data range from 15.18‰ to 18.26‰, the $\delta^{18}O_c$ range from -4.54‰ to -2.94‰, the $\delta^{13}C$ range from -6.49‰ to -11.71‰, and the $^{87}Sr/^{86}Sr$ (n=6) range from 0.70907 to 0.71338. The mean values of the isotopes datasets were compared using a series of Welch's t-tests to determine if there were any significant differences throughout the Talgua operations (Table 6.5). The only differences observed between the operation means were between Operation II and III for $\delta^{18}O_c$ (t=2.285, df=13.949, p=0.038). Exploratory analysis using boxplots were also performed to visualize the range and mean distribution of the isotope datasets by operation. Although the range of $\delta^{18}O_c$ is small, the difference between the mean values for Operation II and Operation III is noticeable (Figure 6.12).

Table 6.5   Mean Isotope Values and T-Test Results by Operation for Talgua

	Talgua Cave							
Operation	**^{87}Sr/^{86}Sr***		**δ^{13}C (‰)**		**δ^{18}O$_p$ (‰)**		**δ^{18}O$_c$ (‰)**	
	Mean	s.d.	Mean	s.d.	Mean	s.d.	Mean	s.d.
I **(n=8)**	0.71026	0.003	-8.09	1.443	16.93	0.604	-3.59	0.280
II **(n=6)**	0.70933	0.003	-8.47	2.180	16.79	0.460	-3.45	0.296
III **(n=18)**	0.71107	0.002	-8.00	1.354	16.74	0.727	-3.83	0.470
t-test **I/II**	*p= 0.757*		*p= 0.718*		*p= 0.637*		*p= 0.395*	
t-test **II/III**	*p= 0.657*		*p= 0.634*		*p= 0.839*		*p= 0.038*	
t-test **I/III**	*p= 0.560*		*p= 0.885*		*p= 0.497*		*p= 0.125*	

* Sample sizes for ^{87}Sr/^{86}Sr are smaller; see paragraph above
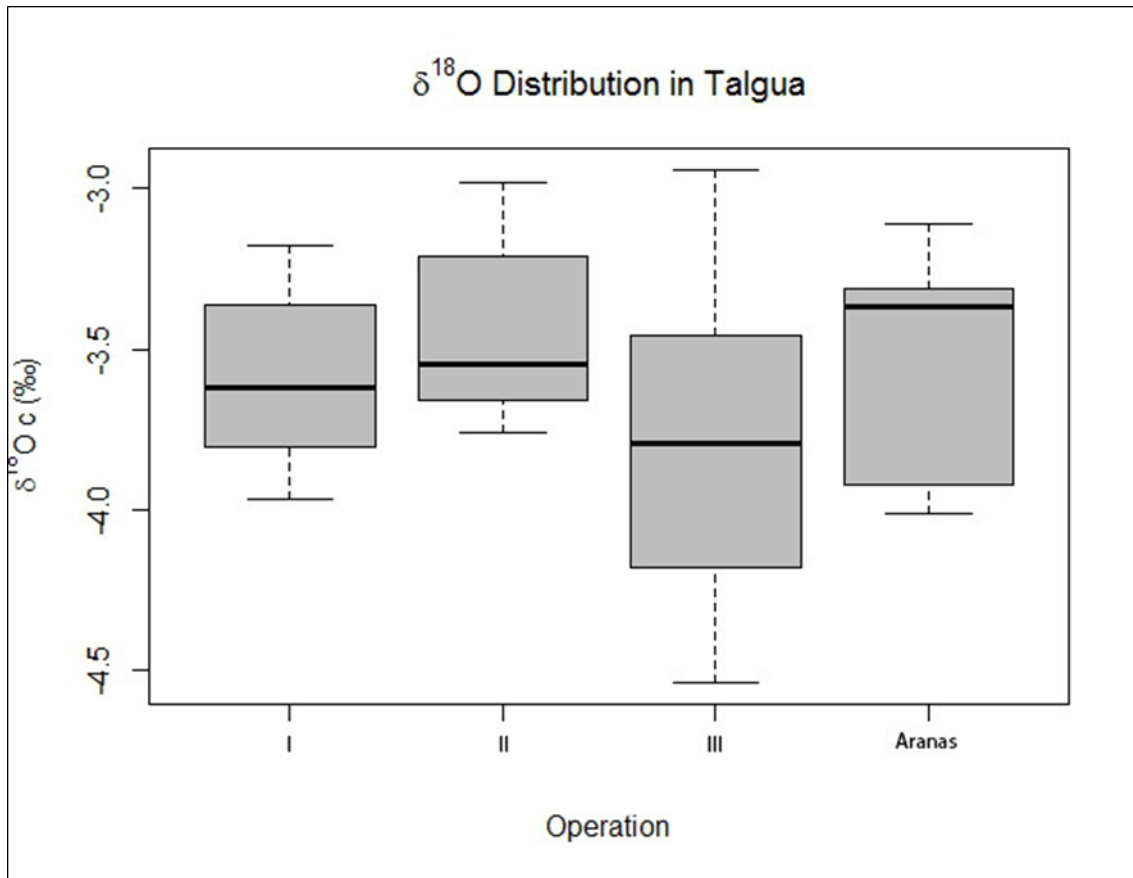
Figure 6.12   Mean $\delta^{18}O_c$ Operation Distribution in Talgua

Only two operations were available for analysis for Arañas, Operation I
(vestibule) and Operation II. A series of Welch's t-tests were performed on the mean
values of the isotope datasets. It has been suggested that the dentition recovered from the
vestibule may have been deposited later (Brady et al., 2000). Therefore, any significant
isotope differences may suggest temporal periods between depositions. Only a single
$^{87}Sr/^{86}Sr$ value was measured from the vestibule, therefore a mean comparison was not
performed between the operations for the $^{87}Sr/^{86}Sr$ data. No significant differences were
observed for the isotope means between the operations at Arañas (Table 6.6).

114

Table 6.6   Mean Isotope Values and T-Test Results by Operation for Arañas

Arañas Cave								
Operation	**$^{87}Sr/^{86}Sr$***		**$\delta^{13}C$**		**$\delta^{18}O_p$**		**$\delta^{18}O_c$**	
	Mean	s.d.	Mean	s.d.	Mean	s.d.	Mean	s.d.
Vestibule (n=2)	0.71008	NA	-7.03	0.720	17.66	0.994	-3.24	0.189
II (n=3)	0.70796	0.001	-7.73	1.179	17.21	0.761	-3.75	0.382
t-test I/II	NA		*p= 0.466*		*p= 0.647*		*p= 0.146*	

* Sample sizes for $^{87}Sr/^{86}Sr$ are smaller; see paragraph above

In order to explore the relationships between the isotope datasets ($\delta^{13}C$, $\delta^{18}O_p$, $\delta^{18}O_c$, and $^{87}Sr/^{86}Sr$) and the spatially structured subdivisions (i.e. lots) in Talgua, IDW was performed in ArcGIS. No distinct visual patterns were observed from the interpolated IDW maps for either the $\delta^{18}O_p$ or $\delta^{18}O_c$ isotopes. This may be attributed to the small ranges of variation in both $\delta^{18}O$ datasets. For instance, the $\delta^{18}O_p$ range only 0.19‰ between the mean lot values throughout Talgua. Therefore, the null hypothesis for research objective 2 is accepted for the $\delta^{18}O$ isotope datasets. The IDW did show possible patterning of the $\delta^{13}C$ and $^{87}Sr/^{86}Sr$ isotopes throughout Talgua, and are discussed below, beginning with the $^{87}Sr/^{86}Sr$ data.

An intra-ossuary analysis of $^{87}Sr/^{86}Sr$ (n=10) revealed possible divisions between $^{87}Sr/^{86}Sr$ values and burial goods, and possible divisions between $^{87}Sr/^{86}Sr$ and lot

location. Contextual artifacts, such as jade, ceramic and marble vessels, and beads were documented in five of the 13 lots sampled for isotopic analyses (Table 6.7). Of those five lots, four were sampled for $^{87}Sr/^{86}Sr$ (n=5). The $^{87}Sr/^{86}Sr$ values associated with these four lots containing artifacts range from 0.71089 to 0.71199 (s.d.=0.001). For instance, Lot II-2 had the most associated burial goods, and included: three vessels with modeled faces, one bird-shaped vessel, and an orange slipped vessel. In this lot two individuals were sampled for $^{87}Sr/^{86}Sr$ (samples 9230=0.71156 and 9344=0.71199), and showed limited variation between the samples for the lot. And the lower $^{87}Sr/^{86}Sr$ values (i.e. 0.70719 to 0.70966) and the highest $^{87}Sr/^{86}Sr$ value (i.e. 0.71338) had no associated documented artifacts present. A student's t-test (unequal variances) show that the mean $^{87}Sr/^{86}Sr$ values between the two groups (0.70967 and 0.71158) were not significantly different (p=0.112).

From the IDW map, there is a division between the lower $^{87}Sr/^{86}Sr$ values located towards the entrance, and the higher $^{87}Sr/^{86}Sr$ values located in Operation III of Talgua. The lowest $^{87}Sr/^{86}Sr$ values are associated with lots I-1 (0.70719) and II-1 (0.70723) (Figure 6.13). These spatial patterns may represent certain social differences in socioeconomic status or perhaps the operations and lots closer to the entrance of the cave may be associated with different interment episodes in time. Unfortunately, neither of these possibilities can be confirmed with certainty, since the all of the radiocarbon dates associated with lots are associated with Operation III.

Table 6.7 ^{87}Sr/^{86}Sr Ratios and Associated Artifacts

| Sample	Operation	Lot	^{87}Sr/^{86}Sr	Artifact Description
9415	I	1	0.70719	None
9318	I	2	0.71147	None
9004	II	1	0.70723	None
9230	II	2	0.71156	3 vessels with modeled faces, 1 bird-shaped vessel, 1 orange slipped vessel
9344	II	2	0.71199	3 vessels with modeled faces, 1 bird-shaped vessel, 1 orange slipped vessel
9397	III	3	0.71184	1 broken vessel and 2 small pieces of jade
9023	III	6	0.70907	None
9132	III	9	0.71162	1 ceramic vessel with an orange slipped rim
9153	III	17	0.71089	2 marble vessels, 1 dichrome jar with red-on-orange geometric designs, 1 modeled face vessel
9375	III	19	0.70966	None
9425	III	8	0.71338	None
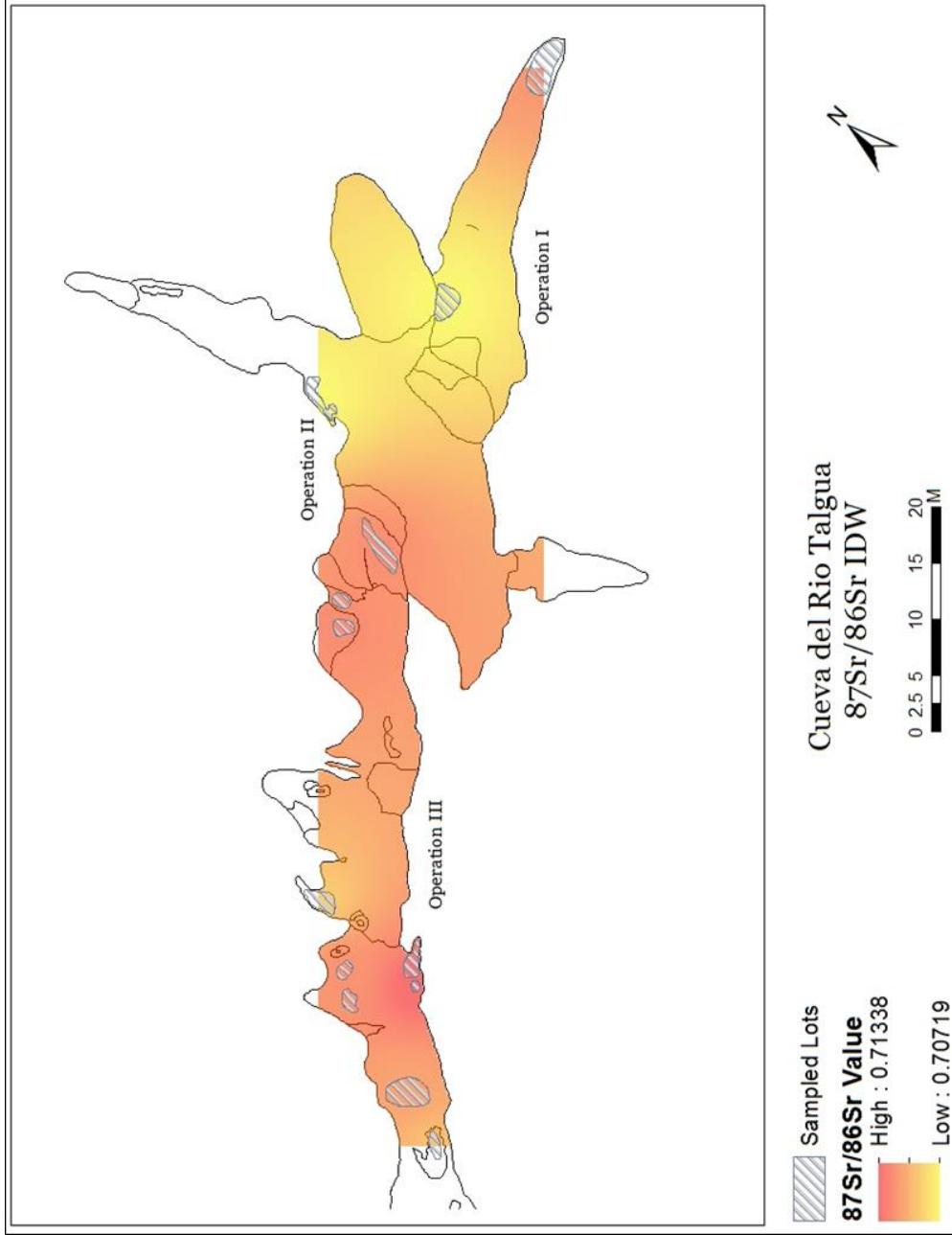
Figure 6.13   IDW of ^{87}Sr/^{86}Sr Values throughout Talgua

The intra-ossuary analysis for the δ^{13}C data (n=32) revealed no possible divisions

between the δ^{13}C value and burial goods, but did show a slight enrichment of δ^{13}C values

in Operation III, when compared to all the lots in Talgua. The five lots with the

documented contextual artifacts had a small range of δ^{13}C (-7.11‰ to -8.65‰), which is

associated with a mixed C_3/C_4 diet. The IDW showed an enrichment in Operation III,

excluding lots III-17 and III-19, which are located at the southern end of the ossuary

(Figure 6.14). Specially, lots III-6 (-6.88‰) and III-8 (-6.83‰) exhibited higher δ^{13}C

values for Talgua. The IDW interpolation for δ^{13}C may be biased since the analysis is

based on mean lot δ^{13}C value. Some lots contained individuals with both lower and

higher δ^{13}C values, therefore a Kruskal-Wallis test and box plots were explored to

determine if the mean δ^{13}C values shown in the IDW were misleading. The distribution

of δ^{13}C by location, or lot/combined lots, also demonstrated the enrichment in δ^{13}C

towards the back of Talgua in Operation III. Although, the lots are not significantly

different from each other (Kruskal-Wallis Chi-squared=4.883; df=8; p=0.77). The box

plot also visually demonstrates the limited variability between the lots (Figure 6.15).

These two exploratory techniques demonstrate that the IDW spatial analysis was

misleading.

The null hypothesis that there are random patterns of δ^{13}C and ^{87}Sr/^{86}Sr values

between the lots in the Talgua Cave ossuary was accepted. The spatial analysis between

the lots for δ^{13}C demonstrated no distinct patterns, and that the individuals interred

throughout Talgua and Arañas consumed variable amounts of C. There may be possible

distinct patterns between the lots for ^{87}Sr/^{86}Sr, but the sample size is too small for a

quantitative analysis.
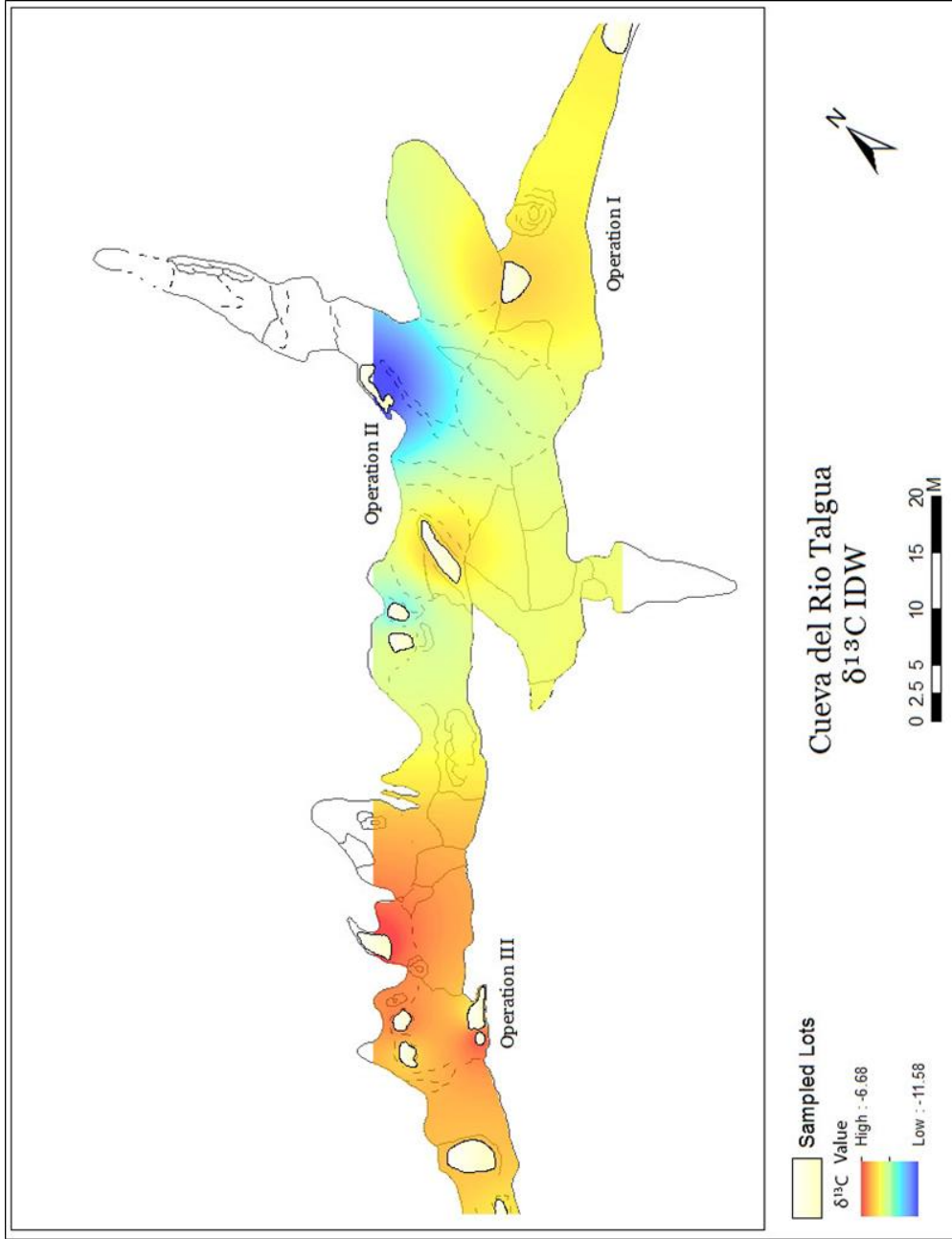
Figure 6.14   IDW of δ¹³C Values throughout Talgua

120
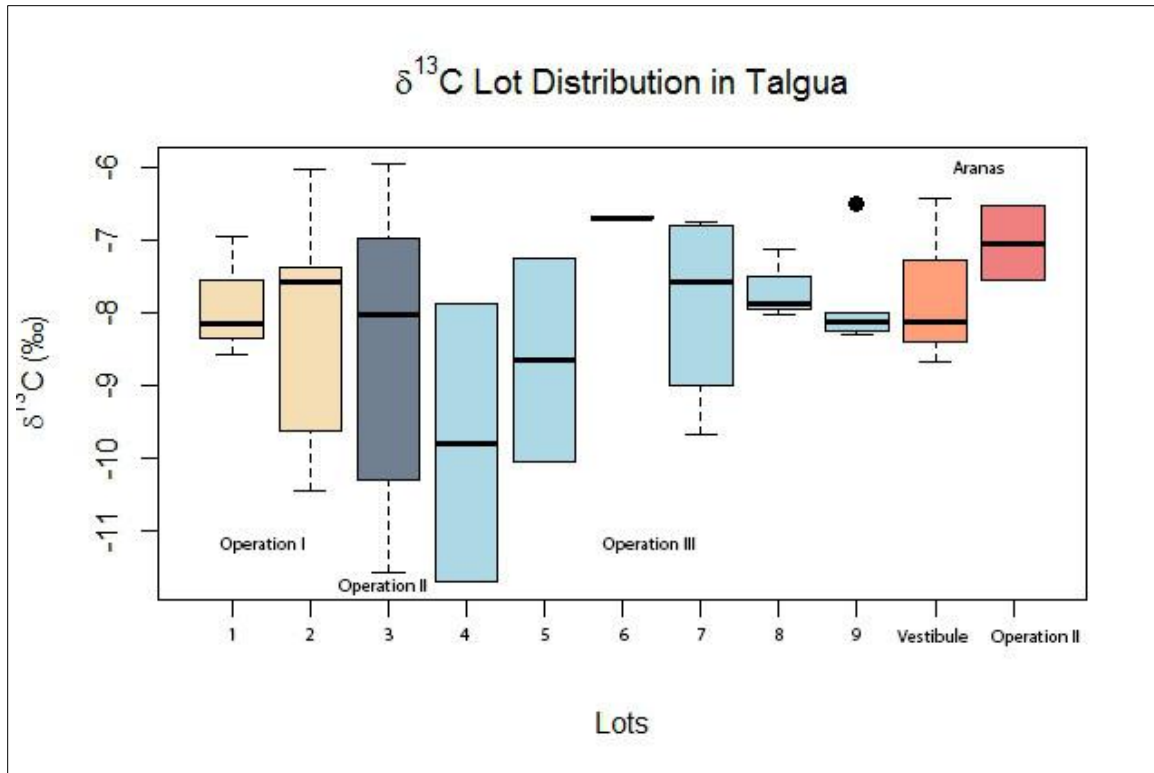
Figure 6.15   Distribution of δ^{13}C by Lot for Talgua and Arañas

6.4.3   Dental metric analysis

- Secondary research objective: To determine if tooth size as a proxy for biological sex is related to geographic origin or diet.

- Question 3: Is there a relationship between isotopic value (δ^{13}C, δ^{18}O$_p$, δ^{18}O$_c$, and ^{87}Sr/^{86}Sr) and tooth size?

- H$_0$: There is no significant relationship between isotopic value and tooth size.

Tooth size was used as a proxy for biological sex to look at gendered activities, such as differential diet (δ^{13}C) and change in residence (δ^{18}O and ^{87}Sr/^{86}Sr). Since the dental metric analysis to determine tooth size is a secondary research objective and

121

cannot be assessed in a quantitative manner due to the limited regional data, a preliminary analysis is presented below. As discussed in Chapter V, the dental metric data were divided into four groups and analyzed by UM1, UM2, LM1, and LM2 using both the Arañas and Talgua cave dentition. A summary of the multivariate and univariate exploratory findings are discussed, then the group results are summarized. The univariate finite mixture results are presented for both the MD and BL measurements. Lastly, tooth size is compared to the sample's corresponding isotopic values ($\delta^{13}C$, $\delta^{18}O_p$, $\delta^{18}O_c$, and $^{87}Sr/^{86}Sr$) to test the hypothesis above. All dental metric data used in this study are listed in Appendix C.2.

Tooth numbers 18, 19, 30, and 31 were available for the mandibular dental metric comparison and tooth numbers 2, 3, 15, and 16 were available for the maxillary dental metric comparison. The multivariate finite mixture's best proportion classification was UM2s (0.514 and 0.486), whereas the univariate normal finite mixture's best proportion classification was the BL data for LM2s (0.507 and 0.493). Overall, the multivariate analysis classified the M2s into more evenly divided subgroups and the univariate approach classified the mandibular BL samples into more evenly proportionate subgroups. The differences observed between multivariate and univariate subgroup classifications are attributed to the negative linear relationship between the BL and MD measurements. For instance, the multivariate mixture model's best subgroup classification (UM2s), exhibited a poor linear MD/BL relationship (y=0.1563x + 10.224, R^2=0.046). Another example is observed in Figure 6.16, where the BL and MD LM1 measurements had a negative relationship (y=0.5725x + 5.928, R^2=0.174), and shows the BL measurements increasing in size, whereas the MD measurements are decreasing.

These poor linear regressions demonstrate that the MD measurements may be affected by attrition. Therefore, only the univariate BL models with higher proportion classifications were be used (i.e. LM1s and LM2s) to test the hypothesis.
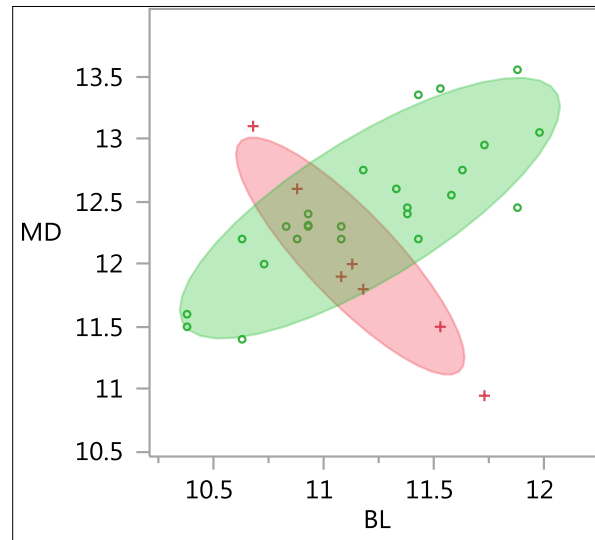
Figure 6.16   Problematic Multivariate Subgroup Classifications for LM1s.

The BL metric data for LM1 (n=33) range from 10.4 mm to 12 mm (mean=11.20 mm, s.d.=0.435), and exhibited a slight bimodal distribution. The finite mixture model (-loglikelihood=18.330, BIC=54.143, AICc=48.883) classified two possible subgroups within the LM1 BL distribution. The likelihood probabilities for compartment one and two were 0.402 and 0.598, respectively. A total of 14 samples (tooth numbers 19 and 30) clustered in compartment one and 19 fell into compartment two. Since two subgroups were identified in the finite mixture model, group LM1s were compared to the corresponding isotopic value (discussed later in this section). On the contrary, the MD measurements (n=32) for LM1s showed no probable subgroups in the mixture model (-

LogLikelihood=27.782, BIC=72.893, AICc=67.872), and range from 10.95 mm to 13.55

mm (mean=12.34 mm, s.d.=0.601). The probabilities for compartments one and two were

0.08310 and 0.91690, respectively, and required no further analysis.

The BL metric data for LM2 (n=17) range from 9.7 mm to 11.7 mm (mean=10.85

mm, s.d.=0.432), and classified two subgroups (proportions 0.507 and 0.493). Sample

9430 was observed with a very low BL measurement (9.7 mm), and influenced the

mixture model considerably. Dental morphology or a specific ancestral trait was not a

factor in the low BL measurement; therefore the sample was included mixture model.

The likelihood of two subgroups in the model (-LogLikelihood=13.318, BIC=40.801,

AICc=42.090) was separated by 8 and 9 samples, respectively. Since two subgroups were

identified in the finite mixture model, group LM1s were compared to the corresponding

isotopic value (discussed later in this section). Additionally, the likelihood of two

subgroups present in the MD dental metric data (n=16) was low (proportions 0.830 and

0.170), similar to the LM1 BL/MD probabilities, and required no further analysis.

The BL metric data for UM1s (n=26) range from 10.9 mm to 13.1 mm

(mean=12.22 mm, s.d.=0.524), and exhibits a normal distribution. The finite mixture

model (-LogLikelihood=17.741, BIC=51.773, AICc=48.483) only identified one

probable cluster (proportions 0.924 and 0.076). No further data analysis is required for

the BL UM1 measurements. On the contrary, the MD metric data range from range 10.3

mm to 12.45 mm (mean=11.33 mm, s.d.=0.650), and classified into two probable

subgroups (-LogLikelihood=23.486, BIC=63.263, AICc=59.973). Subgroups containing

16 samples, proportion 0.624, and 10 samples, proportion of the group 0.376, show a

possible division by UM1 MD tooth size. This tooth size division may not relate to sexual dimorphism, but age.

The UM2 BL metric data (n=31) range from 10.7 mm to 13.15 mm, (11.88, sd. 0.515 [after sample 9111 removal]), with a normal distribution. Sample 9111 (13.55 mm) was an outlier at the highest end of the distribution, and exhibits the three-rooted dental morphology feature. One group was identified by the finite mixture model (-LogLikelihood=22.357, BIC=61.720, AICc=57.215) with the cluster proportions 0.964 and 0.036. The MD measurements for UM2 range from 9.4 mm to 11.9 mm (10.61=mm, s.d.=0.708), and a scatterplot demonstrated a bit of clustering. The finite mixture model (-LogLikelihood=28.512, BIC=74.030, AICc=69.524) classified 22 samples in portion one (0.728) and eight samples in portion two (0.271). Although, likelihood probability suggests possible subgroups for the MD metrics, no further analyses were conducted on the MD groups due to the high amount of wear observed on a majority of the Talgua Cave samples.

Possible male, possible female, and indeterminate individuals were classified from the univariate mandibular BL subgroups. Subgroups for BL LM1 were originally classified into two clusters using the probability proportion output generated from the univariate finite mixture model. The original subgroups or clusters were separated by probabilities greater than 50%. Cluster 1 (n=14) range from 11.35 mm to 12 mm (mean=11.62 mm) and cluster 2 (n=19) range from 10.4 mm to 11.2 mm (10.88 mm). These subgroups were significantly different when compared using the Welch's t-test (p=0.001). Once the samples were separated by 96% probably, there were six possible males, 13 possible females, and 14 indeterminate (Figure 6.20). The mean BL for

possible males (mean=11.83 mm) and possible females (mean=10.76 mm) were

significantly different (p=0.001).
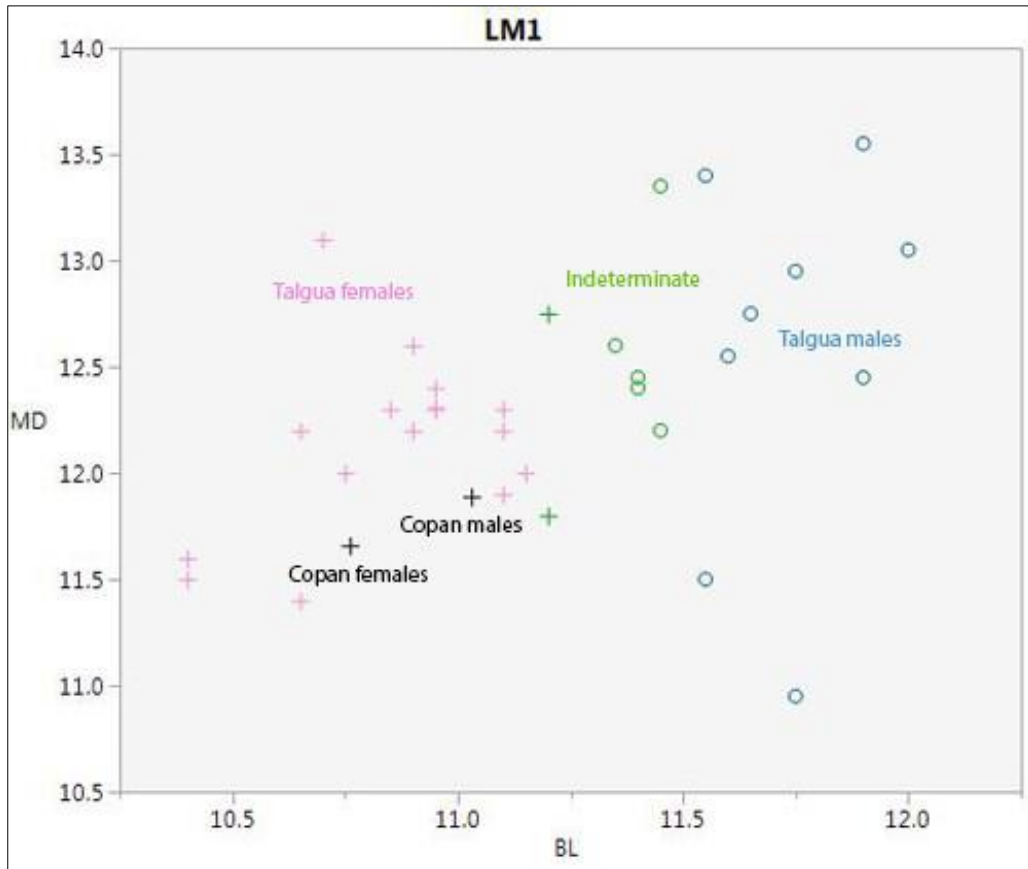
Figure 6.17   LM1 Classification with Scherer (2004) Copán Data

Subgroups for BL LM2 greater than 50% probability grouped into cluster 1 (n=8) range from 9.7 mm to 10.8 mm (mean=10.41 mm) and cluster 2 (n=9) range from 10.9 mm to 11.7 mm (11.23 mm). These subgroups were significantly different when compared by the unpaired 2- tailed student's t-test with unequal variances (p=0.001). Once the samples were separated by 96% probably, there were six possible males and ten

possible females. The possible males (mean=11.45 mm) and possible females (mean=10.23 mm) were still significantly different (p=0.001).

Possible males and females that were identified in the mixture models and further classified into to biological sex using 96% probability were combined to determine if any differences between tooth size and isotopic value were present. For the subsample of isotope measurements, two possible males, six possible females, and three indeterminate individuals were identified (Table 6.7). Only relationships between the possible males/ females and $\delta^{13}C$, $\delta^{18}O_p$, and $\delta^{18}O_c$ values were assessed, since there were only three $^{87}Sr/^{86}Sr$ measurements with possible sex estimation. No significant relationships between $\delta^{13}C$ (p=0.169), $\delta^{18}O_p$ (p=0.383), or $\delta^{18}O_c$ (p=0.906) and tooth size (i.e. possible biological sex were present). Therefore, the null hypothesis is accepted and there are no significant relationships between isotopic values and tooth size.

Table 6.8   Samples with Possible Sex Estimation and Isotope Values

Sample	Cave	Tooth	BL (mm)	$\delta^{13}C$	$\delta^{18}O_p$	$\delta^{18}O_c$	$^{87}Sr/^{86}Sr$	Possible Sex
573	Arañas	31	11.51	-8.12	16.93	-3.92	0.70831	M
695	Arañas	31	11.1	-6.41	16.62	-4.01		I
9021	Talgua	18	10.4	-6.67	18.26	-3.95		F
9023	Talgua	18	10.35	-6.69	15.50	-4.53	0.70907	F
9132	Talgua	19	10.95	-7.11	16.72	-3.78	0.71162	F
9265	Talgua	30	11.1	-7.88	17.10	-3.97		F
9266	Talgua	30	11.9	-8.02	16.92	-3.23		M
9275	Talgua	19	10.85	-8.57	16.93	-3.90		F
9364	Talgua	19	10.9	-7.86	16.92	-3.61		I
9368	Talgua	19	11.1	-11.71	16.96	-3.72		F
9415	Talgua	30	11.2	-6.94	17.19	-3.65	0.70719	I

6.5   Summary

The results from this research project were more informative for the Olancho Valley and Talgua Caves than anticipated. The diagenetic test for CO_3 showed that 10 of the $\delta^{13}C$ and $\delta^{18}O_c$ samples were possibly altered from the depositional cave environment, although removal of the possibly effected samples from the analyses did not change the results. Preliminary analysis of the $^{87}Sr/^{86}Sr$ isotope data showed the mean local $^{87}Sr/^{86}Sr$ signature as 0.71011, which were in disagreement from the geographic assignment tests. When compared to the quantitative assignment model, the exploratory techniques did generate a similar conclusion for sample 9023 as an outlier. Although all of the null hypotheses were accepted certain conclusions can be drawn from the data. The likelihood assignments showed diverse geographic origins, with high probabilities of the interred

individuals originating from areas throughout the Olancho Valley. The intra-ossuary analysis revealed interesting relationships between lots with artifacts and $^{87}Sr/^{86}Sr$ signature, lots containing artifacts having $^{87}Sr/^{86}Sr$ values from 0.71089 to 0.71199. The univariate finite mixture model approach worked best to determine the subgroups for the mandibular BL measurements. Four possible females and two males were identified from the mixture models, but there were no associated isotopic relationships.

CHAPTER VII

CONCLUSION AND DISCUSSION

7.1 Research summary

Traditionally, the *Intermediate Area* was used to define the region of northeast

Honduras as an area where Mesoamerican and South American cultures fused. Early

ideas of the Intermediate Area as a product of the intrusion of core cultural ideas devalue

Honduran prehistory (Lang and Stone, 1984) and inhibit the cultural identity of the

individuals. This depiction is a consequence of the limited research conducted in Lower

Central America, and the dearth of bioarchaeological investigations. Human dentition

from two ossuary caves located in the Olancho Department, Cueva del Río Talgua and

Cueva de las Arañas (Talgua Caves), were used in this research to understand Formative

Period society in northeast Honduras. Specifically, 37 individuals from the Talgua Caves

were assessed using biogeochemistry to understand human movement and mortuary

practice in northeast Honduras during the Formative Period.

There were two primary research objectives: (1) assign geographic origin to a

sample of individuals interred at the Talgua Cave ossuaries, and (2) to understand the

mortuary arrangement in Cueva del Río Talgua using isotopic values. The first portion of

the project used $^{87}Sr/^{86}Sr$ and $\delta^{18}O$ isotope analyses to assign geographic origin to 37

individuals from the Talgua Caves. Likelihood geographic assignment models using

Bayesian probability were used to assign geographic origin on a small-scale quantitative

130

level. These assignment models determined the probability of childhood origin using primarily the first and second molars. The second portion of this research project used multivariate interpolation of $\delta^{13}C$, $\delta^{18}O$, and $^{87}Sr/^{86}Sr$ through inverse distance weighting (IDW) of each isotope dataset in Cueva del Río Talgua to understand the spatial arrangement of the interred individuals. Distinct spatial patterns within Cueva del Río Talgua were tested for differences in diet (i.e. $\delta^{13}C$), geographic origin (i.e. $\delta^{18}O$ and $^{87}Sr/^{86}Sr$), and presence of burial goods (i.e. $\delta^{13}C$ and $^{87}Sr/^{86}Sr$).

The secondary research objective compared tooth dimensions to isotopic value ($\delta^{13}C$, $\delta^{18}O$, and $^{87}Sr/^{86}Sr$). For this study, tooth size was used as a proxy for biological sex to look at gendered activities, such as differential diet ($\delta^{13}C$) and change in residence ($\delta^{18}O$ and $^{87}Sr/^{86}Sr$). Univariate normal finite mixture models were used to classify mesial-distal (MD) and buccal-lingual (BL) dental measurements into subgroups. Individuals from the sub-group with larger dentition were classified as possible male and individuals with smaller dentition were classified as possible female. Lastly, individuals with MD or BL values falling within the middle of the distribution were classified as indeterminate.

Prior to the conclusions of each research objective, the diagenetic test conclusions and insights gained from the exploratory isotope analyses are discussed. Recalling the formulas discussed in Chapter V, after the $\delta^{18}O_C$ values were converted from VPDB to VSMOW values, the diagenetic CO_3 test calculates the offset or the difference between the $\delta^{18}O_P$ and $\delta^{18}O_C$ values (ΔC-P). Using the Martin et al. (2008) 10.6‰ threshold, over a quarter of the $\delta^{18}O_c$ and $\delta^{13}C$ samples (n=10) were modified during deposition. This high rate (27%) is plausible, since the skeletal elements within the Talgua Caves were

covered in calcium carbonate. It is also likely that the CO_3 diagenetic test may be inferring some other sort of information. As previously mentioned, the high offset may not be attributed to alteration in CO_3, but a result from $\delta^{18}O$ variation occurring during mineralization. All exploratory analyses in this research used the original $\delta^{18}O_c$ and $\delta^{13}C$ datasets, along with the modified $\delta^{18}O_c$ and $\delta^{13}C$ datasets (i.e. with the possibly affected samples removed). Overall, the removal of the possibly affected samples did not appear to alter the interpretation of the results. For instance, the $\delta^{13}C$ values (n=37) initially range from -11.71‰ to -5.95‰ with a mean of -8.02‰ for the dataset. After the possibly altered samples were removed (n=27), the range of $\delta^{13}C$ values only slightly change (-11.71‰ to -6.02‰, mean of -8.07‰). Additionally, when both the original and modified $\delta^{13}C$ datasets were input into the IDW, the results of the IDW $\delta^{13}C$ spatial interpolation did not change. Therefore, it is inconclusive if the diagenetic test for CO_3 alteration was a successful test for diagenesis at Talgua Caves. Fortunately for the $^{87}Sr/^{86}Sr$ data, tooth enamel is largely resistant to alterations due to its highly crystalline structure, low organic matter content, and lack of porosity. Numerous studies have demonstrated that bioavailable enamel isotope signatures are reliable with minimal treatment (Slovak and Paytan, 2003).

The results from the exploratory analyses were informative for the Talgua Cave individuals' mortuary practices and diet. The principle component analysis (PCA) demonstrated that the interred at Río Talgua Cave and Arañas Cave most likely originated from a similar population or similar groups living near the ossuaries. The original idea that "the caves were contemporaneous and may represent the mortuary program of one population" was presented by Herrmann (2002: 17). Four samples in the

PCA or two "clusters" showed correlations by $\delta^{18}O_p$ from individuals interred at both Río Talgua and Arañas. Samples 573 (Arañas) and 9415 (Talgua) were related by $\delta^{18}O_p$ (16.93‰ and 17.19‰) and samples 9153 (Talgua) and 9440 (Arañas) had strong $\delta^{18}O_p$ (16.95‰, 16.56‰) correlations. Perhaps, these relationships demonstrate similar childhood geographic origins from areas in the Olancho Valley, and they were interring their dead in both ossuary caves.

Inter-tooth variation among the $\delta^{18}O$ and $\delta^{13}C$ datasets, as discussed in detail in Chapter V, may be the result of weaning. Difference between the M1 and M2 means was observed for both $\delta^{18}O$ datasets. The mean $\delta^{18}O_c$ and $\delta^{18}O_p$ values for M1s were -3.82‰ and 16.72‰ (respectively) and -3.67‰ and 16.99‰ (respectively) for M2s. There was an enrichment in $\delta^{13}C$ between the means for M1s (-8.13‰) and M2s (-7.85‰), which may relate to differences in C_3/C_4 consumption, typically interpreted as weaning (Wright et al., 2010). Although, this relationship was not significantly different based on a one-way ANOVA (F=0.348, p=0.559). Based on a scatter plot, the $\delta^{13}C$ for M1s cluster around -8.5‰ to -6.5‰ (2‰ difference), whereas the M2s range from -10.46‰ to -5.95‰ (4.5‰ difference). The $\delta^{13}C$ M1 values may still suggest a more restricted diet for these younger individuals, based on the smaller 2‰ range.

7.1.1   Research objective 1: geographic origin

Recently, there has been a shift from the use of the faunal baseline towards the isoscape for assessing human movement (Makarewicz and Sealy, 2015). While faunal baselines may help interpret non-locals in a sample, they lack the assignment power to determine geographic origin on the landscape. To test the first hypothesis, the Bataille et al. (2012) $^{87}Sr/^{86}Sr$ isoscapes for the circum-Caribbean region, and a modern $\delta^{18}O$

precipitation isoscape created in IsoMAP were used to assign the bioavailable Talgua Cave signatures. To reiterate the hypothesis for research objective 1:

- H_0: The Talgua Cave $^{87}Sr/^{86}Sr$ or $\delta^{18}O$ bioavailable signatures are assigned with 90% probability to northeast Honduras.

The $^{87}Sr/^{86}Sr$ catchment water isoscape was converted to an $^{87}Sr/^{86}Sr$ archaeological enamel isoscape using 60 available archaeological human and faunal $^{87}Sr/^{86}Sr$ signatures from the circum-Caribbean region. The $\delta^{18}O_p$ Talgua Cave values were converted to $\delta^{18}O_{dw}$ for the modern precipitation isoscape assignments. The Talgua Cave $^{87}Sr/^{86}Sr$ and $\delta^{18}O_p$ geographic assignments were conducted within a Bayesian framework, using the probability that an individual sample was from a particular location, based on the calibrated $^{87}Sr/^{86}Sr$ archaeological enamel isoscape and the geographic assignment function in IsoMAP. Predicted likelihood surfaces were generated from the Bayesian assignments, which showed the high probably areas throughout the circum-Caribbean. Bins were created for the $^{87}Sr/^{86}Sr$ and $\delta^{18}O_p$ Talgua values to ease interpretation, and are discussed in detail in Chapter VI. All the likelihood geographic maps that were generated from the assignments are included in Appendix B.

The hypothesis for research objective 1 was accepted, and all the sampled individuals originated from northeast Honduras. Although some areas outside northeast Honduras are probable for geographic origin, it is more likely that these particular individuals originated from nearby locations. This assumption was based on the fact that the $\delta^{18}O_p$ assignment data complemented the $^{87}Sr/^{86}Sr$ assignments. In addition, the $\delta^{13}C$ Talgua Cave values corroborated the geographic assignments, and the individuals were dominated by a diet high in C_3 plant consumption. For instance, manioc (C_3) has been

suggested as a primary carbohydrate in Formative Period northeast Honduras (Brady et al., 2000). If individuals had higher $\delta^{13}C$ signatures, suggestive of a diet high in C_4 plant consumption, a 'non-local' origin outside of northeast Honduras would have been assumed.

Originally when this hypothesis was proposed, it was unknown that the $^{87}Sr/^{86}Sr$ assignments would have such high cell resolution. This feature of the $^{87}Sr/^{86}Sr$ geographic assignment model made it possible to assess 'local' and 'non-local' individuals. 'Non-local' was defined as individuals that were assigned with no high probability areas within 30 mi (48.3 km) of the Talgua Caves. Based on the 'non-local' definition, sample 9023 was the only non-local identified from the assignment models.

Using the traditional outlier techniques, no 'non-locals' were identified in the $^{87}Sr/^{86}Sr$ Talgua Caves dataset. Four possible 'non-locals' were identified in the $\delta^{18}O_p$ dataset, and two possible non-locals in the $\delta^{18}O_c$ dataset (Table 7.1). Unfortunately, only one $^{87}Sr/^{86}Sr$ measurement was available to compare the traditional techniques and the assignment method to identify possible 'non-local' individuals. These results suggest that the outlier techniques and the assignment methods may be complimentary for assessing 'local' individuals in isotope datasets. In addition to determining if an individual may be 'local', probable likelihood surfaces may help to narrow the possible range of geographic origin, as demonstrated by the $^{87}Sr/^{86}Sr$ assignment models.

135

Table 7.1   Possible 'Non-locals' Identified at Talgua Caves

Sample	Cave	Operation	Lot	$\delta^{18}O_p$	$\delta^{18}O_c$	$\delta^{13}C$	$^{87}Sr/^{86}Sr$
9021	Talgua	III	6	18.26‰		-6.67‰	*Not available*
9023	Talgua	III	6	15.50‰	-4.53‰	-6.69‰	0.70907
9155	Talgua	III	17	15.18‰		-6.49‰	*Not available*
9191	Talgua	III	7		-4.54‰	-6.73‰	*Not available*
9442	Arañas	I	1	18.36‰		-7.54‰	*Not available*

7.1.2   Research objective 2: mortuary arrangement

An intra-ossuary spatial analysis was performed on Cueva del Río Talgua using the $\delta^{13}C$, $\delta^{18}O$, and $^{87}Sr/^{86}Sr$ isotopes from 32 individuals. Individuals were sampled throughout the ossuary by Operation and Lot. The $\delta^{13}C$ and $^{87}Sr/^{86}Sr$ values were also compared to Lots with and without burial goods. To reiterate the hypothesis for research objective 2:

- H_0:   There are random patterns of $\delta^{13}C$, $\delta^{18}O$, and $^{87}Sr/^{86}Sr$ values between the lots in the Talgua Cave ossuary.

The inverse distance weighting (IDW) analyses showed random patterns of $\delta^{18}O_p$ and $\delta^{18}O_c$ throughout Talgua, and the null hypothesis was accepted using $\delta^{13}C$ and $\delta^{18}O$ for research objective 2. The $^{87}Sr/^{86}Sr$ spatial patterns may relate to temporal phases of deposition, with the individuals near the entrance of Talgua being the oldest interments and the individuals in Operation III being deposited later in time. There is no provenience for the single Classic Period radiocarbon date in Río Talgua Cave; therefore it cannot be

used to support the claim that individuals interred in Operation III were more recent. It is

assumptive, but it is possible that the Classic Period date did come from Operation III,

since Brady et al. (2000) did originally propose this idea of temporal deposition.

Additionally, since the majority of the absolute dates are from the Formative Period, it is

safe to assume that most of the interments were deposited earlier in time. Patterns were

evident in the spatial distribution of $^{87}Sr/^{86}Sr$ by lots in Talgua, but due to the small

sample size the hypothesis could not be rejected.

The intra-ossuary analysis for $^{87}Sr/^{86}Sr$ (n=10) also revealed possible divisions

between $^{87}Sr/^{86}Sr$ values and burial goods. Burial goods, such as jade, ceramic and

marble vessels, and beads were documented in five of the 13 lots sampled for isotopic

analyses. The $^{87}Sr/^{86}Sr$ values associated with the lots with artifacts ranged from 0.71089

to 0.71199, and lots without artifacts had lower $Sr/^{86}Sr$ values (i.e. 0.70719 and 0.70723).

Although there were observed differences between the lots with artifacts and the lots

without artifacts, the differences were not significant (p=0.112).

The complete mortuary program of northeast Honduras is not fully understood,

but it does appear that the common Formative Period practice was to inter individuals in

secondary contexts within ossuary caves. This practice of secondary interments in

ossuary caves was common during the Formative Period, and then appears to transition to

residential burial practices in the Classic Period. Evidence of residential burial practice

was recorded at the Talgua Village and has been seen throughout the Ulua Valley in

Western Honduras during this time.

The secondary burial practice may have become less commonly used by

individuals residing closer to the ossuaries, and more frequently used by individuals with

137

geographic origins further from the Talgua Caves. For instance, Dixon et al. (1998)

speculated that Cueva Grande, which is also located in the mountains surrounding the

Olancho Valley, was a pilgrimage site due to the high number of remaining fragmented

artifacts. If the Talgua Caves were important cave sites, like Cueva Grande, individuals

from more distant locations would desire interment at Talgua.

7.1.3   Secondary research objective: tooth size

The secondary research objective was designed to compare tooth size to isotopic

value (δ^{13}C, δ^{18}O, and ^{87}Sr/^{86}Sr) for the Talgua Cave assemblage. For this study, tooth

size was used as a proxy for biological sex to look at gendered activities, such as

differential diet (δ^{13}C) and change in residence (δ^{18}O and ^{87}Sr/^{86}Sr). Finite mixture

models were used to separate any possible sub-groups of the UM1s, UM2s, LM1s, and

LM2s, and the high probability (>96%) samples in the sub-groups were determined as

possible male or possible female. Any samples that had probabilities lower than 96%

were assessed as indeterminate. To reiterate the hypothesis for research objective 3:

- $H_{0:}$ There is no significant relationship between isotopic value and tooth
  size.

The univariate finite mixture models classified two subgroups for the LM1 and

LM2 BL metric data. The BL metric data for LM1 (n=33) range from 10.4 mm to 12 mm

(mean=11.20 mm, s.d.=0.434), and classified the likelihood probabilities for

compartment one and two as 0.402 and 0.598, respectively. Once the samples were

separated by 96% probably, there were six possible males, 13 possible females, and

fourteen indeterminate. The possible males (mean=11.83 mm) and possible females

(mean=10.76 mm) were significantly different (p=0.001). The BL metric data for LM2

(n=17) range from 9.7 mm to 11.7 mm (mean=10.85 mm, s.d.=0.432), and classified two subgroups (proportions 0.507 and 0.493). There were four possible males, five possible females, and eight indeterminate. The possible males (mean=11.45 mm) and possible females (mean=10.23 mm) were significantly different (p=0.001). For the subsample of isotope measurements, two possible males, six possible females, and three indeterminate, individuals had associated isotope values. No significant relationships between $\delta^{13}C$ (p=0.169), $\delta^{18}O_p$ (p=0.382), or $\delta^{18}O_c$ (p=0.906) and tooth size were present. Therefore, the null hypothesis was accepted and there was no significant relationship between isotopic value and tooth size. However, this null relationship of $\delta^{13}C$ provides evidence for equal access to food resources in the Olancho Valley during the Formative Period.

7.2 Interpretations

The biogeochemistry data in this thesis support the ideas that the Talgua Cave individuals were an egalitarian society living in small homesteads around the valleys and on the hillsides of the ossuaries. They consumed minimal amounts of maize, and young children may have had redistricted diets under the age of two. There were no differences in diet for the eleven individuals assigned possible sex estimation. And lastly, short distances were observed from their childhood origins to their final interment at Talgua Caves.

The lack of spatial patterning by isotopic signature within Río Talgua Cave and the absence of gendered dietary activities suggest population egalitarianism. This may be the reason for the absence of a large Formative Period habitation settlement in the Río Talgua drainage or Olancho Valley. A larger habitation site may require control or

139

management over subsistence, thus differences in high and low status interments would be documented with differential access to food resources (i.e. distinct δ^{13}C values).

The δ^{18}O and ^{87}Sr/^{86}Sr individual assignments generated diverse geographic origins within the designated buffer-zone of Talgua Caves. This evidence shows that different kin or ethnic groups from diverse geographic origins were utilizing the ossuaries. Whether the multi-group use of the ossuaries was temporally correlated is unknown, but the intra-ossuary analysis of ^{87}Sr/^{86}Sr shows individuals with lower ^{87}Sr/^{86}Sr signatures interred closer to the entrance in Río Talgua Cave. The diverse geographic origins may also relate to multi-ethnic use of the cave simultaneously. Ethnographic accounts of the Olancho Valley mention the valley as a "mixed area where the highland peoples of Honduras, the varied Lenca tribes, met the peoples of eastern and northeastern Honduras, whose culture was generally of the rain-forest type" (Stone 1957:76). This interpretation is also a reasonable possibility, since individuals interred in lots with artifacts had unique ^{87}Sr/^{86}Sr signatures.

One individual was identified as a possible 'non-local' from the ^{87}Sr/^{86}Sr assignments, and an additional three 'non-local' individuals were identified in the δ^{18}O$_p$ dataset. This small number of 'non-local' individuals provides evidence for minimal human movement into northeast Honduras from outside Lower Central America during the Formative Period. This research supports the ideas that northeast Honduras was not dependent on any external forces, such as the Maya, but was an independent cultural phenomenon that was involved in outside interactions, such as exchange, with external societies. The exchange of goods is present during the Formative Period in northeast Honduras, apparent by the exotic goods (i.e. jade documented at Talgua Caves and

obsidian at Cuyamel Caves). The low number of 'non-local' individuals at Talgua Caves

also suggests that the trade items were acquired by down-the-line exchange processes

rather than through a long-distance trade connection. Down-the-line type of exchange

network has also been documented at the Formative central Honduran site Yarumela,

which had materials with Mesoamerican and South American origins (Dixon et al., 1994;

Lentz et al., 2005). This type of trade network and bioarchaeological evidence of limited

'non-local' individuals at Talgua Caves suggests the surrounding region was culturally

distinct and used certain Mesoamerican or South American cultural features.

7.3   Research limitations and future directions

This section was combined since the research limitations encountered during this

research project lead to the future directions needed to assess geographic origin and

mortuary practices in northeast Honduras. The major impediment encountered during the

research project was limited data. Issues with incomplete data stem from the limited

published archaeological and bioarchaeological investigations conducted in the Lower

Central American region. This limitation most likely affected the archaeological enamel

isoscape that was created for calibrating the Bataille et al. (2012) isoscape, and the

assessment of tooth size. The Bataille et al. (2012) model was calibrated using mean

archaeological $^{87}Sr/^{86}Sr$ values (n=60) from human and faunal tooth enamel. When the

linear regression analysis was conducted the relationship of observed to expected

$^{87}Sr/^{86}Sr$ values was high, but the distribution appeared bimodal. Bataille et al. (2012)

also encountered this problem when comparing the geological expected values to the

plant, animal, and human observed values. The authors attributed this phenomenon to

weathering effect of the bedrock in certain areas.

As for future directions, the first objective should be to attain more human archaeological ^{87}Sr/^{86}Sr data from Lower Central America. The isoscape models appear to be accurate predictors of lower ^{87}Sr/^{86}Sr values, but some issues with the values around 0.71100 may be problematic. Without further ^{87}Sr/^{86}Sr data to calibrate the model, it is difficult to state with certainty that individuals with ^{87}Sr/^{86}Sr values near 0.71100 have high probabilities of geographic origins 20 mi to 30 mi from the Talgua Caves site. Additionally, the limited available dental metric or even skeletal data from Lower Central America and eastern Honduras made the sex estimation impossible on a quantitative scale. Finally, additional fieldwork is needed in the Olancho Valley and surrounding regions. The systematic documentation of caves, especially ossuary caves in this region would help to understand the complete mortuary complex of northeast Honduras during the Formative Period.

Lastly, the sample size for the ^{87}Sr/^{86}Sr dataset was limited to 14 individuals, which restricted the interpretation of the intra-ossuary cave analysis and the comparison of the outlier techniques to the assignment model 'non-local' results. A future direction would be to perform additional ^{87}Sr/^{86}Sr isotope analysis. Additional ^{87}Sr/^{86}Sr data in combination with dental morphology may help answer research questions regarding kinship at the Talgua Caves.

REFERENCES

Ambrose SH. 1993. Isotopic analysis of paleodiets: Methodological and interpretive considerations. In: Standford MK, editor. Investigations of ancient human tissue: Chemical analysis in anthropology. New York: Gordon and Breach. p 59–130.

Ashmore W, Geller PL. 2005. Social dimensions of mortuary space. In: Rakita GM, Buikstra JE, Beck LA, Williams SR, editors. Interacting with the dead: Perspectives on mortuary archaeology for the new millennium. p 81–92.

Attendorn HG, Bowen RC. 1997. Radiogenic and stable isotope geology. London: Chapman and Hall.

Barrantes R. 1993. Evolución en el trópico: los amerindios de Costa Rica y Panamá, Editorial de la Universidad de Costa Rica, San Jose.

Bataille CP, Bowen GJ. 2012. Mapping 87Sr/ 86Sr variations in bedrock and water for large scale provenance studies. Chem Geol 304-305: 39–52.

Bataille CP, Laffoon J, Bowen GJ. 2012. Mapping multiple source effects on the strontium isotopic signatures of ecosystems from the circum-Caribbean region. Ecosphere 3:13-24.

Becquerel AH. 1896. Sur les radiations invisibles émises par les corps phosphorescents. CR Acad. Sci. Paris 122: 501.

Begley CT. 1999. Elite power strategies and external connections in ancient northeast Honduras. PhD dissertation, The University of Chicago, Chicago, IL.

Bender MM. 1968. Mass spectrometric studies of carbon 13 variations in corn and other grasses. Radiocarbon 10: 468-472.

Benedix DC, Herrmann NP, Haskins VA, Flournoy LE. 1999. Analysis of dental remains from Honduran ossuary caves. Poster presented at the Sixty-Eighth. Annual Meeting of the American Association of Physical Anthropologists, Columbus, Ohio.

Bentley RA. 2006. Strontium isotopes from the Earth to the archaeological skeleton: A review. J Archaeol Method Th 13:135–187.

Bisel SC. 1980. A pilot study in aspects of human nutrition in the ancient eastern Mediterranean, with particular attention to trace minerals in several populations from different time periods. Ph.D. Dissertation. University of Minnesota.

Bowen GJ. 2010. Statistical and geostatistical mapping of precipitation water isotope ratios. In: Isoscapes. Springer. p 139–160.

Bowen GJ, Liu Z, Vander Zanden H B, Zhao L, Takahashi G. 2014. Geographic assignment with stable isotopes in IsoMAP. Methods in Ecology and Evolution. 5: 201-206.

Bowen GJ, West JB. 2008. Isotope landscapes for terrestrial migration research. In: Hobson KA, Wassenaar LI, editors. Tracking animal migration with stable isotopes. Oxford: Elsevier. p 79–106.

Bowen GJ, West JB, Miller CC, Zhao L, Zhang T. 2015. IsoMAP: Isoscapes Modeling, Analysis and Prediction (version 1.0). The IsoMAP Project. http://isomap.org.

Brady, JE. 1994. A Report to: The Instituto Hondureno de Anthropologia e Historia, on investigations carried out at La Cueva Del Río Talgua, district of Olancho, Honduras.

Brady JE. 1995. A reassessment of the chronology and function of Gordon's Cave# 3, Copán, Honduras. Ancient Mesoam, 6: 29-38.

Brady JE, Hasemann G, Fogarty J. 1995a. Buried secrets, luminous find: Américas. 48: 6-15.

Brady JE, Hasemann G, Fogarty J. 1995b. Harvest of Skulls and Bones. Archaeology 48:36-40.

Brady JE, Begley CT, Fogarty J, Stierman DJ, Luke B, Scott A. 2000. Talgua archaeological project: A preliminary assessment. Mexicon 22: 111–118.

Brady JE, Stone A. 1986. Naj Tunich: entrance to the Maya underworld. Archaeology 39: 18-25.

Brand WA, Coplen TB. 2012. Stable isotope deltas: Tiny, yet robust signatures in nature. Isot Environ Healt S 48: 393–409.

Brugnoli E, Scartazza A, Lauteri M, Monteverdi MC, Maguas C. 1998. Carbon isotope discrimination in structural and non-structural carbohydrates in relation to productivity and adaptation to unfavourable conditions. In: Griffiths H, editor. Stable Isotopes.: integration of Biological, Ecological, and Geochemical Processes. Oxford: BIOS Scientific Publishers. p 133–144.

Budd P, Montgomery J, Barreiro B, Thomas RG. 2000. Differential diagenesis of strontium in archaeological human dental tissues. Appl Geochem 15:687–694.

Buikstra JE, Ubelaker DH, Haas J, Aftandilian D. 1994. Standards for data collection from human skeletal remains: Proceedings of a seminar at the Field Museum of Natural History, Organized by Jonathan Haas. Arkansas Archeological Survey.

Burton J. 2008. Bone chemistry and trace element analysis. In: Katzenberg MA, Saunders SR, editors. Biological anthropology of the human skeleton. New York: Wiley-Liss. p 443–460.

Burton JH, Wright LE. 1995. Nonlinearity in the relationship between bone Sr/Ca and diet: paleodietary implications. Am J Phys Anthropol, 96: 273-282.

Cabana GS, Clark JJ. 2011. Introduction: migration in anthropology. In: Cabana GS, Clark JJ, editors. Rethinking anthropological perspectives on migration. University Press of Florida.

Campbell NR, Wood A. 1906. The radioactivity of the alkali metals. In Proc. Cambridge Phil. Soc 14:15.

Capo RC, Stewart BW, Chadwick OA. 1998. Strontium isotopes as tracers of ecosystem processes: theory and methods. Geoderma 82:197–225.

Carr C. 1995. Mortuary practices: their social, philosophical-religious, circumstantial, and physical determinants. J Archaeol Method Th 2:105–200.

Cerling TE. 1999. Paleorecords of C_4 plants and ecosystems. In: Sage RF, Monson RK, editors. C_4 plant biology. Academic Press. p 445- 469.

Chacko T, Cole DR, Horita J. 2001. Equilibrium oxygen, hydrogen and carbon isotope fractionation factors applicable to geologic systems. In: Valley JW, Cole DR, editors. Stable Isotope Geochemistry. Reviews in Mineralogy and Geochemistry vol 43.

Cohodas M. 2002. Multiplicity and discourse in Maya gender relations. In Gustafson, Trevelyan A, editors. Ancient Maya Gender Identity and Relations London: Bergin & Garvey, pp. 11–54.

Coplen KT, Hopple J. 1983. Comparison of stable isotope reference samples. Nature 302:236-238.

Craig H. 1957. Isotopic standards for carbon and oxygen and correction factors for mass-spectrometric analysis of carbon dioxide. Geochimica et cosmochimica acta, 12: 133-149.

Cressie NA. 2015. Statistics for spatial data. Second edition. J Wiley.

Cuddy TW. 2007. Political identity and archaeology in northeast Honduras. University Press of Colorado.

Darrah TH. 2009. Inorganic trace element composition of modern human bones: Relation to bone pathology and geographical provenance. Ph.D. Dissertation. University of Rochester, New York.

Dennett CL. 2007. The Río Claro Site (AD 1000-1530), northeast Honduras: A ceramic classification and examination of external connections. MA Thesis. Trent University, Peterborough, Ontario, Canada.

Dennett CL. 2008a. A Modal Analysis of Vessel Appendages from Río Claro (A.D. 1000-1530), Northeast Honduras. La Tinaja: A Newsletter of Archaeological Ceramics 19:12-16.

Dennett CL. 2008b. Río Claro: A Potential CeramicType-Site for Period VI Northeast Honduras. Vínculos 31:79-10

Dennett CL, Healy PF. 2008. Portable Power and Pre-Columbian Polities: Ceramic Figurines from the Northeast and Ulua Valley Regions of Honduras. Paper presented at the 41st Annual Chacmool Conference, University of Calgary, Calgary, Alberta.

Dennett CL, Healy PF. 2012. The Aguan Valley/Coast. In: Kathryn Sampeck, editor. Pottery of Prehistoric Honduras: Regional Classification and Analysis, 2nd ed. Cotsen Institute of Archaeology, University of California, Los Angeles, California.

Dennett CL, McCafferty GG. 2012. Canadian Institutions and Lower Central American Archaeology: An Historical Overview of Research along the Southern Mesoamerican Periphery. Can J Archaeol 36:51–66.

DeNiro MJ, Epstein S. 1978. Influence of diet on the distribution of carbon isotopes in animals. Geochimica et cosmochimica acta 45: 495-506.

Dixon B, Joesink-Mandeville LRV, Hasebe N, Mucio M, Vincent W, James D, Petersen K. 1994. Formative-Period architecture at the site of Yarumela, Central Honduras. Lat Am Antiq 5:70–87.

Dixon B, Hasemann G, Gomez P, Brady J, Beaudry-Corbett M. 1998. Multiethnicity or multiple enigma: Archaeological survey and cave exploration in the Río Talgua drainage, Honduras. Anc Mesoam 9:327–340.

Eerkens JW, Bartelink EJ. 2013. Sex-biased weaning and early childhood diet among middle Holocene hunter–gatherers in Central California. Am J Phys Anthropol 152:471–483.

Ehleringer JR, Bowen GJ, Chesson LA, West AG, Podlesak DW, Cerling TE. 2008. Hydrogen and oxygen isotope ratios in human hair are related to geography. Proceedings of the National Academy of Sciences, 105: 2788-2793.

Ehleringer JR, Thompson AH, Podlesak DW, Bowen GJ, Chesson LA, Cerling TE, Schwarcz H. 2010. A framework for the incorporation of isotopes and isoscapes in geospatial forensic investigations. In: West JB, Bowen GJ, Dawson TE, Tu KP, editors. Isoscapes. Springer Netherlands. p 357-387.

Epstein JF. 1957. Late Ceramic Horizons in Northeastern Honduras. Ph.D. dissertation, Department of Anthropology, University of Pennsylvania. Ann Arbor, University Microfilms International.

Evans ST. 2004. Ancient Mexico & Central America: archaeology and culture history. New York: Thames & Hudson.

Evans I. 2012. Time and space boundaries. In: Nichols DL, Pool CA, editors. The Oxford handbook of Mesoamerican archaeology. Oxford University Press. p 114-128.

Faure G. 1998. Principles and applications of geochemistry: A comprehensive textbook for geology students. New Jersey: Prentice Hall.

Faure G, Powell JL. 1972. Strontium isotope geology. New York: Springer-Verlag.

Faure G. 1977. Principles of isotope geology. NY, New York: John Wiley and Sons.

Faure G, Mensing TM. 2005. Isotopes : principles and applications. Hoboken, N.J.: Wiley.

Fitzsimmons JL. 2012. The living and the dead. In: Nichols DL, Pool CA, editors. The Oxford handbook of Mesoamerican archaeology. Oxford University Press. p 776-784.

Freiwald C. 2011. Maya Migration Networks: Reconstructing Population Movement in the Belize River Valley during the Late and Terminal Classic. Ph.D. dissertation, Department of Anthropology, University of Wisconsin-Madison.

Fry B. 2006. Stable isotope ecology. New York: Springerverlag.

Gándara M. 2012. A Short history of theory in Mesoamerican archaeology. In: Nichols DL, Pool CA, editors. The Oxford handbook of Mesoamerican archaeology. Oxford University Press. p 31-46.

Genoni L, Iacumin P, Nikolaev V, Gribchenko Y, Longinelli A. 1998. Oxygen isotope measurements of mammoth and reindeer skeletal remains: an archive of Late Pleistocene environmental conditions in Eurasian Arctic. Earth Planet Sc Lett 160:587–592.

Goodman AH, Martin DL, Armelagos GJ. 1995. The biological consequences of inequality in prehistory. Revista di Antropologia (Roma) 73:30-45.

Gröning M. 2004. International stable isotope reference materials. In: de Groot, PA, editor, Handbook of stable isotope analytical techniques. Elsevier BV. p 874–906.

Guiteras Holmes C. 1947. Clanes y sistema de parentesco de Cancuc (Mexico). Acta Americana 5: 1-17.

Hakenbeck S. 2008. Migration in Archaeology: Are We Nearly There Yet? Archaeological review from Cambridge 23: 9-26.

Harborne AR, Afzal DC, Andrews MJ. 2001. Honduras: Caribbean coast. Marine Pollution Bulletin 42: 1221-1235.

Harlow GE, Sisson VB, Sorensen SS. 2011. Jadeitite from Guatemala: new observations and distinctions among multiple occurrences. Geologica Acta, 9: 363-387.

Harp EL, Wilson RC, Wieczorek GF. 1981, Landslides from the February 4, 1976, Guatemala earthquake: U.S. Geological Survey Professional Paper 1204-A, 35.

Hasemann G. 1995. Informe sobre excavaciónes en Talgua. Manuscript on file at the Instituto Hondureño de Antropología e Historia.

Healy PF. 1974. The Cuyamel Caves: Preclassic sites in Northeast Honduras. Am Antiquity 39: 435–447.

Healy PF.1975 H-CN-4 (Williams Ranch Site): Preliminary Report on a Selin Period Settlement in Northeast Honduras. Vinculos (Museo Nacional de Costa Rica) 1(2): 61-71.

Healy PF.1978a. Excavations at the Selin Farm Site (H-CN-5), Colon, Northeast Honduras. Vinculos (Museo Nacional de Costa Rica) 4: 57-79.

Healy PF.1978b. Excavations at Río Claro, Northeast Honduras: Preliminary Report. J Field Archaeol 5: 15-28.

Healy PF. 1984. The archaeology of Honduras. In: Lang FW, Stone DZ, editors. The archaeology of lower Central America, A School of American Research Book, University of New Mexico: Albuquerque. p 113-164.

Healy PF, Emery K, Wright LE. 1990. Ancient and modern Maya exploitation of the jute snail (Pachychilus). Lat Am Antiq 1: 170–183.

Healy PF. 1992. Ancient Honduras: power, wealth, and rank in early chiefdoms. In: Lange FW, editor. Wealth and Hierarchy in the Intermediate Area. p 85-108.

Healy PF, Dennett CL, Harris MH, Both A. 2010. A Musical Nature: Pre-Columbian Ocarinas of Northeast Honduras. In: Eichmann R, Hickmann E, Koch LC, editors. Musical Perceptions - Past and Present: On Ethnographic Analogy in Music Archaeology, Veriag Marie Leidorf, Rahden: Germany. p 189-212

Healy PF, Dennett CL, Harris MH, Both AA. 2010. A Musical Nature. Pre-Columbian Ceramic Flutes of Northeast Honduras. Eichmann/Hickmann/Koch, p 189-212.

Hedman K, Hargrave EA, Ambrose SH. 2002. Late Mississippian Diet in the American Bottom: Stable Isotope Analyses of Bone Collagen and Apatite. Midcont J of Archaeol 27: 237–271.

Henderson JS. 1987. Frontier at the Crossroads. Interaction on the Southeast Mesoamerican Frontier, British Archaeological Reports International Series, 327: 455-462.

Henderson IS, Hudson KM. 2012. The southnortheast fringe of Mesoamerica. In: Nichols DL, Pool CA, editors. The Oxford Handbook of Mesoamerican Archaeology. Oxford University Press. p 482-494.

Herrmann NP. 2002. GIS Applied to Bioarchaeology; an Example from the Río Talgua Caves in Northeast Honduras. J Cave Karst Stud 64: 17–22.

Herrmann NP, Benedix DC, Scott AM, Haskins VA. 1999. A Brief Comment on an intentionally modified tooth from the Río Talgua Region, Northnortheast Honduras. Dent Anthropol 13: 9-12.

Hillson S. 1996. Dental anthropology. New York: Cambridge University Press.

Hillson S. 2005. Teeth. New York: Cambridge University Press.

Hodell DA, Curtis J H, Brenner M. 1995. Possible role of climate in the collapse of Classic Maya civilization. Nature 375: 391-394.

Hodell DA, Quinn RL, Brenner M, Kamenov G. 2004.Spatial variation of strontium isotopes (87Sr/86Sr) in the Maya region: A tool for tracking ancient human migration. J Archaeol Sci 31: 585–601.

Hoefs J. 2009. Stable isotope geochemistry. Federal Republic of Germany: Springer-Verlag.

Hoopes JW, Fonseca O. 2003. Goldwork and Chibchan identity: Endogenous change and diffuse unity in the Isthmo-Colombian area. In: Quilter J, Hoopes JW, editors. Gold and Power in Ancient Costa Rica, Panama, and Colombia. Dumbarton Oaks. 49-90.

Iacumin P, Bocherens H, Mariotti A, Longinelli A. 1996. Oxygen isotope analyses of co-existing carbonate and phosphate in biogenic apatite: A way to monitor diagenetic alteration of bone phosphate? Earth Planet Sci Lett 142:1–6.

Jacobi KP. 2000. Last rites for the Tipu Maya: Genetic structuring in a colonial cemetery. Tuscaloosa: The University of Alabama Press.

Joseph AP, Harish RK, Rajeesh Mohammed PK, Kumar V. 2013. How reliable is sex differentiation from teeth measurements. J Oral Maxillofac Pathol 4:289-292.

Joyce RA. 1993. The construction of the Mesoamerican frontier and the Mayoid image of Honduran polychromes. Reinterpreting Prehistory of Central America, 51-101.

Joyce R. 2000. Gender and Power in Prehispanic Mesoamerica. Austin, TX: University of Texas Press.

Joyce R. 2003. Making Something of Herself: Embodiment in Life and Death at Playa de los Muertos, Honduras. Cambridge Archaeological Journal 13:248– 261.

Joyce RA. 2011. 3 in the beginning: The experience of residential burial in prehispanic Honduras. Archeological Papers of the American Anthropological Association 20:33–43.

Joyce RA, Henderson JS. 2010. Being "Olmec" in Early Formative Period Honduras. Anc Mesoam 21:187.

Juarez CA. 2008. Strontium and geolocation, the pathway to identification for deceased undocumented Mexican border-crossers: A preliminary report. J Forensic Sci 53: 46–49.

Juarez CA. 2011. Geolocation: A pathway to identification for deceased undocumented border crossers. Dissertation, University of California-Santa Cruz.

Katzenberg AM. 2008. Stable isotope analysis: A tool for studying past diet, demography, and life history. In: Katzenberg MA, Saunders SR, editors. Biological anthropology of the human skeleton. New York: Wiley-Liss. p 411–441.

Kellner CM, Schoeninger MJ. 2007. A simple carbon isotope model for reconstructing prehistoric human diet. Am J Phys Anthropol 133:1112–1127.

Kieser J. 1990. Human adult odontometrics: The study of variation in adult tooth size. Cambridge studies in biological anthropology.

Kirchhoff P. 1943. Mesoamérica: Sus límites geográficos, composición étnica y caracteres culturales. Acta Americana 1: 92-107.

Knudson KJ, Stojanowski CM. 2008. New directions in bioarchaeology: recent contributions to the study of human social identities. J Archaeol Res. 16: 397-432.

Knudson KJ, Williams SR, Osborn R, Forgey K, Williams PR. 2009.The geographic origins of Nasca trophy heads using strontium, oxygen, and carbon isotope data. J Anthropol Archaeol 28: 244–257.

Knudson KJ, O'Donnabhain B, Carver C, Cleland R, Price TD. 2012. Migration and Viking Dublin: Paleomobility and paleodiet through isotopic analyses. J Archaeol Sci 39: 308–320.

Koch PL, Tuross N, Fogel ML. 1997. The effects of sample treatment and diagenesis on the isotopic integrity of carbonate in biogenic hydroxylapatite. J Archaeol Sci 24:417–429.

Laffoon JE, Rojas RV, Hofman CL. 2013. Oxygen and carbon isotope analysis of human dental enamel from the Caribbean: implications for investigating individual origins. Archaeometry 55: 742-765.

Lange, Frederick W. and Doris Z. Stone. 1984. Introduction. In The Archaeology of Lower Central America, edited by Frederick W. Lange and Doris Z. Stone, pp. 3-12. University of New Mexico Press, Albuquerque, NM.

Lara Pinto G, Hasemann G. 1988. La Sociedad Indígena del Noreste de Honduras en el Siglo XVI:¿ Son la Etnohistoria y la Arqueología Contradictorias? Yaxkin XI 2: 5-28.

Larsen CS. 1997. Bioarchaeology: Interpreting behavior from the human skeleton. New York: Cambridge University Press.

Lee Thorp J, Van Der Merwe N J. 1987. Carbon isotope analysis of fossil bone apatite. South African J Sci 83: 712-715.

Lentz D, Pohl MD, Pope KO. 2005. Domesticated Plants and Cultural Connections in Early Mesoamerica: Formative Period Paleoethnobotanical Evidence from Belize, Mexico, and Honduras. New Perspectives on Formative Mesoamerican Cultures, p 121-126.

Longinelli, A. 1984. Oxygen isotopes in mammal bone phosphate: a new tool for paleohydrological and paleoclimatological research?. Geochimica et Cosmochimica Acta 48: 385-390.

Longinelli A. 1995. Stable isotope ratios in phosphate from mammal bone and tooth as climatic indicators. In Proceedings of the ESF Workshop. p 57-70.

Luke B.A, Begley CT, Chase DS, Ross A.J, Brady J.E. 1997. Rapid-response geophysical site investigations at a pre-columbian settlement in Honduras. In 10th EEGS Symposium on the Application of Geophysics to Engineering and Environmental Problems.

Lu GY, Wong DW. 2008. An adaptive inverse-distance weighting spatial interpolation technique, Computers & Geosciences, 34: 1044-1055.

Luz B, Kolodny Y, Horowitz M. 1984. Fractionation of oxygen isotopes between mammalian bone-phosphate and environmental drinking water. Geochimica et Cosmochimica Acta 48:1689–1693.

Makarewicz CA, Sealy J. 2015. Dietary reconstruction, mobility, and the analysis of ancient skeletal tissues: Expanding the prospects of stable isotope research in archaeology. J Archaeol Sci 56: 146-158.

Marshall JS. 2007. The geomorphology and physiographic provinces of Central America. In: Bundschuh J, Alvarado GE, editors. Central America: Geology, Resources and Hazards. Taylor & Francis. London: UK 1-51.

Martin C, Bentaleb I, Kaandorp R, Iacumin P, Chatri K. 2008. Intra-tooth study of modern rhinoceros enamel $\delta 18O$: Is the difference between phosphate and carbonate $\delta 18O$ a sound diagenetic test? Palaeogeogr Palaeocl 266:183–189.

McCafferty G, Amador FE, Salgado S. 2012. Archaeology on Mesoamerica's southern frontier. In: Nichols DL, Pool CA, editors. The Oxford Handbook of Mesoamerican Archaeology. p 83.

McCafferty GG, McCafferty SD. 2009. Crafting the Body Beautiful: Performing Social Identity at Santa Isabel, Nicaragua. In Halperin CT, Faust KA, Taube R, Giguet A, editors. Mesoamerican Figurines: Small-Scale Indices of Large-Scale Social Phenomena. University Press of Florida, Gainesville, FL. 183-204.

McCafferty GG, McCafferty SD. 2011. Bling Things: Ornamentation and Identity in Pacfic Nicaragua. In Amundsen L, Pickering S, editors. Identity Crisis: Approaches to the Archaeology of Identity,. Proceedings from the 40th Annual Chacmool Conference, University of Calgary, Calgary, AB.

McNatt L. 1996. Cave archaeology of Belize. J Cave Karst Studies, 58: 81-99.

McLachlan G, Peel D. 2004. Finite mixture models. John Wiley & Sons.

Meier-Augenstein W. 2004. GC and IRMS technology for 13 C and 15 N analysis on organic compounds and related gases. In: de Groot, PA, editor, Handbook of stable isotope analytical techniques. Elsevier BV. p 153-176.

Meier-Augenstein W. 2010. Stable isotope forensics: An introduction to the forensic application of stable isotope analysis. Chichester: Wiley Chichester.

Melton PE. 2008. Genetic history and pre-Columbian Diaspora of Chibchan speaking populations: Molecular genetic evidence. Ph.D. Dissertation. University of Kansas.

Miles AW. 2001. The Miles method of assessing age from tooth wear revisited. J Archaeol Sci 28: 973-982.

Milner GR, Wood JW, Boldsen JL. 2008. Advance in paleodemography. In: Katzenberg MA, Saunders SR, editors. Biological anthropology of the human skeleton. New York: Wiley-Liss. p 411–441.

Mook WG. 2006. Introduction to isotope hydrology. Taylor & Francis.

Moyes H, Brady J. 2012. Caves as sacred space in Mesoamerica. In: Holley M, editor Sacred Darkness: A global perspective on the ritual use of caves. University Press of Colorado. p 151-170.

Murrieta-Flores P. 2010. Travelling in a Prehistoric Landscape: Exploring the possible influences that shaped human movement. In Frischer B, Webb Crawford J, Koller D, editors. Making History Interactive. Computer Applications and Quantitative Methods in Archaeology (CAA). Oxford. Archaeopress, British Archaeological Reports S2079: 258-276.

Norr LC. 1991. Nutritional consequences of prehistoric subsistence strategies in lower Central America. Thesis University of Illinois at Urbana-Campaign.

Ortner DJ. 2003. The biology of skeletal tissues. In Identification of pathological conditions in human skeletal remains. Elsevier: San Diego CA. p 11-35.

Parker Pearson M. 1999. The archaeology of death and burial. Phoenix Mill, UK: Sutton.

Paul KS, Stojanowski CM, Butler MM. 2013. Biological and spatial structure of an early classic period cemetery at Charco Redondo, Oaxaca. American journal of physical anthropology 152:217–229.

Pellegrini M, Lee-Thorp, JA, Donahue RE. 2011. Exploring the variation of the δ 18 O p and δ 18 O c relationship in enamel increments. Palaeogeography, Palaeoclimatology, Palaeoecology 310: 71-83.

Philmon KL. 2012. An osteological analysis of human remains from Cusirisna Cave, Nicaragua. MA thesis, Florida Atlantic University, Boca Raton, FL.

Podlesak DW, Torregrossa A M, Ehleringer J R, Dearing MD, Passey B H, Cerling T E. 2008. Turnover of oxygen and hydrogen isotopes in the body water, CO 2, hair, and enamel of a small mammal. Geochimica et Cosmochimica Acta, 72: 19-35.

Pollard AM. 1998. Archaeological reconstruction using stable isotopes. In: Griffiths H, editor. Stable isotopes: Integration of biological, ecological, and geochemical processes. Oxford: BIOS Scientific Publishers Limited. p 285-301.

Price TD, Burton JH, Bentley RA. 2002. The characterization of biologically available strontium isotope ratios for the study of prehistoric migration. Archaeometry 44:117–136.

Price TD, Burton JH, Fullagar PD, Wright LE, Buikstra JE, Tiesler V. 2008 Strontium isotopes and the study of human mobility in ancient Mesoamerica. Latin American Antiquity 19:167-180.

Price TD, Burton JH, Sharer RJ, Buikstra JE, Wright LE, Traxler LP, Miller KA. 2010. Kings and commoners at Copán: Isotopic evidence for origins and movement in the Classic Maya period. J Anthropol Archaeol 29: 15–32.

Price TD, Johnson CM, Ezzo JA, Ericson J, Burton JH. 1994 Residential mobility in the prehistoric Southwest United States: a preliminary study using strontium isotope analysis. J Archaeol Sci 21:315-330.

Price TD, Manzanilla L, Middleton WD. 2000. Immigration and the ancient city of Teotihuacan in Mexico: A study using strontium isotope ratios in human bone and teeth. J Archaeol Sci 27: 903–913.

Prufer KM, Dunham PS. 2009. A shaman's burial from an Early Classic cave in the Maya Mountains of Belize, Central America. World Archaeol 41: 295–320.

Pye K. 2004. Isotope and trace element analysis of human teeth and bones for forensic purposes. Geological Society Special Publications 232: 215–236.

Rhoads ML. 2002. Population Dynamics at the Southern Periphery of the Ancient Maya World: Kinship at Copán. PhD dissertation. The University of New Mexico, Albuquerque, NM.

Rogers RD, Mann P, Emmet PA. 2007. Tectonic terranes of the Chortis Block based on integration of regional aeromagnetic and geologic data. Special Papers-Geological Society of America 428: 65.

Romero J. 1958. Mutilaciones dentarias prehispánicas en México y América en general. Serie Investigaciones 3. Instituto Nacional de Antropología e Historia, Mexico City.

Rue DJ, Freter A, Ballinger D A. 1989. The caverns of Copán revisited: Preclassic sites in the Sesesmil River valley, Copán, Honduras. J Field Archaeol 16: 395-404.

Scherer AK. 2007. Population structure of the classic period Maya. Am J Phys Anthropol 132:367–380.

Schlesinger WH. 2005. Volume editor's introduction. In: Schlesinger WH, editor. Biogeochemistry. Oxford: Elsevier-Pergamon. p xv-xvii.

Schoeninger M J. 1979. Diet and status at Chalcatzingo: some empirical and technical aspects of strontium analysis. Am J Phys Anthropol 51: 295-309.

Schwarcz HP. 2000. Some biochemical aspects of carbon isotopic paleodiet studies. In: Ambrose SH, Katzenberg MA, editors. Biogeochemical Approaches to Paleodietary Analysis, Advances in Archaeological and Museum Science 5. Plenum: New York 189–209.

Schwarcz HP, White CD, Longstaffe FJ. 2010. Stable and radiogenic isotopes in biological archaeology: Some applications. In: West JB, Bowen GJ, Dawson TE, Tu KP, editors. Isoscapes: Understanding movement, pattern, and process on Earth through isotope mapping. Netherlands: Springer. p 335–356.

Scott GR, Turner CG. 1997. Biological consideration: Ontogeny, asymmetry, sex dimorphism, and intertrait association. In: The anthropology of modern human teeth: Dental morphology and its variation in recent human populations. Bristol: Cambridge University Press. p 74-130.

Sheets PD.1992. The Pervasive Pejorative in Intermediate Area Studies. In: Lange FW, editor. Wealth and Hierarchy in the Intermediate Area. Dumbarton Oaks: Washington, DC. p 15-41.

Shimada I, Shinoda K, Farnum J, Corruccini R, Watanabe H, Butters L, Dudar JC, Kaulicke P, Nelson A, Ramirez S. 2004. An Integrated Analysis of Pre-Hispanic Mortuary Practices: A Middle Sicn Case Study 1. Curr Anthropol 45:369–402.

Sillen A. 1981. Strontium and diet at Hayonim Cave. Am J Phys Anthropol 56: 131-137.

Skinner HW, Jahren AH. 2005. Biomineralization. In: Schlesinger WH, editor. Biogeochemistry Vol. 8. Gulf Professional Publishing. 117-184.

Somerville AD. 2010. Telling friends from foes: Strontium isotope and trace element analysis of companion burials from Pusilha, Toledo District, Belize. PhD dissertation, University of California, San Diego, CA.

Somerville AD, Fauvelle M, Froehle AW. 2013. Applying new approaches to modeling diet and status: Isotopic evidence for commoner resiliency and elite variability in the Classic Maya Lowlands. J Archaeol Sci 40: 1539–1553.

Stephan E. 2000. Oxygen isotope analysis of animal bone phosphate: method refinement, influence of consolidants, and reconstruction of palaeotemperatures for Holocene sites. J Archaeol Sci 27: 523-535.

Stephens, L. 2002. Sexualities and genders in Zapotec Oaxaca. Latin American Perspectives, 29(2):41–59.

Stockett MK. 2005. On the importance of difference: re-envisioning sex and gender in ancient Mesoamerica. World archaeolo. *37*: 566-578.

Stojanowski CM, Schillaci MA. 2006. Phenotypic approaches for understanding patterns of intracemetery biological variation. Am J Phys Anthropol 131:49–88.

Stone DZ. 1941 The Archaeology of the North Coast of Honduras. Harvard University, Peabody Museum of Archaeology and Ethnology, Memoir #9(1). Cambridge, MA.

Stone DZ. 1957. The archaeology of central and southern Honduras. Papers of the Peabody Museum of archaeology and ethnology. 49 (3): Cambridge, MA: Harvard University.

Strong, WD. 1935. Archaeological Investigations in the Bay Islands, Spanish Honduras. Smithsonian Institution, Miscellaneous Collections #92. Washington, DC.

Strong WD. 1948. Archaeology of Honduras. In: Steward JH, editor. Handbook of South American Indians. Bulletin No. 143. Washington, DC: Bureau of American Ethnology. p 71-120.

Stronge S. 2012.Examining chronological trends in ancient Maya diet at Minanha, Belize, using the stable isotopes of carbon and nitrogen. MA thesis, Trent University, Canada.

Thompson JS. 1975. The Role of Caves in Maya Culture. In: Mercer H, editor. Introduction to the Hill Caves of Yucatan: Introduction, ix-xliv. Zephryrus Press, Teaneck, New Jersey

Tieszen LL. 1991. Natural variations in the carbon isotope values of plants: implications for archaeology, ecology, and paleoecology. Journal of Archaeological Science, 18: 227-248.

Turner BL. 2008. The servants of Machu Picchu: Life histories and population dynamics in Late Horizon Peru. PhD dissertation, Emory University, Atlanta, GA.

Turner BL, Kamenov GD, Kingston JD, Armelagos GJ. 2009. Insights into immigration and social class at Machu Picchu, Peru based on oxygen, strontium, and lead isotopic analysis. J Archaeol Sci 36:317–332.

Urey HC. 1947. The thermodynamic properties of isotopic substances. J Chemical Society (Resumed), 562-581.

Van der Merwe NJ, Vogel JC. 1978. 13C content of human collagen as a measure of prehistoric diet in woodland North America. Nature 276: 815-816.

Van der Merwe N J, Tykot R H, Hammond N, Oakberg K. 2002. Diet and animal husbandry of the Preclassic Maya at Cuello, Belize: Isotopic and zooarchaeological evidence. Editors, Ambrose SH, Katzenberg AM, In Biogeochemical approaches to paleodietary analysis. Springer US. 23-38.

Vander Zanden HB, Wunder MB, Hobson KA, Van Wilgenburg SL, Wassenaar LI., Welker JM, Bowen GJ. 2014. Contrasting assignment of migratory organisms to geographic origins using long-term versus year-specific precipitation isotope maps. Methods in Ecology and Evolution 5: 891-900.

Viland JC, Henry B. 1996. Late Jurassic deformation in Honduras. Proposals for a revised regional stratigraphy. J S Am Earth Sci 9: 153–160.

Vodanović M, Demo Z, Njemirovskij V, Keros J, Brkić H. 2007. Odontometrics: A useful method for sex determination in an archaeological skeletal population? J Archaeol Sci 34: 905–913.

Vogel, JC, Van der Merwe, NJ.1977. Isotopic evidence for early maize cultivation in New York State. Am Antiquity 42:238-242.

Webb EA, Schwarcz HP, Healy PF. 2004. Detection of ancient maize in lowland Maya soils using stable carbon isotopes: evidence from Caracol, Belize. Journal of Archaeol Sci 31: 1039-1052.

Webster D. 1997. Studying Maya burials. In: Whittington SL, Reed DM, editors. Bones of the Maya: Studies of ancient skeletons. Smithsonian Institution Press. p 3–12.

White WM. 2013. Geochemistry. John Wiley & Sons.

White TD, Black MT, Folkens PA. 2012. Human osteology. Academic Press: 3rd edition.

White CD, Price DT, Longstaffe FJ, 2007. Residential histories of the human sacrifices at the Moon Pyramid, Teotihuacan: Evidence from oxygen and strontium isotopes. Anc Mesoam 18: 159–172.

White CD, Spence MW, Stuart-Williams HL, Schwarcz HP. 1998. Oxygen isotopes and the identification of geographical origins: The valley of Oaxaca versus the valley of Mexico. J Archaeol Sci 25: 643–655.

White CD, Spence MW, Longstaffe FJ, Law KR. 2000. Testing the nature of Teotihuacán imperialism at Kaminaljuyú using phosphate oxygen-isotope ratios. J Anthropol Research 56: 535-558.

White CD, Spence MW, Longstaffe FJ, Law KR. 2004. Demography and ethnic continuity in the Tlailotlacan enclave of Teotihuacan: The evidence from stable oxygen isotopes. J Anthropol Archaeol 23:385–403.

Williams JS, White CD, Longstaffe FJ. 2005. Trophic level and macronutrient shift effects associated with the weaning process in the Postclassic Maya. Am J Phys Anthropol 128: 781-790.

Wright LE. 2005. Identifying immigrants to Tikal, Guatemala: Defining local variability in strontium isotope ratios of human tooth enamel. J Archaeol Sci 32: 555–566.

Wright LE. 2012. Immigration to Tikal, Guatemala: Evidence from stable strontium and oxygen isotopes. J Anthropol Archaeol 31: 334–352.

Wright LE, Schwarcz HP. 1996. Infrared and isotopic evidence for diagenesis of bone apatite at Dos Pilas, Guatemala: Paleodietary implications. J Archaeol Sci 23: 933–944.

Wright LE, Schwarcz HP. 1998. Stable carbon and oxygen isotopes in human tooth enamel: identifying breastfeeding and weaning in prehistory. Am J Phys Anthropol 106:1–18.

Wright LE, Schwarcz HP. 1999. Correspondence between stable carbon, oxygen and nitrogen isotopes in human tooth enamel and dentine: infant diets at Kaminaljuyu. J Archaeol Sci 26: 1159-1170.

Wright LE, Valdés JA, Burton JH, Price TD, Schwarcz HP. 2010 .The children of Kaminaljuyu: Isotopic insight into diet and long distance interaction in Mesoamerica. J Anthropol Archaeol 29: 155–178.

Wright LE, White CD. 1996. Human biology in the Classic Maya collapse: Evidence from paleopathology and paleodiet. J World Prehist 10:147–198.

Wrobel GD. 2003. Metric and Nonmetric Dental Variation among the Ancient Maya of Northern Belize. PhD dissertation. Indiana University, Bloomington, IN.

Wunder MB, Kester C L, Knopf F L, Rye R O. 2005. A test of geographic assignment using isotope tracers in feathers of known origin. Oecologia, 144: 607-617.

Wunder MB. 2010. Using isoscapes to model probability surfaces for determining geographic origins. In: West JB, Bowen GJ, Dawson TE, Tu KP, editors. Isoscapes: Understanding Movement, Pattern, and Process on Earth through Isotope Mapping. Springer Netherlands. p 251–270.

Wunder MB. 2012. Determining geographic patterns of migration and dispersal using stable isotopes in keratins. J Mammal 93:360–367.

Wunder MB, Norris DR. 2008. Improved estimates of certainty in stable-isotope-based methods for tracking migratory animals. Ecol Appl18:549–559.

Zuckerman MK, Armelagos GJ. 2011. The Origins of Biocultural Dimensions in Bioarchaeology. Social Bioarchaeology: 15–43.

APPENDIX A

STANDARD OPERATING PROCEDURES

A.1   Carbonate preparation for enamel apatite SOP

Carbonate Preparation for Enamel Apatite Samples

Caveat:The procedure below represents a basic outline for preparing apatite samples for isotopic analysis by acid digestion. Modification of this procedure may be required for samples of different histories.

Recommended Carbonate Preparation for Tooth Enamel Samples

1.Weigh out 5-10 mg of powdered enamel into a microcentrifuge tube.
2. Add 1 ml of 30% H2O2 (currently located in the lab refrigerator) for 10 mg of sample (scale according to the sample weight).
3. Seal the microcentrifuge tube and agitate (vortex genie) each sample for 30-60 seconds.
4. Loosen the lids (so that gas can escape) and allow samples to sit and react for 24 hours (agitate often).
5. Centrifuge the samples and aspirate the H2O2 away taking care to leave the powder behind.
6. Rinse the sample by adding 1 ml of MilliQ water and agitating. Then centrifuge and repeat for a total of 5 rinses.
7. Once samples have been rinsed 5 times, add 2 ml of 1M acetic acid buffered with calcium acetate to pH of ~5* for 25 mg of sample (scale according to the sample weight). Currently the acetic acid buffered with calcium acetate is found in the flammables cabinet.
8. Agitate samples and allow them to react for 24 hours**.
9. Centrifuge the samples and aspirate the acetic acid buffer solution away taking care to leave the powder behind.
10. Rinse the sample by adding 1 ml of MilliQ water and agitating. Then centrifuge and aspirate as in step 9. Repeat four additional times leaving the powder only (no water) after the final aspiration.
11. Uncap each sample and cover with aluminum foil. Use a sharp to make a small hole in the foil covering each sample tube.
12. Freeze the samples for ~25 minutes or longer.
13. Place samples on a freeze dryer overnight.
14. Weigh out between 0.5 and 1 mg for a Kiel run into sample boats.
15. Vacuum roast the samples for ~ 1 hour at 65°C before running them on a mass spectrometer.

*Buffer solution should be made by mixing a 1M solution of acetic acid with a 1M solution of calcium acetate. Using the Henderson-Hasslebach equation this yields a solution of ~pH 5. Confirm this pH periodically. Do not use buffer solution if pH falls below 4.5.

**Both temperature and time of reaction can affect the C isotope composition of the sample. It is, therefore, imperative to leave samples in solution for exactly 24 hours. This value is not approximate. The reaction time was formerly 12 hours (and may still be 12 hours for enamel) but C isotope composition of dentine carbonate changes rapidly within the first 12 hours, thus 24 hours should give more consistent results.

A.2   Dual-Inlet auto carbonate device SOP

Optima/Prism Run Procedures

Safety:

The primary safety concern in operating the Prism are two-fold:

1) Exposure to liquid nitrogen (LN2) while dispensing. Liquid nitrogen can cause severe freezer burns. Please use closed toed shoes, and personal protective equipment (PPE) when handling liquid nitrogen (cryo-gloves, and face mask). Furthermore, liquid nitrogen boil-off while dispensing from large 230 liter dewars can displace O_2 and lead to dizziness and loss of conciousness. Immediately more away from the liquid nitrogen tank if you notice dizziness while dispensing LN2.

2) Exposure to hot phosphoric acid. Phosphoric acid can cause severe burns, particularly when hot. Use appropriate PPE.

Cleanup:

Points 1 to 3 should be done by the previous user - this is particularly important at weekends so that the water in the hot water bath does not evaporate.

1) Check that the previous run has really finished, and not stalled[1].

2) Turn off the water bath[2].

3) Turn off the cryocooler- this should be left for at least 15 minutes before removing probe and sponges.

4) Fill the trap above the Autocarb rotary pump with LN2 using a funnel.

5) C1, C2, and C3 should be closed; make sure.

6) Open C4

7) Shut the black knob (upwards) to the autcarb rotary pump.

8) Open the carousel and acid bath to atmosphere (black Nupro toggle)*

9) Remove the large stainless steel dewar from the water trap

10) Remove the reaction vessel: remove the clip, lower the magnetic stirrer, and gently detach the reaction vessel from its connection.

11) Unhook the closest water hose and hold; whilst tilting the reaction vessel away from you, allow the water to drain down the other hose.

12) Unhook the other hose, cleaning any water spillage.

13) Connect the two hoses, and seal the reaction vessel connection point with the glass cap and clip.

14) Once the cryocooler probe and sponge have defrosted[3], remove the alcohol trap and allow the probe to drain off exess alcohol.

15) Close the autocarb to atmosphere, and open the carousel to the high conductance vacuum line (black knob downwards). Check the Autocarb vacuum on the computer.

16) Take the acid bath reaction vessel next door and clean it and the boats using the instructions above the sink.

17) Reset the carousel.

For the Optima: Click on the carousel icon, move box to far left (zero), then advance the carousel to position "9".

For the Prism: Go to "Prep", and "reset carousel".

Check that the carousel is advanced slightly past, and not directly above the "O" port.

18) Fill the water bath with DI water to ca. 1 cm from the top[4].

19) Remove the previous runs data sheets from the printer using line/form feed, write down the date, user name, instrument name and store.

20) When the Autocarb Pirani gauge has reached 1E-3, place a spare stainless steel dewar filled with hot tap water on the water trap. Top off the water trap above the Autocarb pump with LN2.

21) Open C3, observing the pressure increase on the autocarb Pirani gauge.

22) During this interval weigh out standards, and note down order of samples/standards[5].

23) Close C3 and, once cool, remove the heater tape.

1 The run program should be DI233, do not use DI247. Following the completion of a run, the message window should say, "autorun finished" in green. If the program/computer has crashed, or the program has stalled for some reason (e.g., for being out of LN2 or

printer paper), check with the previous analyzer/P.I. to discuss whether or not to continue the previous run.

2 If the temperature is <90°C, notify previous analyzer.

* black Nupro toggle valves are closed, when the toggle is parallel with the pipe work, and open when standing up. Make sure the axle is correctly inserted, otherwise the valve will not open/close.

3 Don't try to remove if still frozen, otherwise the pipe may crack.

4 Don't use tap water!!!!

5 Use Carrera Marble standard, unless there is a need for recalibration. For the prism, two grains is sufficient for a small analysis, for the Optima, five grains or less is normally too small. For a full sample run, the first five, the middle three and the last three are generally standards. Standards and samples can be separated by an empty boat, if desired.

Startup:

1) Check that C2 and C3 are closed

2) Put the alcohol[1] trap up, insert the probe, surround with foam and insert thermometer.

3) Turn on Cryocooler

4) While there is no gas in the inlet, note the Ion Gauge reading. (Just after run finishes. Both valves closed.)

5) Get samples and standards ready.

6) Close the autocarb carousel from the rotary pump, undo the carousel bolts , and open to atmosphere with the nearest black Nupro toggle valve.

7) Open the carousel carefully. Use a kimwipe to remove lint from all parts of the carousel. If the carousel disc has been contaminated with acid, boil for a minute in DI water, and wipe the rest of the carousel with a damp kimwipe.

8) Load samples/standards

9) Replace the top of the carousel, making sure the screws are equally positioned[2].

10) Make sure the water bath is full.

11) Put a PTFE coated magnet in the reaction vessel: small magnets fro forams, medium for carbonate powders, large for apatite powders.

12) Pour green phosphoric acid so that it just covers the magnet (>10ml)[3].

13) Unclamp and remove the glass cap underneath the carousel. Clean the black o-ring with a dry kimwipe.

14) Place reaction vessel on top of the magnetic stirrer, and then replace the clip, making sure that the vessel is not tilted. Move the stirrer up.

15) Unfasten the water hoses from each other, and clamp those on the reaction vessel.

16) Turn on the water bath[4]. Make sure the hoses do not leak.

17) Isolate the carousel from atmosphere (black Nupro toggle valve), and open the other toggle to the rotary pumps via the capillary (not the direct route[5]. see (19).

18) Go to "Prep" and turn on the magnetic stirrer. Make sure it is at top speed (dial underneath).

19) Keep checking the autocarb Pirani gauge. Wait ten minutes after it has reached 1E-3, then shut from the capillary route to the rotary, and open the direct route (knob down).

20) While waiting for the carousel, fill in the log. Go to "Analysis", "Batch Edit", load "Isocarb", and go to "Setup". "Release All" to overwrite. Close and open window to make sure that the data has been saved correctly.

21) Make sure the parameters are set correctly ("Analysis", "Edit Parameter Files"). For seconds for apatites (Optima only). For reference gas parameters see the table below.

22) Load reference gas[6] (Under "Prep"). Follow the directions that appear on the screen.

23) Check the alcohol trap temperature. It needs to be < -85°C

24) Similarly the water bath should be at 90°C and the acid should be stirred and pumped while hot for at least 1 hour before starting the analysis.

25) Fill and hook up the large LN2 dewar.

26) Once the reference gas is loaded, go to "Scans" and load CO2. Check that the peak is flat and drag the centering line to the center of the flat part of the peak. Fill in the acceleration voltage on the sheet, and note the minimum beam size (Major m/z = 44 beam).

27) To start the run, go to "Analysis" and "Autorun start/stop". Once you get the green colored message "Autorun initialized", close

the carousel section from the pump (black knob upwards).

1 100% ethanol. Add LN2 if necessary (in fume cupboard if possible, away from ovens/flames) so that the mixture is around -50°C, since cryocool takes a long time to cool the trap.
2 Don't overtighten.
3 Make sure that acid does not come in contact with the mouth of the reaction vessel; if it does, use a dry kimwipe to clean thoroughly.
4 This takes 40 minutes to reach 90.2°C from cold.
5 Otherwise the carousel is showered with powdered samples.
6 The Refgas sequences for the Optima and Prism are different, so make sure you follow the instructions carefully.

A.3 Thermo-Chemical elemental analyzer (TCEA) SOP

THERMO-CONVERSION ELEMENTAL ANALYZER (TCEA) STANDARD OPERATING PROCEDURES

Safety Warnings

In this procedure you may potentially come in contact with acarite (a very strong base), and magnesium perchlorate. Ascarite, in particular, and magnesium perchlorate can cause sever burns to eyes, skin and internal organs. Please wear personal protective equipment and work in the fume hood with these materials.

The TCEA operates at a very high temperature. Be thoughtful when working with this instrument as some components can be very hot and cause skin burns.

Phase 1: Perform TCEA Maintenance

1. Replace the graphite crucible every 75-100 samples.
2. Remove the reactor and clean the glassy carbon tube and glassy carbon grains after every 200-250 samples.

Phase 2: Warm-Up the day prior to running

1. Close SGE valve at MS source & turn on Conflo He dilution.
2. Make sure SGE valve for gas bench, GC, or LC valve is also closed.
3. Clean glassy carbon tube and glassy carbon grains if needed (see below).
4. Set the temperature controller ramp rate.
   a. On Jumbo controller (one on the right) press and hold in the P button for 5 seconds, until the Pb.1 option shows, and release button immediately.:
   b. Now press the P button multiple times to cycle through the options, until you reach rasd.:
   c. Use the Up and Down buttons to select ramp rate. Note the units are °C/min. Never heat or cool in increments > 5°C/min. Ramp rate guidelines: At 1°C/min it takes roughly 20 hours to heat from room temperature to working temperatures of ca. 1400°C. Typically, heat overnight at 1-2°C/min. Cool at 3°C/min.:

5. Set He flow to 0.6 bar.
6. Set Jumbo controller to ramp up to the desired operating temperature overnight.
   a. Press P twice to get to SP.
   b. Use the up and down buttons to set the desired operating temperature.
   c. Once the temperature is set wait roughly 2-3 seconds for the display to blink off and back on. Immediately press P again. The present temperature of the reactor should show.
   d. Watch the cycling yellow lights of the controller and observe that they are applying power to the heating element. Also, confirm that the element is heating and at the selected rate.

Phase 2: The day of the run

0. If running phosphates, procure dry ice (located in 137 Sinsheimer and in the hallway across from 339 PSB, delivered every Tuesday and Friday).
1. Set He and Purge He carrier gas flow to 1.7 bar.
2. Open the CO tank and regulator valves in the fume hood. Check both the cylinder valve and the regulator valve are open. (Temporary: attach the Variac power supply to the automatic shutoff valve on the CO line in the fume hood. This is to bypass a defective circuit powering this valve).
3. Open CO gas tanks by opening the valves below the peripheals benchtop.
4. Close the isolation valve on the zero blank autosamper (ZBA).
5. Load samples and vent the ZBA carousel cavity
   a. Open the vent valve on the top of the ZBA.
   b. Open the three knurled set screws to open the ZBA lid.
   c. Press the manual advance on the ZBA controller and be sure the carousel port is advancing past the drop hole. Adjust the carousel position with the manual advance jog switch on the back of the ZBA controller.
   d. Load samples.
   e. Close the lid being sure to check that the o-ring is seated properly and firmly tighten the three knurled set screws.
   f. Open the in-line Purge line valve (slide barrel towards ZBA) and turn up the auxillary He flow to 1.5 bar. Test that He is flowing using the leak detector or flow meter.

6. Allow the ZBA sample cavity to vent for 5 minutes:
   a. Then close the valve.
   b. Close the in-line Purge line valve (slide barrel away from ZBA) and turn down the auxillary He flow by backing off on the auxillary He regulator by many turns.

7. Set the 4-port valve under the benchtop so that the TCEA is going to the desired mass spectrometer.

8. Set the communication switch box: Select Sherlock/Columbo EA/TCEA communication switch box according to the instrument being used.

9. On the Conflo, turn the dilution on.

10. Turn off source at the computer and then open the SGE valve at the mass spectrometer source. Be sure the other peripheral SGE valves are closed.

11. Check that the vacuum pressure is between 7-e7 to 3e-6 mBar range, and then turn the source back on. If outside this range, close the source SGE valve and see the lab manager.

12. Select CO gas on the mass spectrometer software, and monitor mass 28 background. If it is less than 1000 mV, then turn off dilution.

13. Open the Instrument Control software module and scan mass 28 for background stability. Wait until the background trace flattens out and stabilizes, then stop scan.

14. Return to Acquisition software and begin a standard on-off sequence for CO. You should achieve better than 0.1‰ precision for the standard on off δ^{18}O.

15. While the standard on-off are going, prepare a sequence file for the run.

16. If running phosphates, crush up some dry ice and add it to ethanol, to make a dry ice-ethanol slush. Add this to slush to a small glass dewar (found at the back of the TCEA peripheral). Place the coiled 1/16 stainless steel line into the trap, such that the coil is at the bottom of the dewar.

17. Turn the 2-way valve, that is downstream of the coil at the back of the TCEA peripheral, such that gas from the TECA travels towards the mass spectrometer and not to waste.

18. Start sequence.

19. Log use on the SIL web-based form.

20. Monitor at least the first few standards to ensure instrument is performing properly.

Run Shutdown:

1. Close SGE valve at the mass spectrometer source.

2. Close CO valve on front of the peripheral benchtop. Close CO valves at the gas cylinder and regulator located in the fume hood. Shut off the Variac too (if necessary).

3. Turn on the Conflo III dilution (Isodat software).

4. Set the temperature controller ramp rate to 3°C/min:
   a. On Jumbo controller (one on the right) press and hold in the P button for about 5 seconds, until the Pb.1 option shows, and release button immediately.
   b. Now press the P button multiple times to cycle through the options, until you reach rasd.
   c. Use the Up and Down buttons to select ramp rate. Note the units are °C/min. Never heat or cool in increments > 5°C/min. Ramp rate guidelines: At 1°C/min it takes roughly 20 hours to heat from room temperature to working temperatures of ca. 1400°C. Typically, heat overnight at 1-2°C/min. Cool at 3°C/min.

5. Set He carrier flow to 0.6 bar.

Note: Be very careful that the pressure doesnt drop below this flow rate. The carrier flow drops very slowly and operators have allowed the flow to drop to zero, at which point the furnace control is shut-off and resulting in rapid cooling of the furnace. Once the pressure reaches 0.6 bar, be sure that if you can increase the pressure by turning up the regulator, to confirm the pressure is not still dropping. Rapid uncontrolled cooling can cause very expensive repair and instrument down-time.

6. Set Jumbo controller to ramp down to room temperature:
   a. Press P twice to get to SP.
   b. Use the up and down buttons to set the furnace temperature to 23°C.
   c. Once the temperature is set wait roughly 2-3 seconds for the display to blink off and back on. Immediately press P again. The present furnace temperature should be displayed.
   d. Confirm that the heating element is cooling at the selected rate.

MAINTENANCE PROCEDURES:

1. Replace the graphite crucible every 75-100 samples. A crucible can be removed if the temperature of the furnace is in standby conditions (i.e., with the furnace temperature at 600°C), but not at operating temperature!

2. Remove the reactor and clean the glassy carbon tube and glassy carbon grains after every 200-250 samples.
   a. Clean the glassy carbon grains. Using a Kim-Wipe, roll the glassy carbon grains in the Kim-wipe between your fingers to wipe off the carbon ash.
   b. Clean the glassy carbon tube. Using a Kim-Wipe, wipe off as best as possible the carbon ash and other residues from the outside of the glassy carbon tube. Wad up a Kim-wipe into a roll and insert it into the glassy carbon tube. Using a 3/16 wooden dowel, push the Kim-Wipe forwards and backwards inside the glassy carbon tube a few times to remove the residues

(carbon deposits).

3. Reassemble the glassy carbon tube reactor.
    a. Add Silver to the base of the glassy carbon tube. Insert the glassy carbon tube onto the reverse flow assembly inside the TCEA unit and put in silver wool from the top. You want about 0.5 cm of silver wool in the bottom. Recycle old wool if it doesnt look too tarnished. Use a 3/16 wood dowel to compact the silver wool into position at in the glassy carbon tube. Remove glassy carbon tube from the reverse flow assembly.
    b. Add glassy carbon chips to the glassy carbon tube such that the chips are 28.5 - 29 cm. from the top of the glassy carbon tube.
    c. Add a graphite crucible (if running solid samples).

4. Clean the alumina tube by wadding Kim-Wipes and using a wooden dowel to pass the Kim-Wipes back and forth inside the alumina tube.
5. Reassemble the reactor column.
    a. Remove the cooling fan at the bottom of the TCEA furnace, and carefully place it on the bench outside the furnace cavity.
    b. Insert the alumina tube into the TCEA furnace and secure it below in the reverse flow assembly.
    c. Insert the glassy carbon tube inside the alumina tube, and press down over the o-ring fitting of the reverse flow assembly. The top of the glassy carbon tube will be about 1 cm below the top of the alumina tube.
    d. Attach the top connection (Zero Blank Autosampler for solid samples, injection port for liquid samples) to the alumina tube. Use the strap wrench to tighten the top knurled nut. Be sure to hold the bottom reverse flow assembly and push it up into the top connection to ensure a secure connection.

    Note: Failure to achieve a leak tight connection at this point likely means you will need to cool the furnace down the following day, and will loose 1-2 days without any analyses.

    e. Place the bottom stainless steel spring below the reverse flow assembly. This is critical in that the reverse flow assembly would otherwise pop off when at operational He carrier gas flow pressures.
    f. Position the fan in its slot at the bottom of the furnace cavity and replace the front door of the furnace.

167

A.4 Sr SOP

A   Scope and Applicability

This method describes the setup and operation of the Neptune *Plus* High-Performance Multi-collector inductively-coupled plasma mass spectrometer (ICP-MS) for the measurement of $^{87}Sr/^{86}Sr$ (strontium) isotope ratio of samples in liquid matrix via self-aspiration. Prior to isotopic analysis, strontium is purified and concentrated using an automated off-line column chemistry system, prepFAST; see SOP *4.2.607 Offline strontium purification via prepFAST*.

B   Summary

For self-aspiration, strontium is purified and concentrated in at least 1 ml 2.4% HNO_3. A reference material, SRM® 987, is used as an in-situ standard and brackets every three (3) samples. Prior to starting the plasma, ensure that there is enough argon for the analysis run, the water-cooling system is operating properly, and the correct introduction system (*e.g.* torch, spray chamber, nebulizer, and sipper) is set up.

C   Requirements

C.1   Safety

Several solutions used in this method are mixed from concentrated nitric acid. Wear safety glasses and gloves when handling all solutions. Frocks and Crocs™ must be worn at all time while in the clean lab that houses the Neptune.

C.2   Training

Must complete lab safety training. Must know the location of emergency showers and chemical material safety data sheets (MSDS). Must have received training in clean room conduct.

C.3   Instrumentation/Equipment

- NEPTUNE *Plus* High-Performance Multicollector ICP-MS
- Safety glasses
- Gloves
- Tyvex frock and Crocs™

C.4   Consumables

Table 1: Materials, cost, storage, safety information

Material	Cost	Storage	Safety Information
Ultrapure water		N/A	None

Proprietary information –
Not for distribution.   Page 1/7   IsoForensics Inc.

168

D   Procedure

NOTE: Contact facility manager/technician for troubleshooting issues not described in this document.

D.1   Pre-startup check routine.

D.1.1   Check primary argon tank (and, if applicable, secondary argon tank) in Room 484. There must be at least 100 psi inside the tank to fire the plasma. Pressure can be increased by using the pressure-building (warming) loop.

D.1.2   Check main chiller in Room 484. Main power box in Room 484 must be on. Filter light on chiller in the clean lab, Room 479, should be green.

    D.1.2.1   If light is green precede. If light is red, contact facility manager/technician for instructions.

D.1.3   Verify instrument is setup for *Self-aspiration Sr* method.

D.1.4   Check spray chamber and nebulizer. The in-run blank for a cleaned spray chamber is ~5-10 mV ^{88}Sr while the blank for a dirty spray chamber is ~20mV ^{88}Sr. If spray chamber is dirty, excessive condensation is present within the spray chamber, or previous in-run blanks are high, follow *D.2 Clean spray chamber and nebulizer*. If clean, skip D.2 and go to D.3.

D.2   Clean spray chamber and nebulizer.

D.2.1   Plasma must be OFF and analyzer gate must be CLOSED.

D.2.2   Stop the peristaltic pump.

D.2.3   Remove the clamp holding the spray chamber to the torch.

D.2.4   Release the connector from the sample tubing to the nebulizer.

D.2.5   Remove the nebulizer from the spray chamber; place nebulizer on a clean lint free cloth and allow nebulizer to air dry.

D.2.6   Rinse spray chamber several times with ultrapure (MilliQ$^{®}$) water.

D.2.7   Dry spray chamber with argon.

D.2.8   Reassemble the clean spray chamber to the torch.

D.2.9   Insert nebulizer into spray chamber but leave ~5 mm between nebulizer and spray chamber body.

D.2.10 Reattach the sample tubing to the nebulizer.

D.3   Start Neptune *Plus* (in Tune Window and ESI SC AutoSampler).

D.3.1   In the 'Watch Parameters' panel, verify that 'HV on' and 'Analyzer Gate Open' is turned off.

Proprietary information –
Not for distribution.   Page 3/7   IsoForensics Inc.

169

D.3.2 In the 'Watch Parameters' panel, check 'fore', 'high', and 'ion getter' vacuum pressures. Pressure should be x.xxe-3, x.xxe-7, and x.xxe-9 respectively. Record pressures in personal lab notebook.

D.3.3 In the 'Chart Recorder' panel, save chart recorder file from previous analytical run (if applicable) and start a new chart.

D.3.4 In the 'Start and Stop Plasma' panel, lick "On" to start plasma. Select "No" when prompted by pop-up box to start peristaltic pump. Note start time on a new log sheet.

D.3.5 Listen for interface pump to begin a high-pitched whine.

D.3.6 Keep watch on the "Forward Power" and "Reflected Power" reading on the Neptune control panel during ignition of the plasma. If power is applied but plasma is not lit, abort immediately by clicking "Emerg. Off" in the 'Start and Stop Plasma' Panel in Tune window or press the "RF" button on the Neptune control panel. Contact facility manager.

D.3.7 In the 'Inlet System' tab, load the tune file "Neptune_Tune LR Self 100uL.sle". The forward power on the Neptune control panel is 1198-1203 W.

D.3.8 In the 'Watch Parameter' panel, open the analyzer gate and turn on high voltage ('HV').

D.3.9 Start peripump. In ESI SC Autosampler window, open 'FAST' (a new window will appear).

D.3.9.1 In the 'Peripump' tab, set the peristaltic pump #1 and #2 speed to 2.5 rpm and start pump ('Run').

D.3.10 In the 'Watch Parameter' panel, check 'fore', 'high', and 'ion getter' vacuums. Record pressures on log sheet and compare to pressures recorded previously in personal lab notebook.

D.3.11 In 'Chart recorder' panel, start a new chart recorder.

D.4 Tuning (in Tune Window).

D.4.1 In 'Scan Control' tab, check that 'Selected Mass' is '86Sr', 'Selected Cup' is 'C (Far.)'.

D.4.2 In 'Center Cup' tab, check that 'Faraday' is check marked and 'Mode' is Faraday (indicated by green dot).

D.4.3 In 'Detector Calibration' tab, run instrument Baseline/Gain calibration by clicking 'Gain' (Analyzer Gate need to be closed). This process will take ~10 minutes. This is a good time to prepare stock solutions and reference materials. The calibration is complete when buttons become available again. Re-open analyzer gate.

D.4.4 Set probe to ultrapure (MilliQ®) water for a few seconds then to 2.4% TMG HNO_3 blank solution.

D.4.5 In the 'Scan Control' tab, acquire blank reading by clicking 'Set'. Record the ^{88}Sr signal intensity in 'Watch Parameter' panel (Cup H2), and the peristaltic pump speed in the log sheet. If blank signal intensity is high, *i.e.* >5mV, consider cleaning spray chamber following *D.2 Clean spray chamber and nebulizer* if running low concentration samples.

D.4.6 Set probe to 100ppb SRM® 987 in 2.4% TMG HNO_3 standard solution.

Proprietary information –
Not for distribution.   Page 4/7   IsoForensics Inc.

170

D.4.7 Adjust X-axis and Y-axis accordingly to capture signal intensity.

D.4.8 If the instrument is in tune, the signal intensity reading from Cup H2 should be ~5-7V. In addition, note signal intensity from the previous run. A significant decrease in intensity indicates the instrument should be re-tuned.

D.4.9 If needed, tune the instrument.

D.4.9.1 In 'Inlet System' tab, change "Sample Gas", and "X- and Y-positions" to maximize signal intensity.

D.4.9.2 Save and overwrite tune file ("Neptune_Tune LR Self 100uL.sle").

D.4.10 Record the ^{88}Sr signal, concentration of tuning solution, and speed of the peristaltic pump during tuning on the log sheet.

D.4.11 In the 'Scan Control' tab, click 'Peakcenter' to run a peak center. Peak center is complete when status window states "Peak center successful!"

D.4.12 In the 'Scan Control' tab, click 'Peakscan' to run a peak scan. H2, H1, Ax, and L1–L4 should be well aligned and have good peak shapes (*i.e.* peaks have flat tops and fairly steep sides).

D.4.13 Rinse spray chamber with 2.4 % HNO$_3$.

D.4.13.1 Set probe to ultrapure (MilliQ$^®$) water for 10 seconds.

D.4.13.2 Set probe to 2.4% HNO$_3$. Wait for signal in chart recorder window to return to near baseline (recorded 'blank').

D.5 Starting a sample sequence.

NOTE: Analyze samples in ascending order of concentration (lowest to highest); ideally concentrations for all samples in a sequence should be between 50 and 100 ppb Sr.

D.5.1 Place samples in Autosampler Rack 1, starting at Position 1.

D.5.2 Replenish 100 ppb SRM$^®$ 987 in 2.4% TMG HNO$_3$ (Rack 0, Position 2 in autosampler). Each SRM analysis uses ~0.5 mL of solution.

D.5.3 Discard remaining Blank Solution (Rack 0, Position 1 in autosampler) in appropriate waste container and replenish with new 2.4% TMG HN0$_3$ solution.

D.5.4 Replenish the autosampler water rinse container with ultra-pure (MilliQ$^®$) water (Rack 0, Position 5 in autosampler).

D.5.5 Replenish the autosampler acid rinse container with 2.4% TMG HNO$_3$ (Rack 0, Position 6 in autosampler).

D.5.6 Open SRM$^®$ 987 solution, Blank Solutions, and rinse solutions.

D.5.7 Create run sequence.

D.5.7.1 Open 'Sequence Editor' window.

D.5.7.2 Open sequence "Sr self-aspiration 100uL Template.seq".

D.5.7.3 In 'Sample ID' column, enter sample information into 'SMP' slot.

171

D.5.7.4 In 'Filename' column, autofill sample information by clicking icon.

D.5.7.5 In 'Method File' column, verify that the appropriate method file is selected.

D.5.7.6 In 'Tune Parameter' column, verify that the appropriate tune file is selected.

D.5.7.7 In 'Status' column, verify that corresponding lines are enabled.

D.5.7.8 In the 'Sequence Editor' window, click "Save" icon located in the top left corner to save sequence.

D.5.8 Close the FAST window (not ESI SC Autosampler).

D.5.9 In the 'Sequence Editor' window, click "Start – Go" icon located in the top left corner to begin run.

D.5.10 When prompted, check the box for "Online ASCII Export"

D.5.11 Note run start time and 14-digit identifier on log sheet.

D.5.12 In the 'Sequence Editor' window, choose option 'Switch plasma off' under 'Execute' menu. DO NOT select this option if there will be another run soon after the current run is completed.

D.5.13 Check the main instrument waste reservoir. If the reservoir is half-full, empty it using peristaltic pump into acid waste container.

D.6 If autosampler is operating incorrectly, restart ESI software.

D.6.1 Close all program associated with controlling the Neptune *Plus* instrument.

D.6.2 Reopen ESI software, and initialize the autosampler by clicking 'Initialize autosampler."

D.6.3 Verify the correct 'FAST Method File' is loaded.

D.6.4 Reopen 'Tune' & 'Sequence Editor' software. Restart the run sequence.

D.7 Monitor the first two blanks and SRM® 987 standards. Acceptable SRM® 987 ^{87}Sr/^{86}Sr range is 0.710270 – 0.71032. If the first two standards are not within acceptable range, contact facility manager/technician immediately for additional help.

D.8 Use TeamViewer to remotely monitor run using ID: 416015826. A password is required. Password is reset by closing TeamViewer. (Check and verify credentials are up-to-date)

Proprietary information –
Not for distribution.   Page 6/7   IsoForensics Inc.

172

APPENDIX B

LIKELIHOOD ASSIGNMENT MAPS
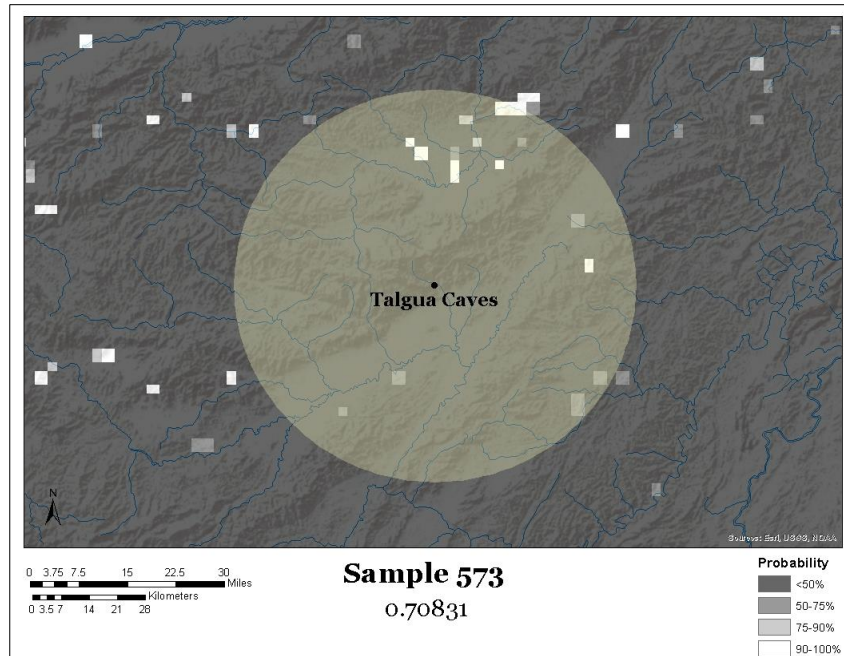
Figure B.1 $^{87}Sr/^{86}Sr$ Assignment for Sample 573
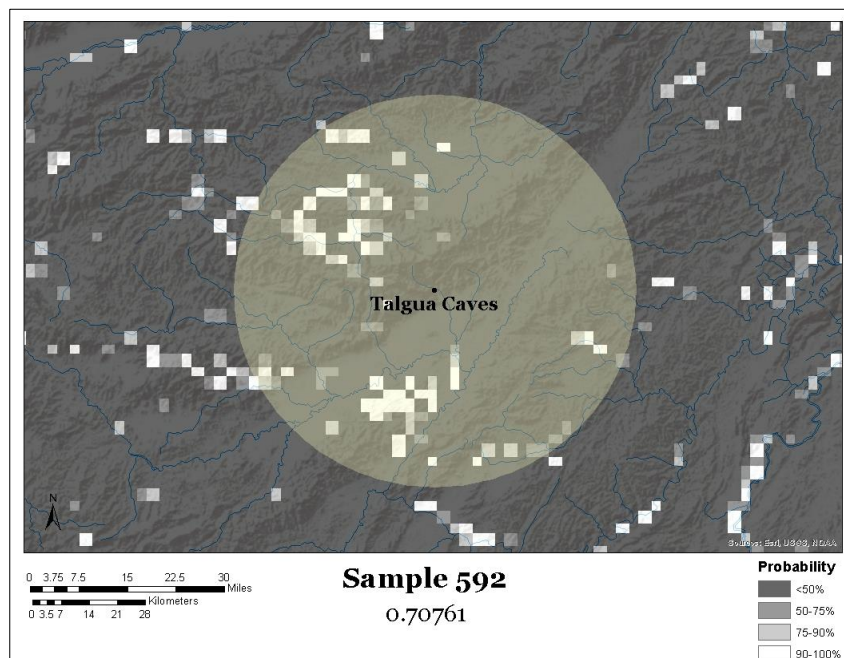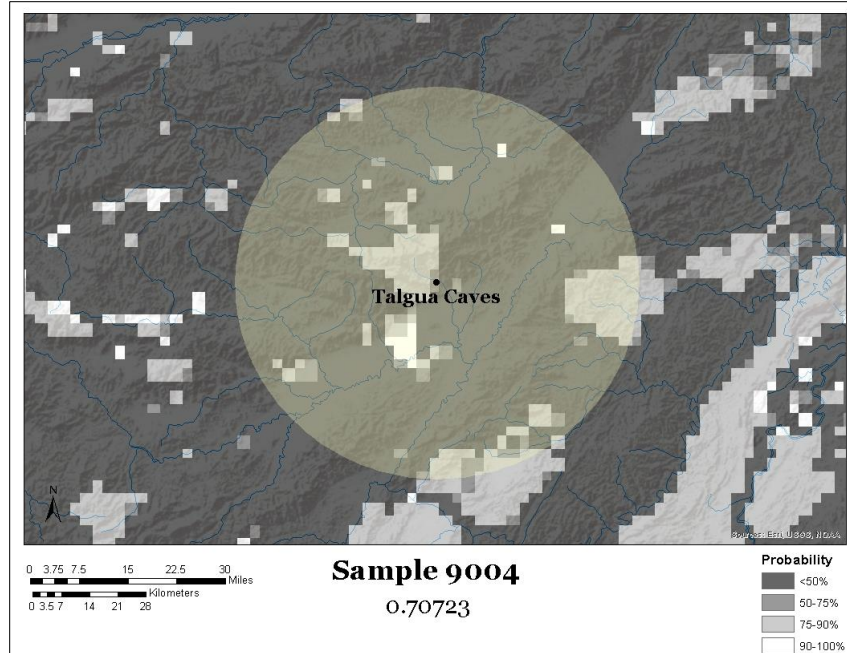

Figure B.2 $^{87}Sr/^{86}Sr$ Assignment for Sample 592
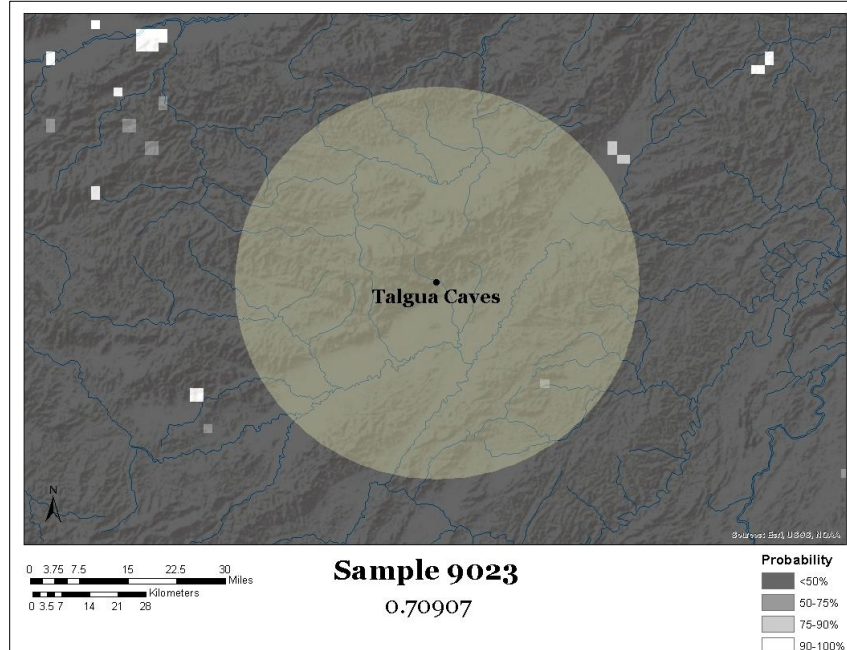
Figure B.3 $^{87}Sr/^{86}Sr$ Assignment for Sample 9004

Figure B.4 $^{87}Sr/^{86}Sr$ Assignment for Sample 9023

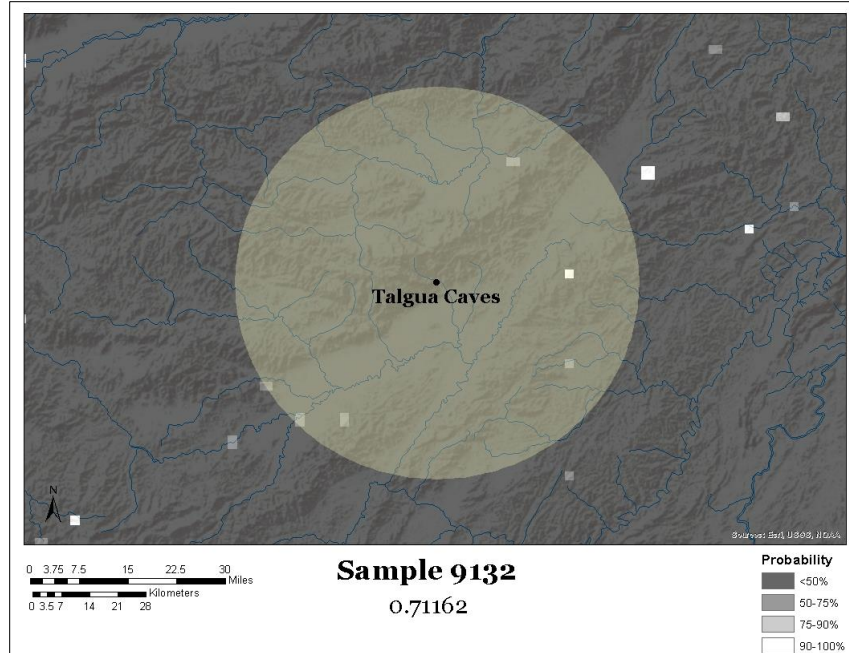Figure B.5 ^{87}Sr/^{86}Sr Assignment for Sample 9132
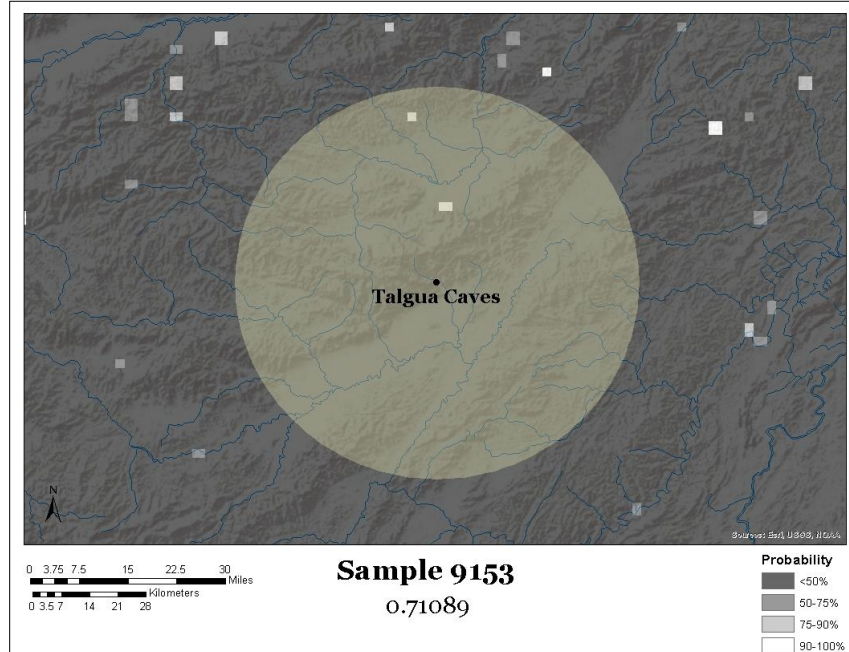
Figure B.6 ^{87}Sr/^{86}Sr Assignment for Sample 9153
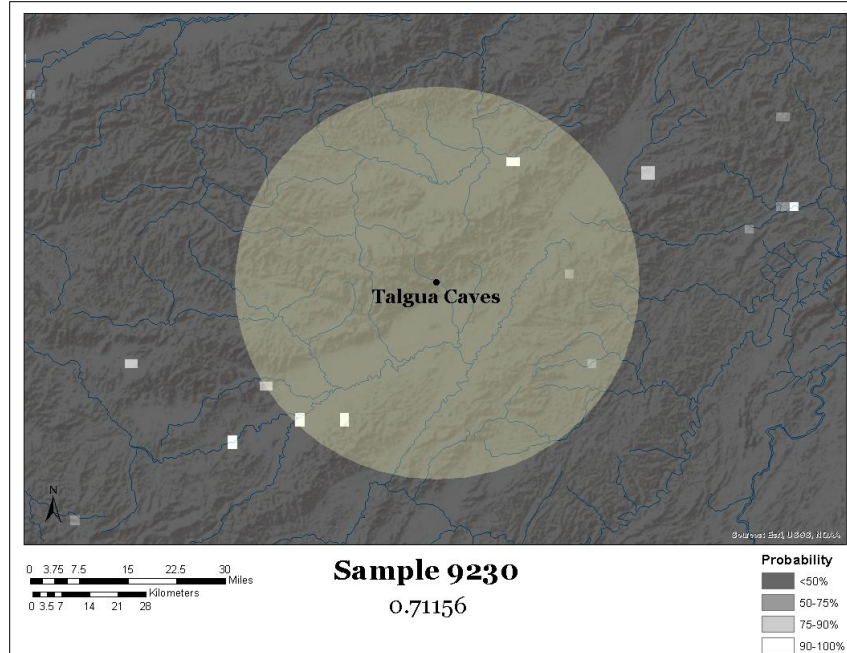
Figure B.7 $^{87}Sr/^{86}Sr$ Assignment for Sample 9230

Figure B.8 $^{87}Sr/^{86}Sr$ Assignment for Sample 9318
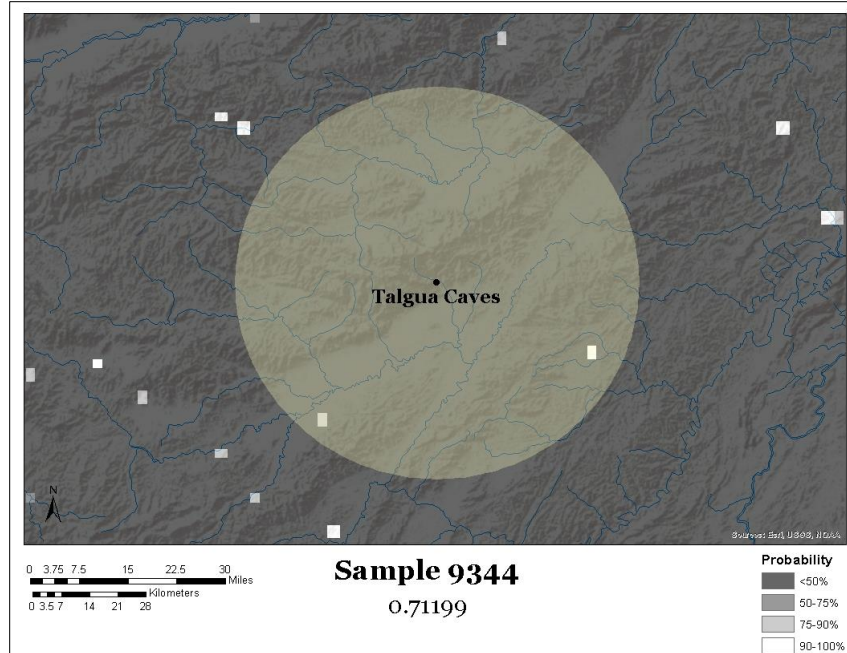
Figure B.9 $^{87}Sr/^{86}Sr$ Assignment for Sample 9344
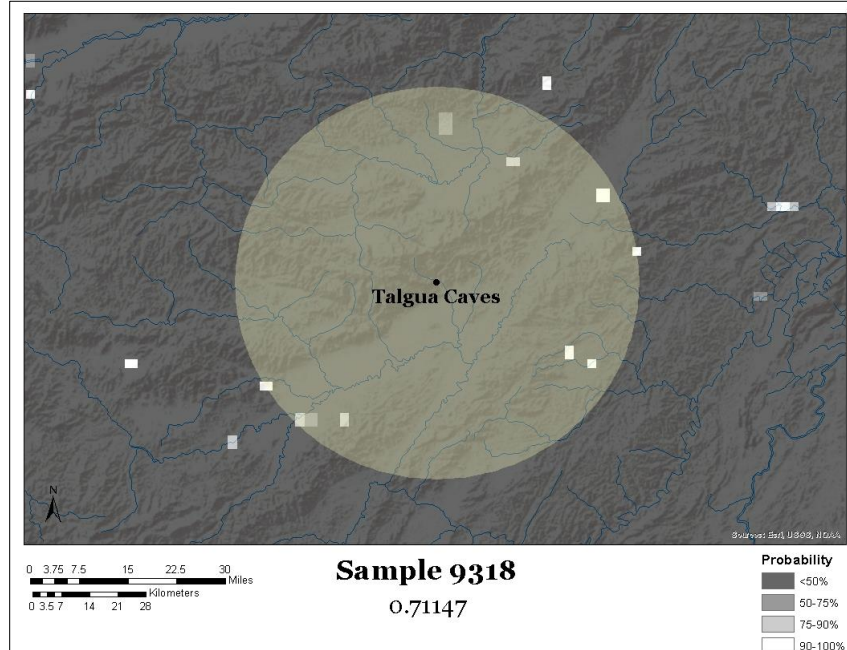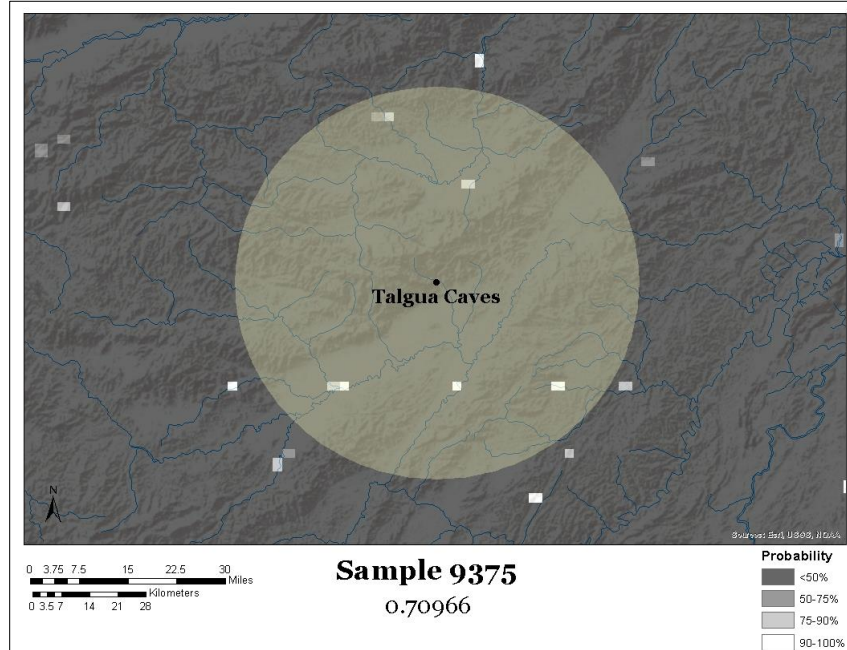

Figure B.10 $^{87}Sr/^{86}Sr$ Assignment for Sample 9375
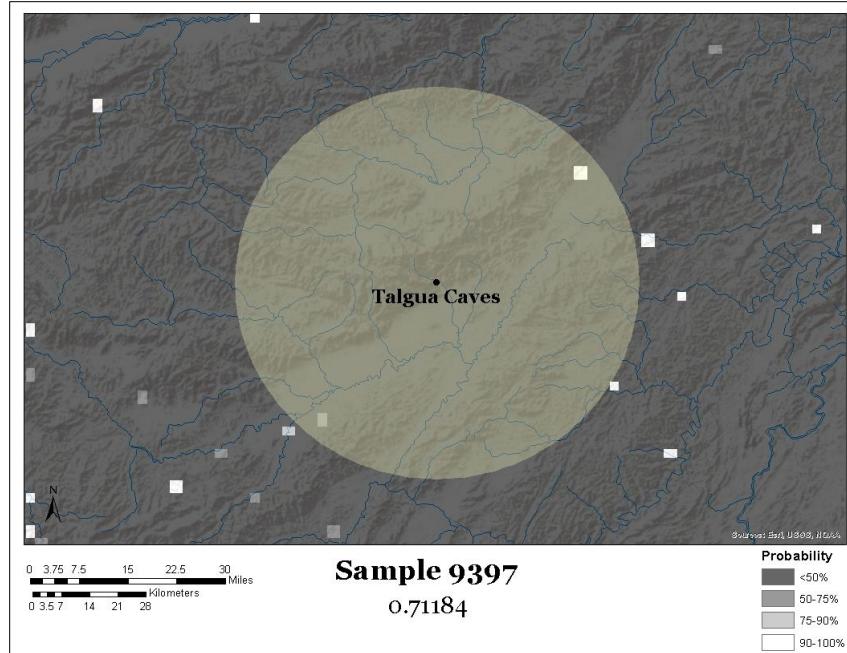
Figure B.11 $^{87}Sr/^{86}Sr$ Assignment for Sample 9397
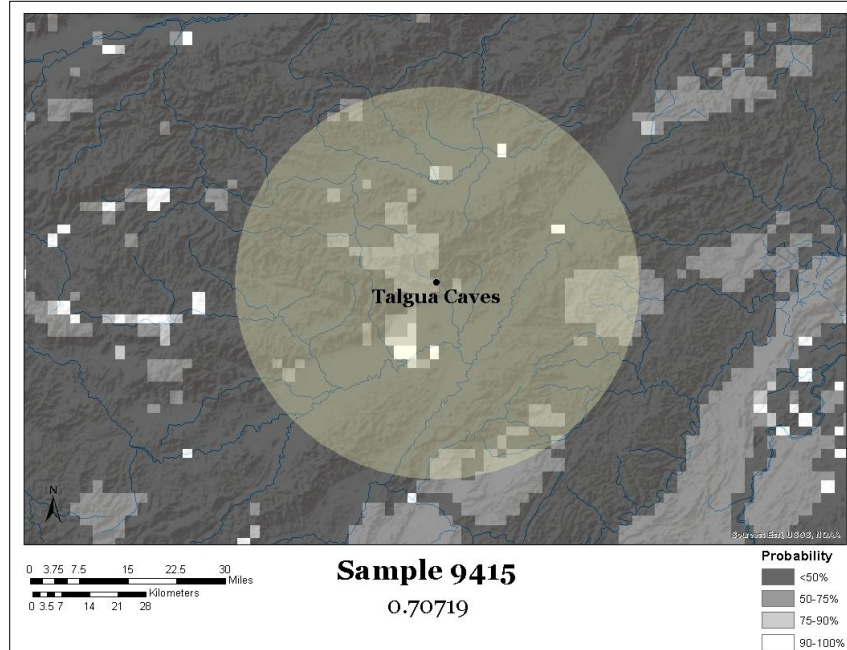
Figure B.12 $^{87}Sr/^{86}Sr$ Assignment for Sample 9415

Figure B.13 ^{87}Sr/^{86}Sr Assignment for Sample 9425

Figure B.14 ^{87}Sr/^{86}Sr Assignment for Sample 9440

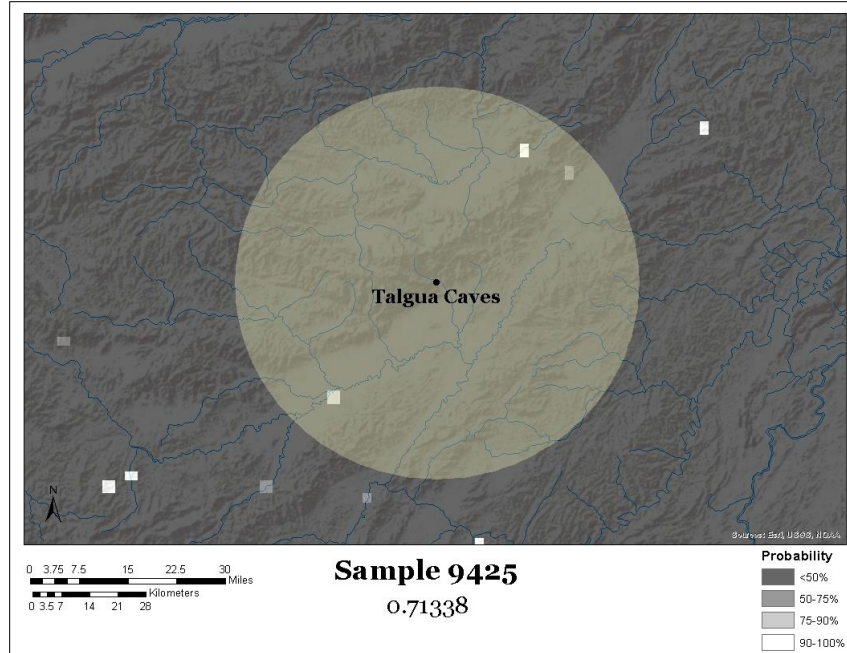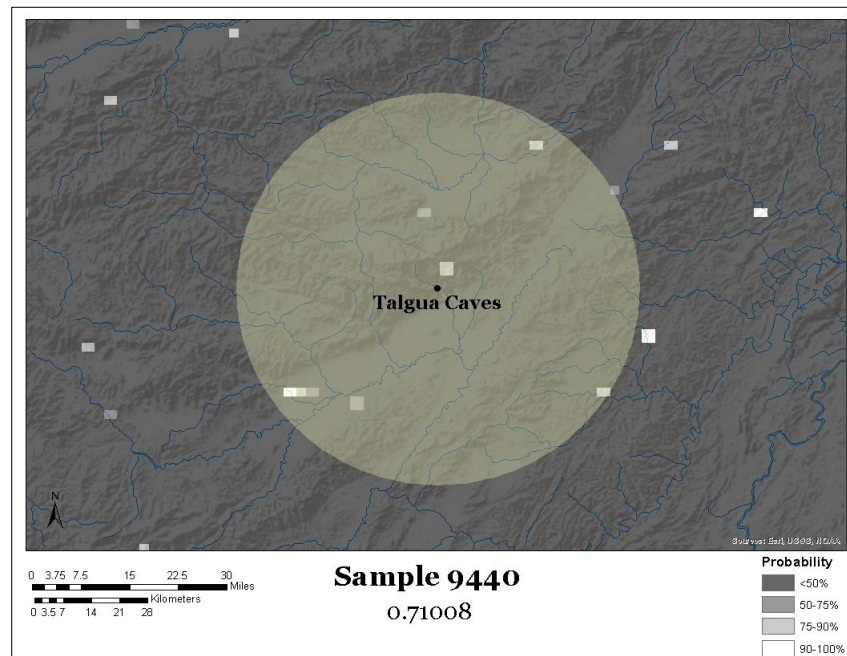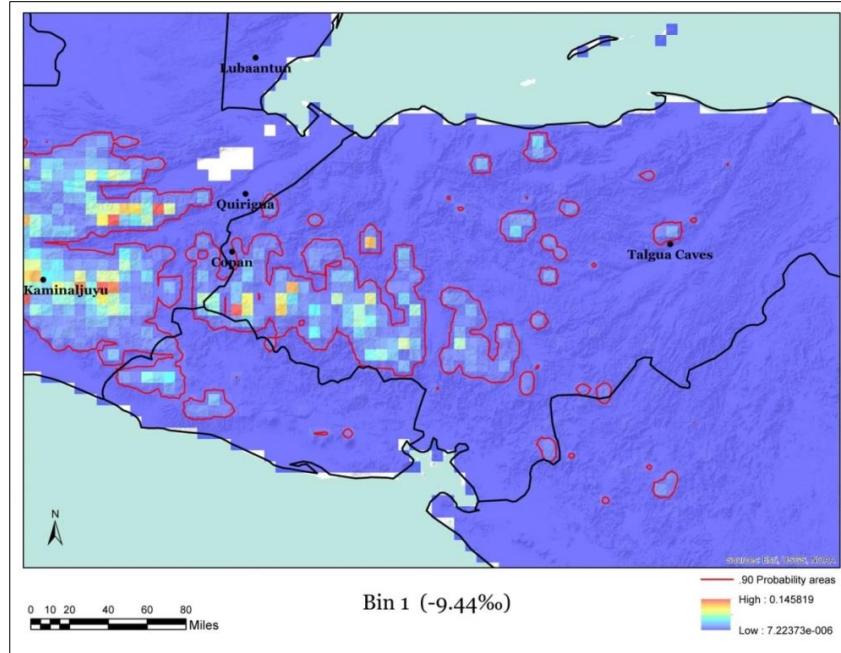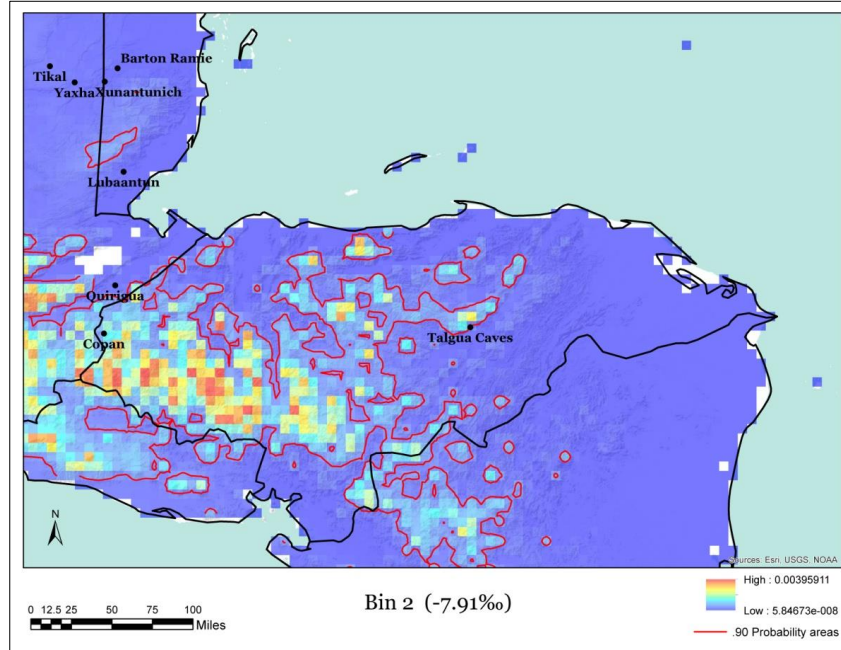Figure B.15 $\delta^{18}O_p$ Bin 1 Assignment

Figure B.16 $\delta^{18}O_p$ Bin 2 Assignment
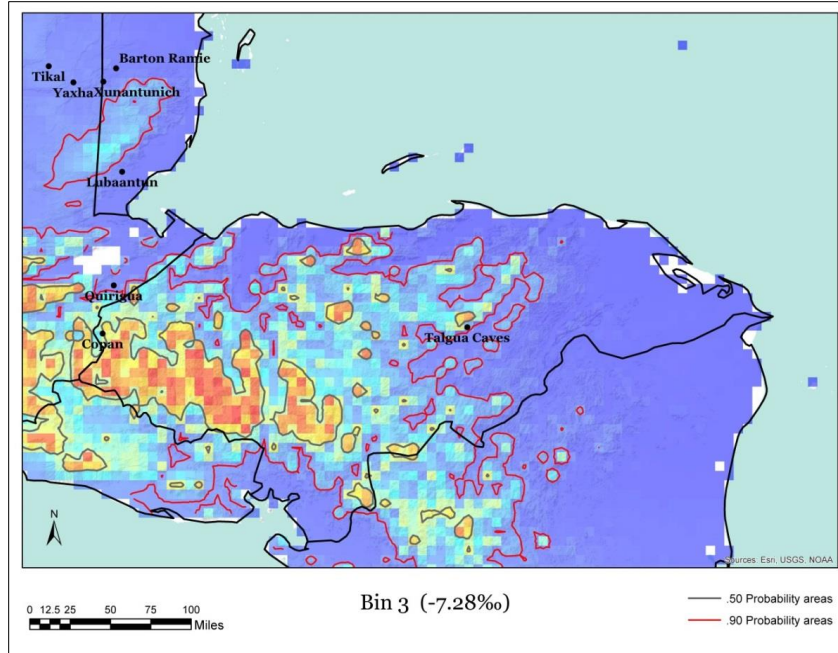
Figure B.17 $\delta^{18}O_p$ Bin 3 Assignment
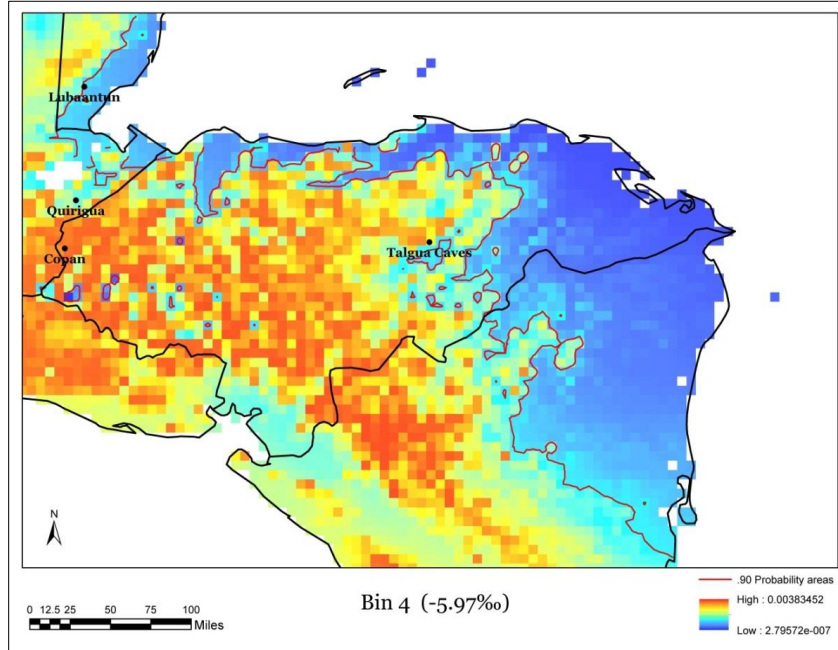

Figure B.18 $\delta^{18}O_p$ Bin 4 Assignment

APPENDIX C

DATA SHEETS

C.1 Assignment catchment model calibration data

Site	Latitude	Longitude	Bioavailable $^{87}Sr/^{86}Sr$	Catchment $^{87}Sr/^{86}Sr$	Type	Source
Abaj Takalik	14.638	-91.733	0.70410	0.70486	Fauna	Price et al. (2010)
Aquateca	16.412	-90.188	0.70750	0.70710	Fauna	Price et al. (2010)
Atitlan	14.700	-91.200	0.70420	0.70496	Fauna	Price et al. (2010)
Baking Pot	17.203	-89.019	0.70866	0.70772	Human	Freiwald (2011)
Balamku	18.560	-89.944	0.70830	0.70802	Fauna	Price et al. (2010)
Barton Ramie	17.203	-89.019	0.70862	0.70772	Human	Freiwald (2011)
Becan	18.517	-89.467	0.70820	0.70772	Fauna	Price et al. (2010)
Blackman Eddy	17.217	-88.917	0.70856	0.70764	Human	Freiwald (2011)
Bonampak	16.704	-91.065	0.70770	0.70706	Fauna	Price et al. (2010)
Brook Site	17.070	-61.700	0.70886	0.70841	Fauna	Laffoon et al. (2012)
Buenavista	17.084	-89.134	0.70861	0.70727	Human	Freiwald (2011)
Cahal Pech	17.146	-89.074	0.70847	0.70706	Human	Freiwald (2011)
Calakmal	18.114	-89.809	0.70770	0.70772	Fauna	Price et al. (2010)
Campeche	19.850	-90.531	0.70820	0.70802	Fauna	Price et al. (2010)
Chaa Creek	17.179	-89.349	0.70950	0.70772	Human	Freiwald (2011)
Champoton	19.344	-90.724	0.70830	0.70880	Fauna	Price et al. (2010)
Chiapa de Corzo	16.700	-93.000	0.70740	0.70780	Fauna	Price et al. (2010)
Chichen Itza	20.683	-88.569	0.70870	0.70802	Fauna	Price et al. (2010)
Coba	20.495	-87.736	0.70820	0.70880	Fauna	Price et al. (2010)
Cocales	14.392	-91.197	0.70420	0.70499	Fauna	Price et al. (2010)
Colha	17.950	-88.367	0.70820	0.70773	Fauna	Price et al. (2010)
Copan	14.840	-89.140	0.70690	0.70721	Human	Price et al. (2010)
Ek Balam	20.891	-88.136	0.70860	0.70880	Fauna	Price et al. (2010)
El Chayal	14.717	-90.033	0.70610	0.70492	Fauna	Price et al. (2010)
El Chorro de Maita	21.090	-75.740	0.70829	0.70744	Fauna	Laffoon et al. (2012)
El Mirador	17.755	-89.920	0.70790	0.70772	Fauna	Price et al. (2010)
Escarcega	18.606	-90.746	0.70810	0.70802	Fauna	Price et al. (2010)
Floral Park	17.200	-88.950	0.70853	0.70759	Human	Freiwald (2011)
Izapa	14.923	-92.180	0.70470	0.70500	Fauna	Price et al. (2010)
Kaminaljuyu	14.633	-90.549	0.70520	0.70486	Human	Wright et al. (2010)
Los Buchillones	22.140	-78.310	0.70830	0.70863	Fauna	Laffoon et al. (2012)
Lubaantun	16.281	-88.965	0.70700	0.70748	Fauna	Price et al. (2010)
Maisabel	18.490	-66.390	0.70895	0.70880	Fauna	Laffoon et al. (2012)
Mayapan	20.629	-89.461	0.70880	0.70802	Fauna	Price et al. (2010)
Mirador	17.755	-89.920	0.70720	0.70772	Fauna	Price et al. (2010)
Nohmul	18.217	-88.585	0.70860	0.70880	Fauna	Price et al. (2010)
Oxlontok	20.560	-89.954	0.70880	0.70880	Fauna	Price et al. (2010)
Palenque	17.484	-92.046	0.70874	0.70772	Fauna	Price et al. (2010)
Paso de las Amada	14.877	-92.490	0.70480	0.70500	Fauna	Price et al. (2010)
Piedras Negras	17.167	-91.263	0.70800	0.70723	Fauna	Price et al. (2010)
Pontreno del Mango	21.030	-75.770	0.70728	0.70764	Fauna	Laffoon et al. (2012)
Pook's Hill	17.154	-88.852	0.70845	0.70767	Human	Freiwald (2011)
Quirigua	15.269	-89.040	0.70730	0.70789	Fauna	Price et al. (2010)
Rio San Pedro	17.276	-90.982	0.70750	0.70719	Fauna	Price et al. (2010)
San Cristobal	16.737	-92.638	0.70760	0.70770	Fauna	Price et al. (2010)
Sandy Ground	18.200	-63.090	0.70891	0.70856	Fauna	Laffoon et al. (2012)

Site	Latitude	Longitude	Bioavailable $^{87}Sr/^{86}Sr$	Catchment $^{87}Sr/^{86}Sr$	Type	Source
Saturday Creek	17.334	-88.817	0.70869	0.70772	Human	Freiwald (2011)
Shoal Bay East	18.250	-63.030	0.70914	0.70856	Fauna	Laffoon et al. (2012)
Siho	20.487	-90.151	0.70870	0.70880	Fauna	Price et al. (2010)
Tikal	17.222	-89.624	0.70812	0.70772	Human	Wright (2005)
Tizimin	21.136	-88.146	0.70890	0.70880	Fauna	Price et al. (2010)
Tonina	16.901	-92.010	0.70790	0.70821	Fauna	Price et al. (2010)
Tulum	20.215	-87.429	0.70800	0.70880	Fauna	Price et al. (2010)
Xunantunich	17.084	-89.134	0.70862	0.70727	Human	Freiwald (2011)
Yaxchilan	16.900	-90.967	0.70820	0.70706	Fauna	Price et al. (2010)
Yaxha	17.078	-89.403	0.70790	0.70880	Fauna	Price et al. (2010)

C.2 Dental metric data

Sample	Tooth	MD (mm)	BL (mm)	Sample	Tooth	MD (mm)	BL (mm)
486	3	10.3	10.9	9230	2	10.1	11.3
487	15	12.19	9.95	9235	15	11.4	11.85
489	2	9.7	10.7	9239	14	10.45	11.15
572	3	10.75	12.08	9240	3	11.4	12.1
573	31	12.28	11.51	9249	19	12.55	11.6
655	15	11.04	11.94	9251	31	11.55	11.2
692	30	12.31	10.95	9253	19	12.2	10.65
695	31	12.85	11.1	9254	18	12.2	10.65
9002	3	11.05	12.15	9255	31	12.1	10.25
9003	15	11.42	12.5	9256	30	11.5	10.4
9005	19	11.5	11.55	9258	31	12.05	10.7
9009	19	11.9	11.1	9259	2	11.3	11.25
9021	18	11.15	10.4	9260	15	11.45	11.45
9023	18	11.25	10.35	9264	19	12.2	11.45
9025	30	13.35	11.45	9265	30	12.3	11.1
9030	14	10.55	11.5	9266	30	12.45	11.9
9031	14	11	12.2	9275	19		10.85
9059	19	13.4	11.55	9277	30	11.6	10.4
9060	30	13.05	12	9278	31	10.55	10.8
9061	19	13.55	11.9	9281	30	12.75	11.65
9062	30	13.1	10.7	9283	2	11.3	12.35
9064	31	11.2	10.9	9286	15	11.15	12.3
9065	31	12.5	11.1	9297	19	12.45	11.4
9066	30	12	11.15	9298	18	11.8	11
9108	15	10.25	11.25	9299	31	12.25	10.45
9109	15	11.3	12.05	9300	30	12.4	11.4
9111	15	11.5	13.55	9302	18	11.85	11.3
9112	2	10.6	13.15	9303	2	11.1	12
9113	3	11.8	12.75	9304	2	11.2	12.5
9114	14	12.25	12.7	9318	15	10.55	11.8
9115	3	12.45	12.75	9344	2	10.6	11.75
9116	14	12.4	12.8	9349	19	12.2	10.9
9117	2	9.45	11.7	9351	30	12	10.75
9132	19	12.4	10.95	9352	2	11.9	11.4
9133	3	12.2	12.5	9356	2	10.6	12.6
9153	3	12.15	12.7	9357	3	11.35	12.35
9154	3	11.55	12.4	9358	15	10.95	12.3
9155	3	10.8	12.35	9364	19	12.6	10.9
9177	19	12.6	11.35	9365	30	12.75	11.2
9178	19	12.3	10.95	9368	19	12.2	11.1
9179	30	11.4	10.65	9375	2	9.5	11.55
9180	30	10.95	11.75	9376	15	9.4	11.15
9185	2	11.2	11.4	9377	3	11.6	11.75
9187	3	11.4	12.8	9378	14	11.6	11.65
9188	14	11.2	13.1	9396	3	10.8	11.9
9189	15	10.6	11.8	9397	2	9.9	12.05
9190	14	11.85	12.35	9398	15	9.7	12.2

186

Sample	Tooth	MD (mm)	BL (mm)	Sample	Tooth	MD (mm)	BL (mm)
9191	14	11.65	12.3	9399	2	10.7	12
9201	30	12.95	11.75	9401	3	10.85	12.05
9202	31	12.7	11.7	9415	30	11.8	11.2
9203	18	12.9	11.3	9416	14	10.5	12.4
9204	19	12.3	10.85	9425	15	10.35	11.9
9219	14	10.55	11.95	9428	2	9.7	12.1
				9430	18	10.05	9.7